INTERIM REPORT,EL 1/88
SEPTEMBER 1994

EL 1/88

M BENDALL

CONTENTS

1 COPY OF PROMOTIONAL PAPER ON THE TASMANIAN AGSO PROJECT

2 PHOTOGRAPHS OF THE DEPT OF MINES' DRILL HOLE AT DOUGLAS RIVER WHERE M BENDALL COLLECTED SAMPLES

3 COPY OF A PAPER ON HYDROCARBON BIOMARKERS, THERMAL MATURITY AND DEPOSITIONAL SETTINGS OF TASMANITE OIL SHALES BY REVILL, VOLKMAN ET AL.

TCR 94-3636

94-3636

AMG REFERENCE POINTS ADDED

TASMANIA
DEVELOPMENT
AND RESOURCES

AGSO
AUSTRALIAN
GEOLOGICAL SURVEY
ORGANISATION

EL1/88

TASMANIA NGMA PROJECT "TASGO":

Geological Framework of an "Island State with Potential"

Mineral Resources Tasmania (MRT)

and the

Australian Geological Survey Organisation (AGSO)

Draft Proposal for a new National Geoscience Mapping Accord (NGMA) Project 1994 to 1997

Second Draft, 29 July 1994.

TO CAROL BACON
Personal copy

Sept 1994.

EXECUTIVE SUMMARY

The National Geoscience Mapping Accord (NGMA) is a cooperative arrangement between the Commonwealth and the States, through AGSO and State/Northern Territory Geological Surveys, to provide a new generation of geoscience maps and data sets for Australia through the utilisation of state-of-the-art technologies and the collaboration of Governments, the minerals and petroleum industries, and universities.

This draft document gives an outline of a 3-year NGMA Project designed to increase exploration, development and investment in Tasmania. A strategy, work plan and multidisciplinary activities to improve the definition of Tasmania's minerals and petroleum potential is proposed.

This is to be achieved largely through the acquisition and interpretation of new state-of-the-art geophysical data, supplemented by some review work to provide a framework at depth for the surface mapping to fit into and for the State's mineral and petroleum potential to be reassessed through the better understanding that will emerge.

859004

CONTENTS

OUTCOMES

Increased exploration, development and investment in Tasmania through

- improved definition of minerals and petroleum prospectivity zones, especially those not being explored,
- more efficient exploration in strategic prospectivity zones
  - based on a better understanding of Tasmania's deep structure, its known mineralisation, and a better understanding of the potenetial for petroleum.

PREAMBLE

Tasmania has a good coverage of geological maps (Attachment 1). The State is richly endowed with world-class deposits of copper-zinc-lead-silver-gold, significant tin, tungsten, gold and iron, and lesser platinum group-metal deposits (Attachment 2). This extensive suite of mineral deposits is located in a small land mass, more than adequately serviced by towns, roads, power and other necessary infrastructure.

Not surprisingly, the 1993 Commonwealth Government's Task Force on Regional Development considered Tasmania's best opportunity for growth to be in minerals processing. Legislative, regulatory and policy changes recently enacted and initiated by "Tasmania-Development and Resources", emphasise the State's pro-development platform.

Geological maps are the primary information source that minerals and petroleum companies use to begin their assessments of risk associated with exploration. The maps are also a key data set used in resource assessments, helping to underpin Government decisions on multiple land use issues.

It is clear that the current availability of quality geological maps alone is insufficient to sustain the level of exploration activity required for a healthier State economy with considerable minerals processing potential. In consequence, more scientific innovation to supplement the mapping effort is required. It now seems a good time *to place this mapping in a framework* through the acquisition of new information on the State's geology *at depth*.

It is proposed that this be via high-technology studies. The character of Tasmania's principal geological structures *at depth* cannot be uniquely determined from surface mapping. Several models exist for some key structures, but they vary considerably. They must be tested before they can reliably used to generate new ideas for exploration.

It is known that the land mass of Tasmania is made up of several "provinces" of old rocks between which lie narrower geological "troughs" with slightly younger rocks (Attachment 3). Both the provinces and the troughs contain mineralised belts (Attachment 4). These features are now anchored to the Earth's deep crust by a pedestal of unknown rocks through which fluids containing the minerals have passed. The pathways of these former fluid systems also need to be defined, where possible.

Covering the junction of two major provinces is the Tasmania Basin. It has considerable coal resources and would be prospective for petroleum if its strata are sufficiently thick. However, this basic information on the basin's thickness is not known with sufficient certainty, largely due to the cover of younger rocks.

Offshore, younger basins adjoin Tasmania's western and northern margins but these are poorly explored. Their known geological histories appear similar to the oil-generative Gippsland Basin which has sustained much of Australia's petroleum needs for a long time.

The Tasmania NGMA Project has been designed to provide some answers and to find missing links. If successful, a *framework* for understanding the relationships of the various "bits" that make up Tasmania at depth will emerge. Ideally, present and future geological mapping can then be placed in and integrated with this framework.

If so, the State's minerals and petroleum systems can then become better understood, hence the importance of this project for exploration, development and investment in Tasmania.

OBJECTIVE

Define and characterise the large scale structure of Tasmania to provide a framework for existing mapping, thereby

- constraining models for the State's geological evolution

- as an input to improved minerals and petroleum exploration strategies
- for developing new insights towards the understanding of the State's minerals and petroleum resources.

STRATEGY

The project will place Tasmania in its regional southeast Australian context. The building blocks of Tasmania will be defined. How the mineral and petroleum systems fit into this framework will be ascertained. The specific steps in this strategy are illustrated in Fig. 1 (overleaf) and outlined as follows:

- Define and explain Tasmania's place within the continent
- Determine the size, shape and distribution of the tectonic elements which comprise the geology of Tasmania
- Define the internal structure of the tectonic elements and characterise the boundaries between them
- Examine if there is a relationship between known mineralisation and major structures, and resolve the shape, direction and dip of the major structures
- Define the fluid flow paths of mineral systems and build models for exploration
- Highlight features pertinent to understanding the petroleum potential of Tasmania.

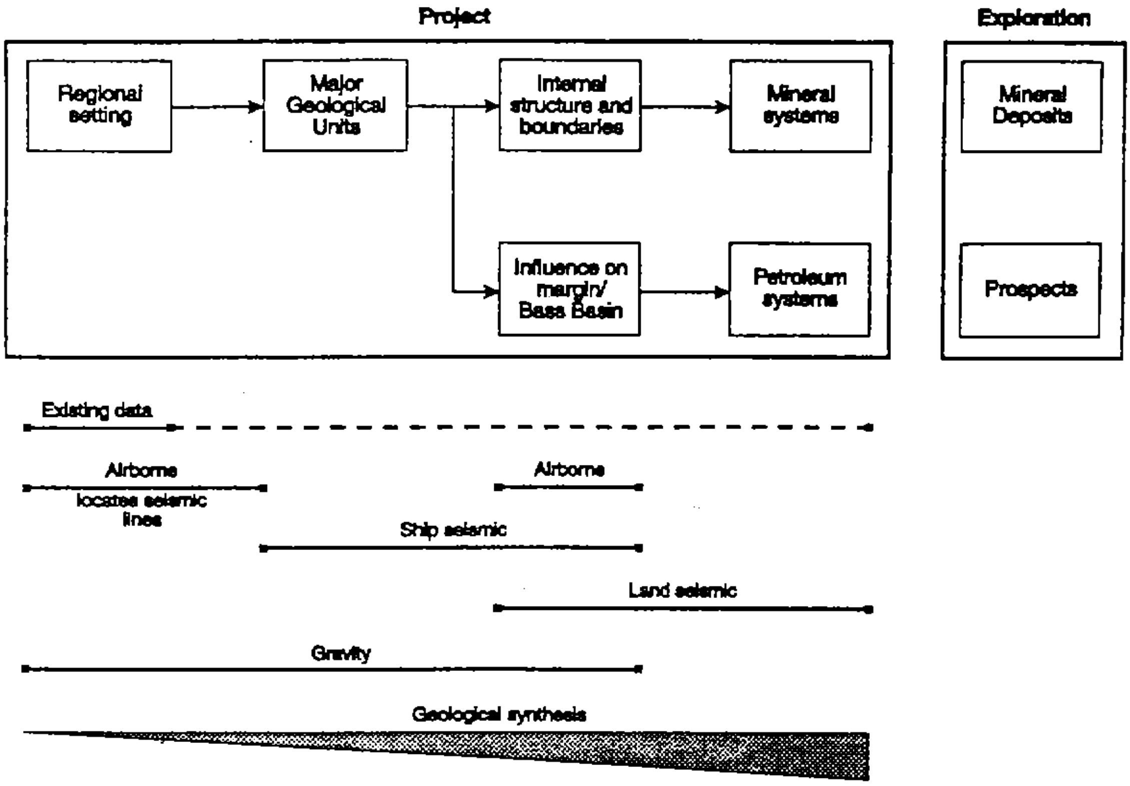

Fig. 1: Project Strategy

WORK PLAN

Collate the existing geophysical (particularly gravity and magnetic), geochronological and geological data to

- define the main geological events that built Tasmania
- relate the events in time and effect to those observed on the mainland and along the continental margin.

Collect new quality airborne magnetic data around the margins of Tasmania (Attachment 5) in order to

- better define the main tectonic elements
- position a number of regional seismic reflection profiles offshore.

Collect regional seismic reflection profiles along the northern, western and southern margins (Attachment 6) to

- define the structure in the upper 10 to 20 km of the crust
- characterise the internal structure of major crustal blocks and the geometry of their boundaries including the Dundas Trough and Arthur Lineament.

Continue profiling along the eastern margin to allow a piggyback refraction/tomographic experiment in order to

- define the structure of the lower crust.

Record seismic reflection profiles onshore across tectonic element boundaries and mineralised zones (Attachment 6) and in particular

- the Dundas Trough and its relationship to the adjacent Rocky Cape and Tyennan Blocks in west Tasmania
- structures associated with gold mineralisation in the northeast
- experimental recording to attempt to image Permo-Triassic sedimentary rocks of the Tasmania Basin beneath Jurassic dolerite cover in central and eastern Tasmania.

TIMETABLE

The project will take 3 years. It will comprise a number of linked sub-projects as outlined below and with timing of key elements indicated in Fig. 2.

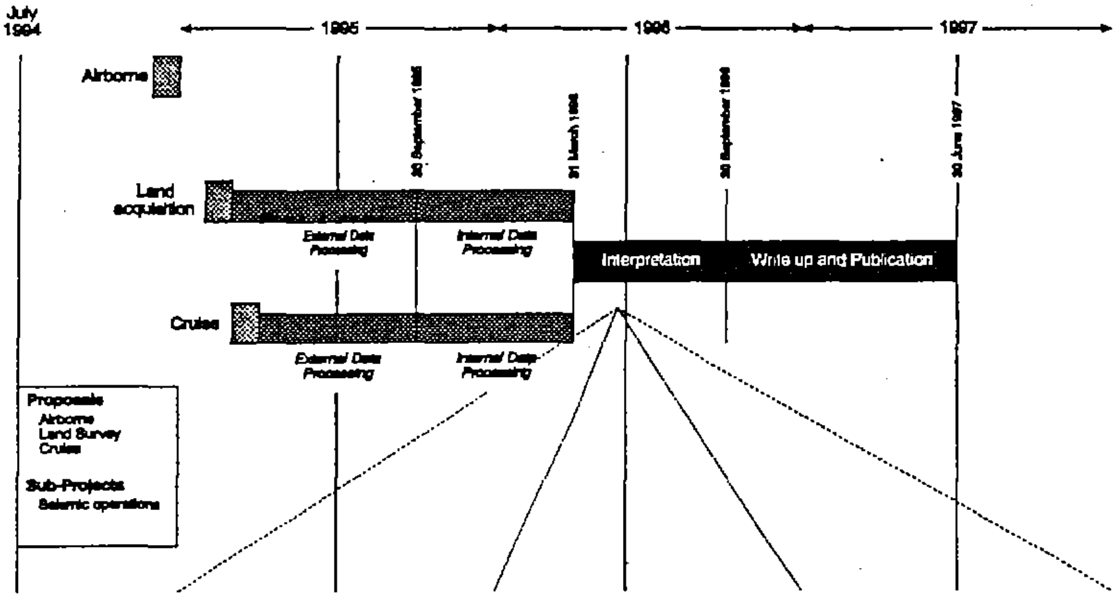

Fig. 2: Project Timetable

SUB-PROJECTS

1. Geological Synthesis at Plate/Framework and Element Scales.

The sub-project will be a compilation and review of existing knowledge and concepts. Its objective is to define, within logistic constraints, the optimum positions for seismic reflection and refraction profiles along the northern, western and southern coastlines.

The primary products of the sub-project will be a new 1:500,000-scale strato-tectonic map for Tasmania and time-space plots of depositional, igneous, mineralising and deformational events for each tectonic element.

These products will be comprehensive new style summaries of Tasmania's geology valuable for anyone wanting to explore or study Tasmania. They will be updated during the life of the project. The first editions are expected to be available from December 1994 as computer-generated, date-stamped paper copies printed at cost on demand.

2. Dating Tasmania's Geological Events.

Recent zircon dating has revealed the presence of a previously unknown basement beneath the rocks exposed at the surface. The significance of this basement will be assessed especially during interpretation of the seismic surveying.

More dating by this technique will be carried out where such work can be justified in terms of the project's purpose. Priority will be accorded to dating that can constrain the timing of poorly dated tectonic events and which can improve the geochronological timescale through ascertaining the duration of key fossil zones.

3. New Aeromagnetic Data Acquisition and Interpretation

New aeromagnetic data, mostly at 500m line spacing, will be collected over up to four areas: the northeast, northwest, west and south (Attachment 5). The coverage will extend from the onshore areas to the continental shelf. This will provide geological correlations between areas covered by shallow water and help to position marine seismic reflection profiles (see below). The outputs of this sub-project will be new airborne magnetic maps and images, each with an interpretation. Fieldwork is scheduled for the second half of 1994.

4. Three Dimensional Control of Models of the Tasmanian Crust

Estimates exist for the thickness of the crust for many of Tasmania's tectonic elements but they need to be confirmed. The internal structure of the various tectonic elements and the nature of the boundaries between them are poorly known at depth. The main outcomes of this sub-project will be well constrained 3-D models of the Tasmanian crust and key structures.

This is to be achieved through the acquisition and interpretation of new seismic reflection profiles and gravity surveys along these traverses. The marine seismic profiles will be shot along the northern, western and southern margins.

Prior to the marine surveying, an array of refraction recorders.will be established across Tasmania to acquire data for an experimental tomographic and 4-D modelling study by the Australian Geodynamics Cooperative Research Centre.

Onshore, seismic surveying will be undertaken in the Dundas Trough, across the Arthur Lineament and across another lineament that may have significance for gold mineralisation in the northeast. Experimental recording to determine the thickness of the Tasmania Basin will also be attempted.

Weather conditions will be a substantial limiting factor so fieldwork is scheduled for summer and early autumn of 1995. Data processing will begin when fieldwork is complete. Preliminary sections will be available about six months after fieldwork and final sections a further six months later.

5. Tectonic Synthesis of Tasmania

The tectonic synthesis sub-project will effectively take over where the first sub-project finishes. It will take the tectonics elements map and test it with the results of geophysical interpretations. A final version of the proposed new 1:500,000-scale stratotectonic map will then be produced with cross sections incorporating the results of seismic interpretation.

6. Reviews

It is planned to carry out some additional review work of existing information to provide impartial and dispassionate constraints (or the elimination of existing constraints) as baseline information for taking into account when the results of the new geophysical work are being interpreted.

Such summary reviews will be available in draft form in readiness for the interpretation of the seismic data and are currently planned as follows:

- the degree of biogeographic provincialism (if any) in Tasmania's palaeontological record
- geochemical characteristics of Tasmania's mafic and ultramafic rocks, their degree of similarity to others in the Tasman Fold Belt System and the "affinities" of such compositions
- geochemical characteristics of Tasmania's calc-alkaline rocks and a comparison with that in other parts of the Tasman Fold Belt System and the southwest Pacific islands
- an historical review of models proposed for the tectonic evolution of Tasmania and the tectonic significance of structures if known
- a summary of the distribution, mineralogy, intensity and geochemistry of hydrothermal alteration
- a summary of any potential petroleum habitat information.

Where the expertise or knowledge required in these undertaking resides outside of AGSO and MRT, scientists from other organisations will be invited to collaborate.

7. Mineral Systems of Tasmania

Key information revealed from the interpretation of new geophysical surveys will be combined with information compiled from the relevant reviews above to define and characterise Tasmania's mineral systems. Emphasis will be placed on depth characteristics and any areas outside the main prospectivity zones found to be suitable for exploration. This information will be available towards the end of the project.

8. Petroleum Systems of Tasmania

The Larapintine, Gondwanan and Austral Petroleum Systems (defined by Marita Bradshaw, AGSO, *PESA Journal* 21, p. 43-53, 1993) are all present in Tasmania. Information acquired during the project will be added to existing knowledge to provide more information about each system and their potential in and around Tasmania. The outcome of this study will also be available towards the end of the project.

PARTICIPATING ORGANISATIONS

A list of the organisations and the nature of their possible involvements is outlined below to give an impression of the extent of collaboration being proposed. It is emphasised that talks and negotiations are either still at an early stage or have not yet been undertaken in some instances.

AGSO

- project coordination
- geochronology
- airborne geophysics and interpretation
- land seismic and gravity surveying, and interpretation
- marine seismic and gravity surveying, and interpretation
- review studies, geological syntheses and map compilation.

MRT

- geological synthesis, map compilation and review studies
- magnetic, gravity and seismic interpretations
- databases.

Australian Geodynamics Cooperative Research Centre

- Tomography
- 4-D Modelling (technological aspects; to be confirmed).

Centre for Ore Deposit and Exploration Studies (CODES)

- ore deposit modelling and ore environment geochemistry (to be jointly discussed and confirmed)

University of Tasmania and other Universities

- contributions of first-hand knowledge and information on tectonics, gravity, mineral deposits, maturation, heat flow and other disciplines deemed to be relevant (to be discussed and confirmed).

Companies

- the project hopes that exploration companies will make contributions to the work plan. CRA, RGC, Pasminco and Aberfoyle are known to be currently active in Tasmania.

FURTHER PROJECT INFORMATION

Dr Tony Brown
State Chief Geologist
Mineral Resources Tasmania
P O Box 56
ROSNY PARK, TAS., 7018

Telephone: (002) 338 365
Fax: (002) 338 338.

Mr A N (Tony) Yeates
Project Coordinator
Australian Geological Survey Organisation
GPO Box 378
CANBERRA ACT 2601

Telephone: (06) 249 9335
Fax: (06) 249 9983.

ATTACHMENT 1: Series Geological Mapping Coverage of Tasmania

(a) 1: 250,000 Scale (There is complete Coverage)

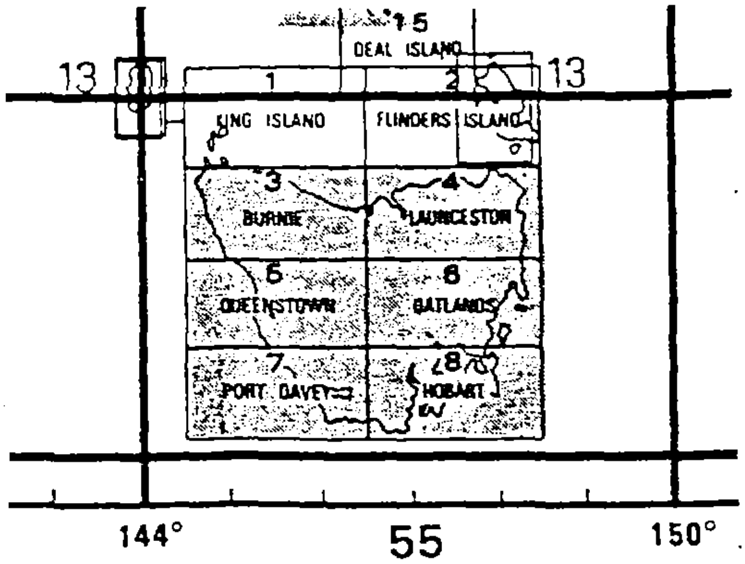

(b) 1: 50,000 Scale Coverage

5 cm

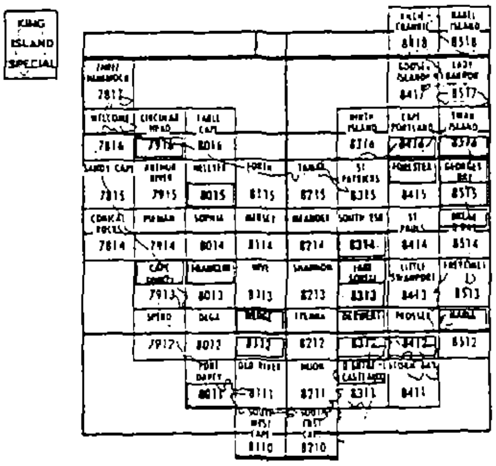

Blue Tier	8515-I,IV	Pedder	8112-II,III
Boobyalla	8416-II,III	Ringarooma	8415-I,IV
Brighton	8312-I,IV	Saint Helens	8515-II,III
Davey	8011-II,III	Saint Marys	8514-I,IV
Eddystone	8516-II,III	Saint Valentines	8015-II,III
Hobart	8312-II,III	Smithton	7916-II,III
Huntley	8112-I,IV	Sorell	8412-II,III
Kingsborough	8311-I,IV	Strahan	7913-I,IV
Lake Mary	8314-II,III		
Lake Sorell	8313-I,IV		
Lyell	8013-I,IV		
Maria	8512-I,IV		
Oatlands	8313-II,III		

Note: Several areas are also covered by non-serial Special Maps (e.g. Mt. Read Volcanics 1: 100,000 Scale; Corbett et al., 1988).

ATTACHMENT 2: Chronology of Lithogenesis, Events and Mineralisation in Tasmania (Collins & Williams, 1986).

Age	Sedimentation and volcanic activity	Tectonic and igneous activity	Mineralization
Quaternary	Fluvial and coastal deposits Widespread glaciation		
	------------------ Erosion ------------------		
Tertiary	Shallow-marine sand Basalt lava flows Terrestrial clay, sand, gravel		Alluvial Sn, Au, Os-Ir; Chromite, lateritic Ni
Cretaceous	------------------ Erosion ------------------	Formation of troughs and separation of Australia and Antarctica Syenite intrusion (SE Tasm.)	Au in syenite
Jurassic		Epeirogenic deformation Intrusion of dolerite	
Triassic	Terrestrial sandstone, coal measures		
Permian	Shallow glacio-marine mudstone, sandstone, minor oil-shale, terrestrial coal measures Widespread glaciation (tillite)		Sn in "fossil" placers
Carboniferous		Lateral movement along Tamar fracture system	
Devonian	Local cave deposits in Gordon Limestone *NE Tasm.* *Dacitic ignimbrite, intra-caldera sheet*	Granitoid intrusions (high level, mainly S-type) *NE Tasm.* *Granitoid intrusions (S and I-type, minor alkali feldspar granite)*	Granitoid-related mineralization Sn greisen (*Anchor*); Sn, W vein (*Aberfoyle, Storeys Ck*, Oakleigh Ck, Interview R.); W skarn (King Is., Kara); Sn carbonate-replacement (Renison, Cleveland, Mt. Bischoff); Ag—Pb—Zn vein (Zeehan, Mt. Farrell, Magnet); Au reef (Beaconsfield, *Lefroy, Mathinna*)
	----------------- Unconformity -----------------	OROGENY (correlated with Tabberabberan	
Silurian	Shallow marine quartz sandstone, mudstone, minor limestone *Deep marine turbidite quartzwacke, mudstone*		
Ordovician	Shallow marine limestone (Gordon Limestone) Shallow marine and terrestrial quartz sandstone, conglomerate *Mudstone, minor turbidite quartzwacke* = = = ? = = = ? = = =	Thermal event	Stratabound veined and disseminated Pb—Zn sulphides (Zeehan) in Gordon Limestone
Cambrian	Local turbidite quartzwacke and volcanic-volcaniclastic sequences	Local deformation associated with emergence of Tyennan geanticline	
	-- Unconformity ---		
	Mudstone, turbidite lithic-wacke, chert conglomerate (Dundas Group) Rhyolitic—andesitic, subaerial—subaqueous volcanics and volcaniclastics (Mt. Read Volcanics)	Subvolcanic granitoids and porphyritic intrusions in Mt. Read Volcanics	Volcanogenic massive sulphide deposit Disseminated Cu—Ag—Au (Mt. Ly massive, bedded Zn—Pb—Cu—Ag— (Rosebery, Hercules, Que River, Hellyer) in Mt. Read Volcanics
	--------- Erosion --------- = = = ? = = ? = = =	Local erosion Emplacement of mafic—ultramafic masses during mild compression	Os—Ir, Ni sulphides, Cr in serpentinize ultramafics; Cu—Ni sulphides in gabl (Cuni)
	Deeper marine mudstone, turbidite lithic-wacke, basaltic volcanics, chert, limestone (Crimson Creek Formation)		Cu in basalt
Eocambrian	Shallow-marine quartz sandstone, dolomite	Development of narrow depositional troughs during tension	
--------------	----------------Unconformity----------------	--------------- Structural hiatus ---------------	
Late Proterozoic		PENGUIN OROGENY — local metamorphism (Arthur Lineament), granitoid intrusion (S-type, King Is.)	
	Turbidite quartzwacke, mudstone, minor basaltic volcanics, dolomite—magnesite (Burnie, Oonah Formations) Shallow-marine quartz sandstone, mudstone (Rocky Cape Group)	Dolerite intrusion, mafic—ultramafic emplacement	Volcanogenic massive magnetite—pyrite — associated with basaltic volcanism (Savage River)
		-------- Structural/metamorphic hiatus -------- FRENCHMAN OROGENY	
	Metamorphosed successions derived from shallow-marine quartz sandstone, mudstone (Tyennan region)	Mafic intrusions (now amphibolite), eclogite	

Pre-Carboniferous data for western Tasmania is shown in normal type and for northeast Tasmania in italics.

ATTACHMENT 3: Tectonic Elements (Corbett & Turner, 1989).

AMG
332000E,
5460000N

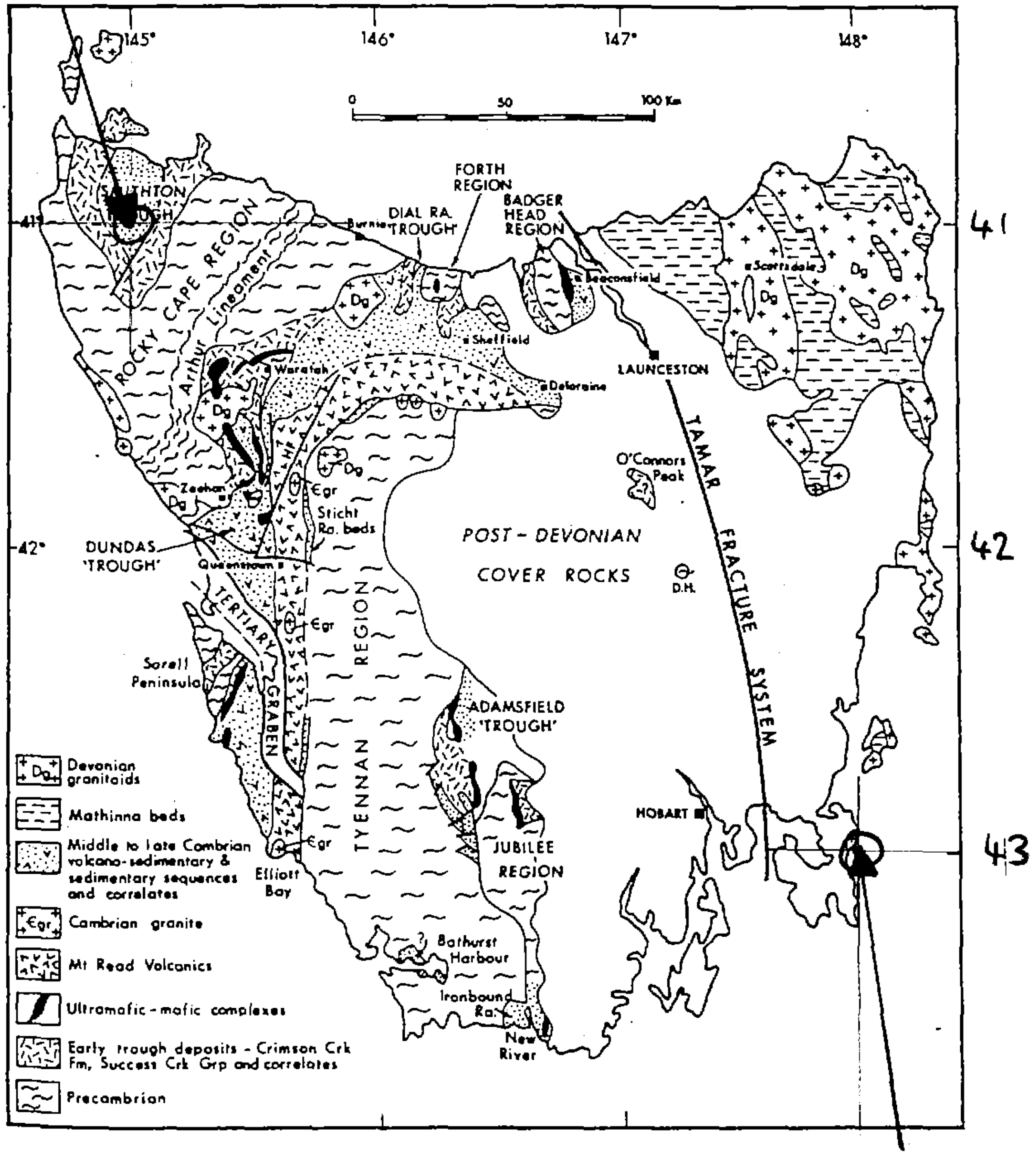

AMG
581500E,
5238500N

5 cm

AMG REFERENCE POINTS ADDED

ATTACHMENT 4: Major Mineral Belts in Tasmania and their Ages (ABARE: National Agricultural and Resources Outlook Conference 1992).

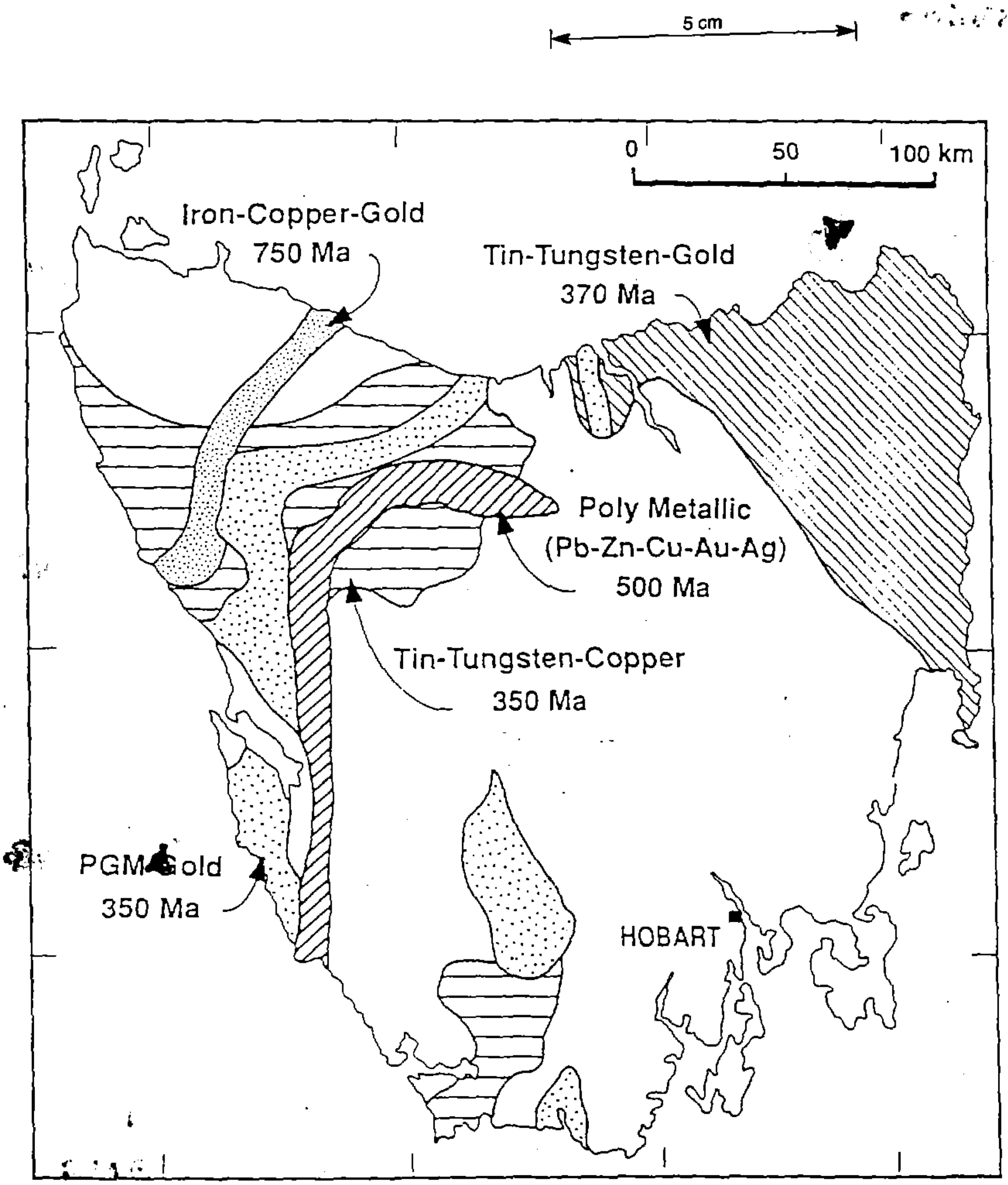

859019

ATTACHMENT 5: Locations of Indicative Aeromagnetic Surveying; Areas are ranked in order of priority. Note: Areas 1, 2 and 3 have now been joined.

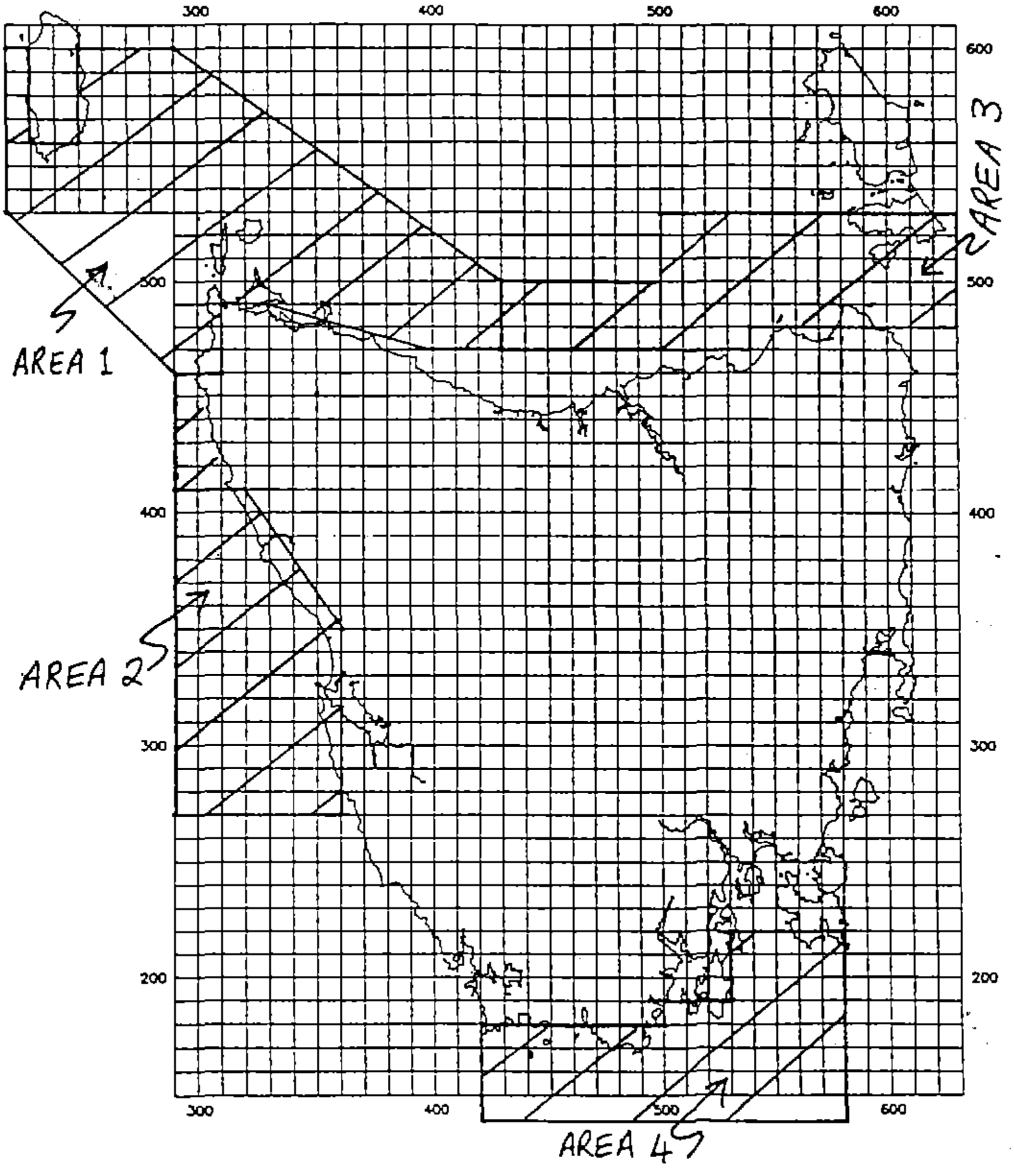

AREA 1: to survey relationship of Smithton Trough and Arthur Lineament to Precambrian Blocks

AREA 2: to survey the contacts of the Arthur Lineament and Dundas Troughs where they abut Precambrian Blocks.

AREA 3: to survey the east and west Matthina Beds contact and two contrasting regions of granitoids and the "Tamar Lineament".

AREA 4: to survey a possible basement disjunction beneath the Tasmania Basin and obtain an estimate of the basin's thickness.

ATTACHMENT 6: Locations of Indicative, Logistically Feasible Seismic Traverses to Examine the Internal Structure of Tectonic Elements and the Relationships Between Elements at Depth (Base Map after Corbett & Turner, 1989).

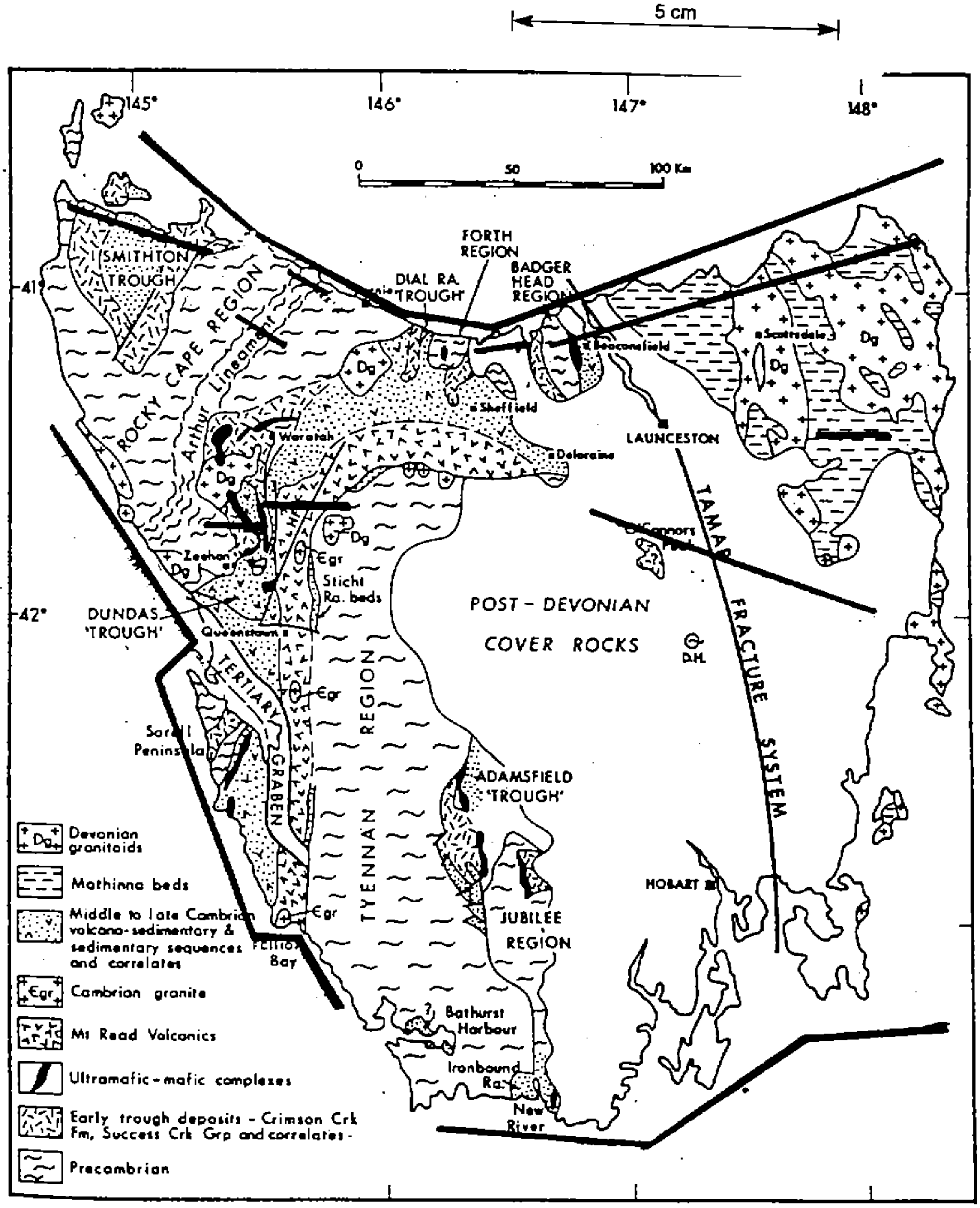

▬ logistically feasible seismic traverse

Three new National Geoscience Mapping Accord projects

Tasmanian onshore studies to be supported by RV *Rig Seismic*

AGSO and Mineral Resources Tasmania (MRT) joined forces in July to initiate a three-year NGMA project in Tasmania. The main objectives of this project are to characterise the large-scale geological structure of the island; to provide a three-dimensional framework that will support existing detailed geological maps; and to determine how mineral and petroleum systems fit into this framework. By helping to constrain models of the State's geological evolution, this framework will make an invaluable contribution to the development of improved minerals and petroleum exploration strategies.

The project will augment MRT's detailed geological mapping. It will reveal the size, shape, distribution, and internal structure of the tectonic elements of Tasmania, and ascertain if there is a relationship between known mineral deposits and the major structural elements. Eventually it will attempt to determine the fluid-flow paths of the mineral systems, and construct new exploration models.

The project will collate all geological and geophysical data; undertake new geochronological studies; acquire new airborne magnetic data around the margins of Tasmania, and seismic reflection profiles around the island; carry out a refraction/tomographic experiment to define the structure of the lower crust; and record seismic reflection profiles onshore across tectonic element boundaries in order to determine the nature of those boundaries. All the data collection will take place within the first year of the project (1994–95). Owing to the ruggedness of the terrain, and the difficulty and expense of shooting seismic profiles onshore, AGSO will deploy RV *Rig Seismic* to generate profiles around the island. Thus a ship will be used for the first time to support the NGMA.

Further information about the project can be obtained from Tony Yeates, *Project Coordinator, AGSO (tel. (06)2499335, fax (06)2499983)*, or Tony Brown, MRT Chief Geologist (tel. (002)338365, fax (002)442117).

Northern Australian basins resource analysis to focus on petroleum and mineral systems

AGSO, the Northern Territory Geological Survey (NTGS), and the Geological Survey of Queensland (GSQ) are about to embark on a new NGMA project — 'northern Australian basins resource analysis'. This project will focus on the regional structure and stratigraphic framework that define the dimensions, character, timing, and distribution of the major petroleum and mineral systems operating in northern Australia — between the Victoria River Basin and the Mount Isa basin. Its outcome will help to influence the future economic development of this region, by promoting more efficient and cost-effective exploration.

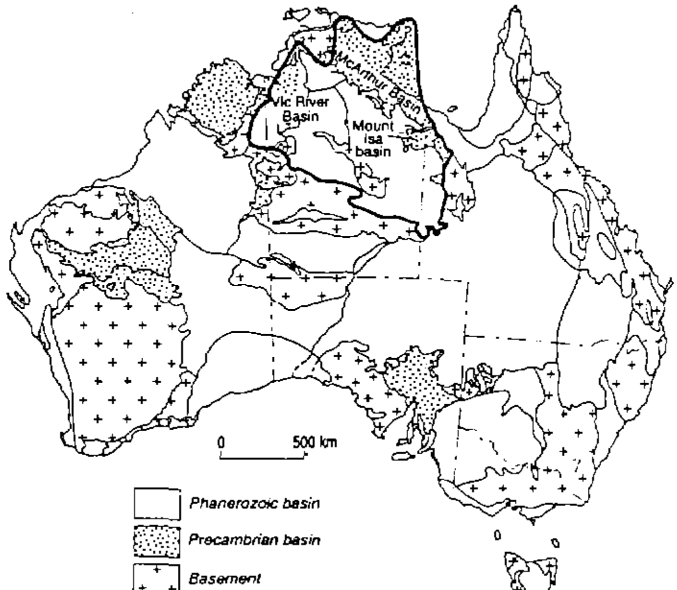

Study area (circumscribed by heavy line) of the 'northern Australian basins resource analysis'.

The project, in partnership with the minerals and petroleum industries and geoscience researchers, will consist of four phases of parallel activities. Phase I will concentrate on the nature of the basement under northern Australia. Phase II will focus on the stratigraphic framework of the Mesoproterozoic of the northern Australian basins. Phase III will map the distribution and character of key play elements in the region, and phase IV will map the extent and character of petroleum and mineral systems. The emphasis initially will be on phases I and II.

Activities during the first year (1994–95) will include interpreting gravity and magnetic data; mapping basement characteristics; compiling events that have impacted on the evolution of the basement and overlying basins; re-evaluating and synthesising regional outcrop data and recently published NTGS 1:250 000 geological maps; and re-evaluating parts of the structure and stratigraphy of Mount Isa and the MacArthur Basin with the help of petroleum-industry subsurface data. These activities will identify both gaps in the coverage and uncertainties in the region's evolution that activities during the second year and beyond will attempt to resolve.

Contacts for further information are: Peter Southgate, AGSO (tel. (06)2499206, fax (06)2499983); Barry Pietsch, NTGS (tel. (089)895214, fax (089)814806); and Peter Green, GSQ (tel. (07)2371414, fax (07)2354074).

Pilbara mapping sighted on promoting base- and precious-metal exploration

A new project agreed to between AGSO and the Geological Survey of Western Australia began in July 1994. It involves mapping fifteen 1:100 000 Sheet areas covering granite–greenstone terrane in the Pilbara Craton in northwestern Western Australia over a period of three years.

Work has begun in the west Pilbara, where first-edition 1:250 000 geological maps are recognised as being out of date. Thereafter, it will be extended to the eastern Pilbara Craton, where it will focus on key areas — specifically on resolving a number of problems that have been recognised since the last comprehensive review of the geology undertaken in the mid-1970s.

The work will be directly relevant to exploration for stratabound base-metal deposits currently taking place in the greenstone sequences, and should attract new interest in the multitude of other minerals known in the region — including gold, nickel, tin, tantalum, iron ore, and platinum. Apart from its economic interest, the craton is recognised as containing some of the best exposed granite–greenstone sequences in the world, and the mapping is expected to throw further light on the evolution of the early crust.

Contacts for further information are: Lynton Jaques, Chief, AGSO Division of Regional Geology & Minerals (tel. (06)2499745, fax (06)2499983); and Peter Dunn, Assistant Director, GSWA Precambrian Geology & Mineral Resources Branch (tel. (09)2223172, fax (09)2223633).

AGSO Journal 15(2) published

AGSO recently released the latest number of the *AGSO Journal of Australian Geology & Geophysics* — volume 15, number 2 — which contains the following papers:

- Diagenesis of Jurassic and Lower Cretaceous sandstones of the Eromanga Basin in New South Wales; F. He & P.J. Conaghan; pp. 191–215.
- Mapping ^{137}Cs at Maralinga nuclear test site, South Australia, using conventional 4-channel airborne gamma-ray spectrometry; B.R.S. Minty & R.C. Brodie; pp. 217–222.
- The Great Cumbung Swamp — terminus of the low-gradient Lachlan River, eastern Australia; P.E. O'Brien & R.V. Burne; pp. 223–233.
- A new structure in pollen assigned to *Sriatopodocarpites* Sedova 1956 and *Protohaploxypinus* Samoilovich emend: Morbey 1975 from the Late Permian (Tatarian) of the Russian Platform; C.B. Foster & A.V. Gomankov; pp. 235–238.
- First record of Tethyan palynomorphs from the Late Triassic of East Antarctica; C.B. Foster, B.E. Balme, & R. Helby; 235–238.
- Early Silurian (Llandovery) conodonts from the Barbwire Terrace, Canning Basin, Western Australia; R.S. Nicoll, K.K. Romine, & S.T. Watson; pp. 247–255.

This issue of the *AGSO Journal* costs $40 + postage and handling charges of $5 (in Australia) or $15 (overseas). The *AGSO Journal* is available by subscription at a cost of $80 to individuals or $120 to corporations for four quarterly numbers.

859022

Monday, August 22, 1994

$3m new lode of mining knowhow

By MARY ROSE

A JOINT federal-state geological survey would provide an explosion of new information for use in the search for minerals and petroleum in Tasmania, Premier Ray Groom said yesterday.

The $3 million, three-year program was jointly announced by state Mines Minister Mr Groom in Hobart and federal Resources and Energy Minister David Beddall in Canberra.

The federal and state governments will share the cost of the National Geoscience Mapping Accord, under which seismic shock waves will be used to map the deeper levels of the earth's crust under Tasmania.

It is expected to allow better identification of the structures controlling the location of mineral and petroleum deposits.

Mr Groom said the state would provide $400,000 to $500,000, mostly in kind, for the project.

About $150,000 in support had been allowed for this financial year, he said.

He and Mr Beddall said results from the NGMA project were expected to boost exploration and investment in Tasmania.

Research teams from Tasmania Development Resources and the Australian Geological Survey Organisation would collaborate to study structures at depths to 40 kilometres, Mr Groom said.

The managing geologist for TDR's Mineral Resources Tasmania, Geoff Green, said Tasmania had been trying to have such a study done for 20 years.

Ray Groom: seismic shock waves will be used to map the deeper levels of earth's crust.

But the wait probably was worth it because of the improvement of technology and ideas of geology in that time, Dr Green said.

"This is big-picture stuff," he said.

TDR geological maps will be used as a starting point for research into the size, shape, distribution and internal structure of Tasmania's geological features.

"Tasmania is naturally endowed with world-class deposits of copper, zinc, tin, silver and gold and rich supplies of tungsten and iron and possibly valuable petroleum reserves," Mr Groom said.

"A better understanding of Tasmania's geology will help the State Government attract investment in Tasmania's mineralised belts, particularly areas offshore which may contain oil but have so far been poorly explored."

As well as seismic studies, Mr Beddall said the project would involve flying aeromagnetic surveys over Tasmania's coasts to define potential petroleum-bearing areas.

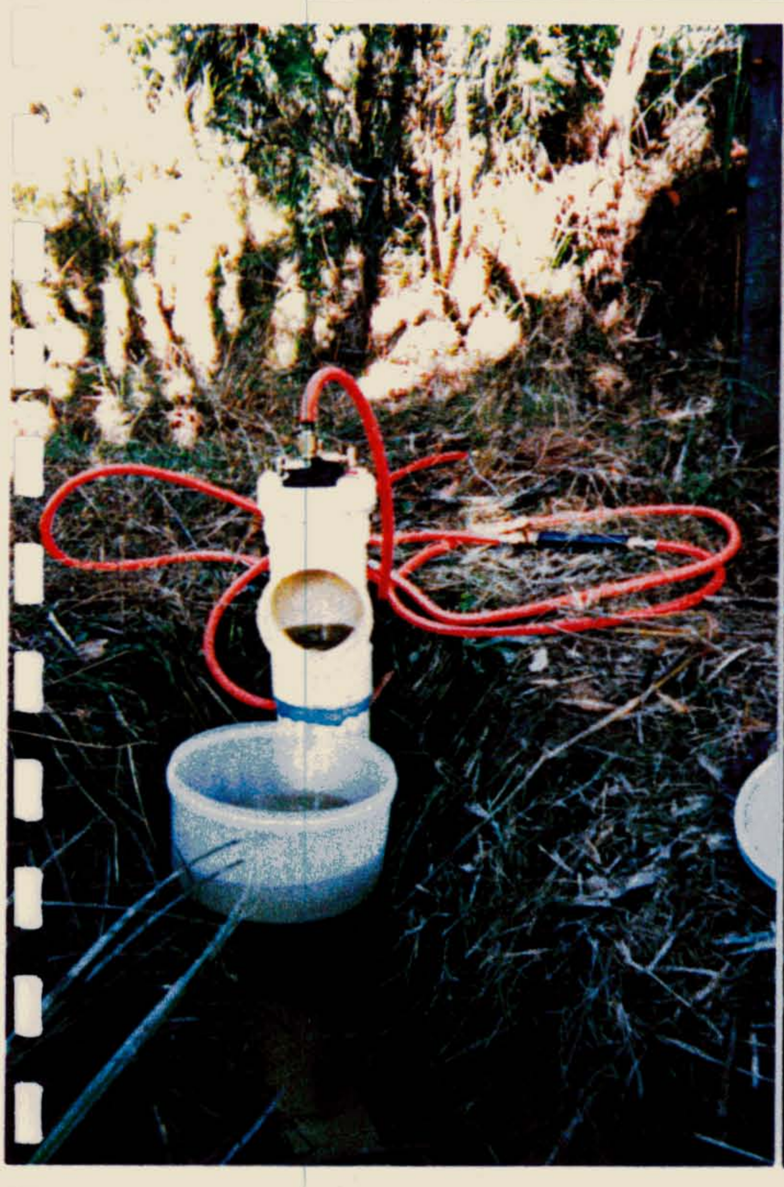

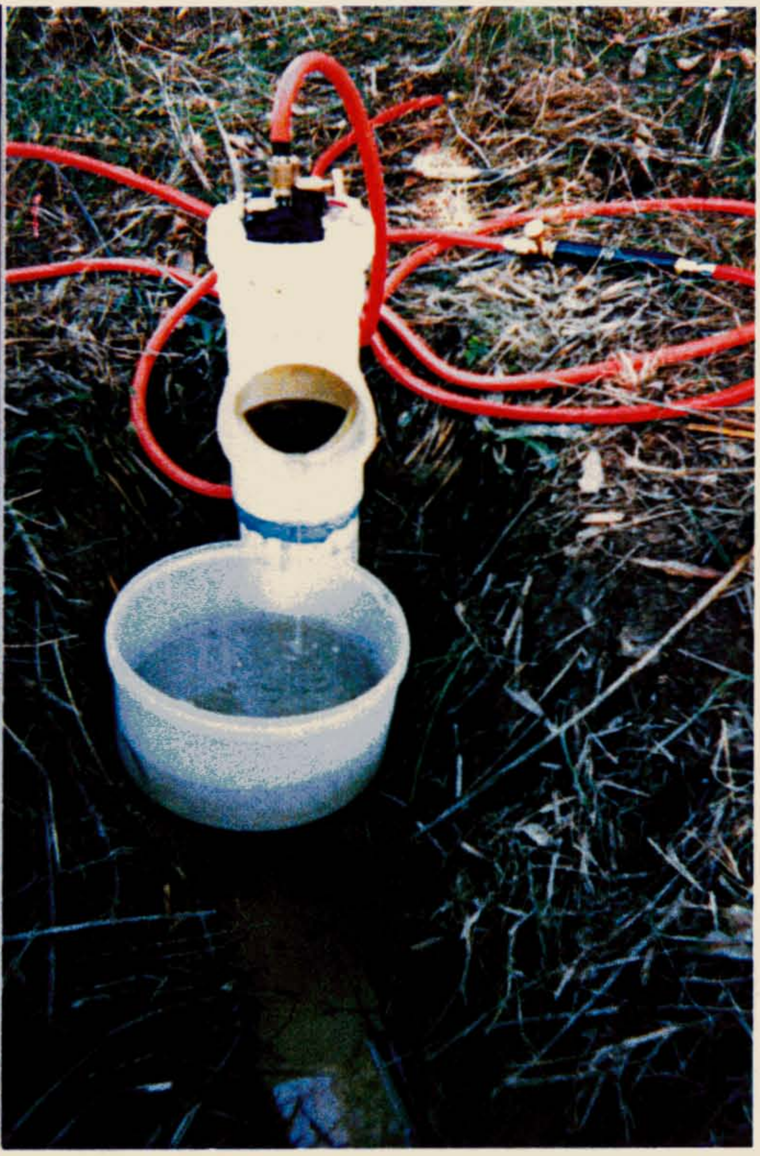

859023

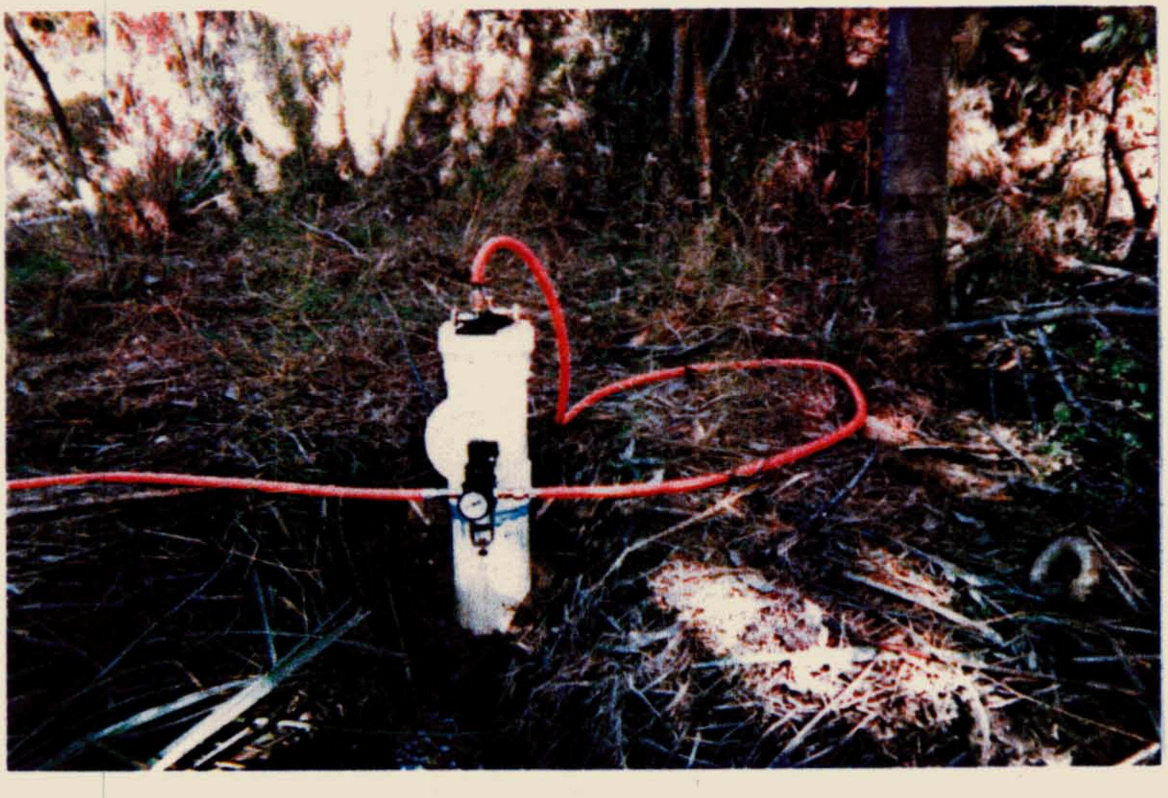

859024

Revised version 21-01-94 for *Geochimica et Cosmochimica Acta*

Final Top copy less Fig 4 [illegible]
Fig 5-10 - [illegible]

Hydrocarbon biomarkers, thermal maturity and depositional setting of tasmanite oil shales from Tasmania, Australia.

A. T. REVILL[1], J. K. VOLKMAN[1], T. O'LEARY[1], R. E. SUMMONS[2],
C. J. BOREHAM[2], M. R. BANKS[3] and K. DENWER[3,4]

[1] CSIRO Division of Oceanography, GPO Box 1538, Hobart, Tasmania 7001, Australia

[2] Australian Geological Survey Organisation, GPO Box 378, Canberra, ACT 2601, Australia

[3] Geology Department, University of Tasmania, GPO Box 252C, Hobart, Tasmania 7001, Australia

[4] Present address: RGC Exploration, PO Box 1166, Milton, Queensland 4064

Abstract- This study represents the first geological and organic geochemical investigation of samples of tasmanite oil shale representing different thermal maturities from three separate locations in Tasmania, Australia. The most abundant aliphatic hydrocarbon in the immature oil shale from Latrobe is a C_{19} tricyclic alkane, whereas in the more mature samples from Oonah and Douglas River low molecular weight *n*-alkanes dominate the extractable hydrocarbon distribution. The aromatic hydrocarbons are predominantly derivatives of tricyclic compounds, with 1,2,8-trimethylphenanthrene increasing in relative abundance with increasing maturity. Geological and geochemical evidence suggests that the sediments were deposited in a marine environment of high latitude with associated cold waters and seasonal sea-ice. It is proposed that the organism contributing the bulk of the kerogen, *Tasmanites*, occupied an environmental niche similar to that of modern sea-ice diatoms and that bloom conditions coupled with physical isolation from atmospheric CO_2 led to the distinctive "isotopically heavy" $\delta^{13}C$ values (-13.5 ‰ to -11.7 ‰) for the kerogen. $\delta^{13}C$-data from modern sea-ice diatoms (-7‰) supports this hypothesis. Isotopic analysis of *n*-alkanes in the bitumen (-13.5 ‰ to -31 ‰) suggest a multiple source from bacteria and algae. On the other hand, the *n*-alkanes generated from closed-system pyrolysis of the kerogen (-15 ‰) are mainly derived from the preserved *Tasmanites* biopolymer algaenan. The tricyclic compounds (mean -8 ‰) both in the bitumen and pyrolysate, have a common precursor. They are consistently enriched in ^{13}C compared with the kerogen and probably have a different source from the *n*-alkanes. The identification of a location where the maturity of the tasmanite oil shale approaches the "oil window" raises the possibility that it may be a viable petroleum source rock.

The only lithological distinction between the oil shale and surrounding mudstone is that the former contains abundant algal remains. These are dominated by the unicellular alga *Tasmanites punctatus* Newton (1875) whose biological affinities have been suggested to lie with the extant green alga *Pachysphaera pelagica* Ostenfeld (1899) (WALL, 1962). Initially, the tasmanite was thought to have been deposited in an extensive lake (MILLIGAN, 1852), but the discovery of marine fossils (GOULD, 1861) precluded this. Recent work has suggested a nearshore marine origin (BANKS, 1962; CALVER et al., 1984) with the oil shale representing a period of algal blooms (CALVER et al., 1984; CLARKE, 1989). This hypothesis is further supported by comparison of the known occurrence of tasmanite with the inferred palaeogeography of Tasmania during the early Tamarian (BANKS and CLARKE, 1987; Fig. 3).

There has been much discussion about the correct nomenclature for the abundant microfossils found in the tasmanite (see WALL, 1962). The term spore has been used (SIMONEIT and BURLINGAME, 1973) while studies of some modern prasinophycean genera (*Pachysphaera, Halosphaera and Pterosperma*) have shown that the asexual reproductive cycle consists of a phycoma (cyst) and a motile stage (PARKE and HARTOG-ADAMS, 1965; PARKE, 1966; PARKE et al., 1978). GUY-OHLSON (1988) identified various developmental stages of *Tasmanites* in the Jurassic of Sweden and concluded that the fossil cysts were phycomata. Recent studies (BOALCH and GUY-OHLSON, 1992; GUY-OHLSON and BOALCH, 1992) have indicated that the morphology of fossil *Tasmanites* are sufficiently close to some rarely found living specimens of *Pachysphaera* that the genus *Tasmanites* suffices for both. TAPPAN (1980) indicates that the term phycoma describes the non-motile stage specific to prasinophytes and therefore, to use this description would indicate an acceptance that *Tasmanites punctatus*, found in Tasmanian tasmanite, is the equivalent of a modern prasinophyte. To avoid any taxonomic inference, the abundant microfossils in these samples will be referred to as *Tasmanites* or simply fossils. Although known to range from the Cambrian (540 Ma)

INTRODUCTION

The oil prospectivity of onshore Tasmania has long been problematical. Interest in the possibility of finding oil has been stimulated by repeated reports of bitumen strandings on western and southern beaches since the late 19th century (TWELVETREES, 1917). This interest has continued, despite the fact that these coastal bitumens are now thought to arise from Mesozoic or Cainozoic offshore sediments that are poorly represented onshore (VOLKMAN et al., 1992). There have been, however, numerous reports over the last century of oil-seeps onshore (BENDALL et al., 1991) suggesting the possibility that older onshore rocks may also be a source of petroleum. Central to much of this interest has been the organic-rich tasmanite oil shale (subsequently referred to simply as "tasmanite" or "oil shale") which occurs particularly in the north-west of the state (Fig. 1). JAMES et al. (1932) reported that the oil shale was retorted to liberate hydrocarbons as early as 1910, and this carried on until the 1930's, producing about 1.13 megalitres of shale oil.

The tasmanite occurs as a distinctive band low in the Quamby Mudstone. The stratigraphy of Late Palaeozoic sediments in Tasmania has been the centre of much research interest (see CLARKE and FARMER, 1976; CLARKE, 1989) due to the difficulty of applying the (warm water based) internationally accepted biostratigraphic divisions to the cold water environment of Tasmania at this time. Because of this difficulty, the more appropriate Rekunian Series has been proposed (CLARKE and BANKS, 1975; CLARKE and FARMER, 1976) with a sub-division, the Tamarian stage, within which is the Quamby Mudstone (Fig. 2). That part of the Quamby Mudstone containing the oil shale has consistently yielded stage 2 microfloras (TRUSWELL, 1978) and a Faunal Zone 1 macrofauna (Fig. 2; CLARKE and BANKS, 1975). The age has been given as either Early Permian (FOSTER and WATERHOUSE, 1988) or Late Carboniferous (CLARKE, 1992) [i.e. a little older or a little younger than 290 my BP, taken as the age of the beginning of the Permian by HARLAND et al. (1990)].

to present, *Tasmanites* and related forms occur in high concentrations only in the tasmanite deposits of Tasmania (Permian) and Alaska (Jurassic) with other less abundant occurrences in the Sahara and Brazil (AQUINO NETO et al., 1992).

The fossils were spheroidal, but become disc shaped with sediment compaction, ranging in size from <0.1 mm to >0.6 mm in diameter. The wall of the fossil is formed of two to three layers, with the outer layer rarely preserved. The middle layer forms the bulk of the wall, the inner layer being thin and fibrous (KANTSLER, 1980).

The algal origin for the tasmanite and its organic richness has led to a wide range of geochemical studies of the kerogen. Data have been presented on carboxylic acids (BURLINGAME et al., 1969; SIMONEIT and BURLINGAME, 1973), and more recently the hydrocarbon content (PHILP et al., 1982; AZEVEDO et al., 1990; SIMONEIT et al., 1990; AZEVEDO et al., 1992). These studies have identified novel aliphatic and aromatic compounds, but all have been based on samples from the one site at Latrobe (Fig. 1), where the oil shale is relatively immature. In this paper we report a comprehensive organic geochemical study of the tasmanite oil shale, including a comparison of immature and mature samples from different locations in Tasmania.

EXPERIMENTAL

Samples

Samples were collected from rock outcrops at Oonah, Latrobe in the Mersey Valley and from a core taken at Douglas River (Fig. 1; for stratigraphy see Fig. 2). The rock sample from Latrobe shared many of the characteristics of that from Oonah, except that it came from a continuous 1.8 m seam, 21.4 m above the basal conglomerate within the Spreyton beds (Fig. 2). A spore concentrate was obtained from a sample collected at Oonah by density separation of the fossils from the crushed rock using ferric chloride.

Extraction

Total solvent-extractable compounds were obtained by sonication of the crushed rock samples (*ca.* 50 g) with chloroform/methanol (2:1, 3 x 50 ml). The composition of a portion of the total extracts was determined either by gravimetry after fractionation or by Iatroscan thin-layer chromatography-flame ionisation detection, using hexane as the developing solvent (VOLKMAN et al., 1986). Saturated and aromatic hydrocarbons were isolated by applying 30 mg of extract to a glass column containing 3 g of silicic acid (100-200 mesh) capped with 1 g of activated alumina (BDH). Aliphatic hydrocarbons were eluted with hexane (20 ml) and a second fraction containing aromatic hydrocarbons was obtained by eluting with hexane:toluene (1:1; 20 ml). Resins and ashphaltenes were eluted with chloroform (20 ml) and methanol (10 ml).

Analyses

Hydrocarbon fractions were analysed by capillary gas chromatography on a 50 m non-polar methyl silicone fused silica capillary column (HP-1, 0.32 mm i.d., 0.25 μm film) with on-column injection and hydrogen as the carrier gas. The temperature program was 45 °C for 1 minute, followed by a ramp to 120 °C at 30 °C min^{-1} then a ramp to 310 °C at 4 °C min^{-1}. The oven was then maintained isothermally for 15 min.

Biomarker information was obtained by gas chromatography-quadrupole mass spectrometry (Hewlett Packard 5790 MSD with HP 5890 GC and 59970A computer workstation) in selected ion monitoring (SIM) mode. Typical conditions were: electron multiplier 2200 V, transfer line 310 °C, electron impact energy 70 eV. GC conditions were as above except that helium was used as carrier gas. Samples were also analysed using metastable reaction monitoring GC-MS using a VG 70E instrument fitted with an HP 5790 GC and controlled by a VG 11-250 data system. The GC was equipped with a HP

Ultra-1 capillary column (50 m x 0.2 mm i.d.) connected to a OCI-3 cooled on-column injector (SGE) with a retention gap of uncoated fused silica (0.5 m x 0.33 mm i.d.). The oven was programmed from 50 °C to 150 °C at 10 °C min^{-1} and then to 300 °C at 3 °C min^{-1} with a final hold time of 30 min. The carrier gas was hydrogen with a linear flow of 30 cm s^{-1}. The mass spectrometer was operated with a source temperature of 240 °C , ionisation energy of 70 eV and interface and re-entrant at 310 °C. In full scan mode the MS was operated from *m/z* 650 to *m/z* 50 at 1.8 s per decade and an inter-scan delay of 0.2 s. In MRM mode, the magnet current and ESA voltage were switched to sequentially sample 26 selected parent-daughter pairs. The sampling time was 40 ms per reaction with a 10 ms delay giving a total cycle time of 1.3 s.

Gas chromatography-isotope ratio mass spectrometry (GC-IRMS) was carried out as described by HAYES et al. (1990) using a Finnigan-MAT 252 isotope ratio mass spectrometer linked to a Varian 3400 GC via a cupric oxide combustion furnace operated at 900 °C. Isotopic calibration was made using an external primary CO_2 standard introduced via a sample bellows and change-over valve and checked using deuterium labelled *n*-alkanes as internal standards. The latter, in hexane, were co-injected with the sample onto a J&W DB-5 capillary column (30 m x 0.25 mm i.d.) using a Varian SPI injector. The oven was programmed from 50 - 300 °C at 6 °C min^{-1}.

Closed-system Pyrolysis

Kerogen was isolated from the tasmanite shale by standard acid digestion techniques, and pyrolysed in evacuated quartz tubes for 72 hours at 300 °C, 330 °C and 350 °C, in the presence of water. Only liquid products were isolated and these were treated in the same way as other extracts. Rock-Eval derived kinetic parameters on whole rock samples of Latrobe tasmanite (AGSO #1995) were determined by Daniel Jarvie, Humble Instruments, Humble, Texas.

RESULTS AND DISCUSSION

Geological Setting of the Tasmanite Oil Shale

The tasmanite at Oonah consists of two seams, separated by up to 6.7 metres of siltstone. The lower and upper seams contain two and three *Tasmanites*-rich beds respectively. These beds consist of a multiplicity of lenses, each up to about a millimetre thick and a few centimetres long, separated by silt layers. The beds generally show a gradually increasing concentration of algal remains upwards. The fossil content decreases rapidly at the top of each bed. The oil shale contains fossils in spherical or flattened forms, the latter being much more common. Spherical *Tasmanites* are observed in fossil-poor sediment, but are absent or rare in fossil-rich sediment (Table 1), and tend to be filled with framboidal pyrite with or without collophane. The flattened disks are probably produced by compaction of the spheroidal form. The fossils exist as thin- and thick-walled specimens, the latter having two distinct walls (Fig. 4). The samples from Oonah contain relatively high levels of clay and silt (quartz) grade sediments. The fossil-rich sediments also contain a greater abundance of elongate, horizontal, silica-filled burrows (Table 1).

In the sample from Latrobe, silica-filled burrows are less prevalent and smaller than in the sediments from Oonah. The oil shale at this site exhibits large scale lensing as well as the small scale lensing noted above. This suggests a fluctuating environment, and the oil shale maintains a constant thickness possibly indicating an almost flat sea floor.

Within the core taken from Douglas River, two beds of oil shale can be recognised between 320 and 321.5 m (CALVER et al., 1984). The lower bed exhibits a fossil morphology very similar to that from Latrobe. The upper bed has a thin (20 cm thick) basal conglomerate which fines upwards into the oil shale. Similar small scale structures to those in the sample from Latrobe can be observed and the top of the shale is characterised by flame structures. The oil shale is overlain by a thin fining upwards sequence (*ca.* 50 cm thick) commencing with conglomerate. Dispersed *Tasmanites* are observed in the silt at the top of this sequence.

Bulk Parameters

Bulk parameters are given in Table 2. The samples from Oonah represent a span from the upper tasmanite seam to below the lower seam.

Total organic carbon (TOC) concentrations are consistently greater in the immature sample from Latrobe and the more mature Douglas River sample than in that of intermediate thermal maturity from Oonah (Table 2). There appears to be no direct correlation between organic carbon content and sulphur concentration in the Oonah sediments, except possibly in the upper seam (Fig. 5). The majority of sulphur is framboidal (Table 1) with the greatest concentration coinciding with the fossil-rich sediments. In the sample from Latrobe, pyrite is present in lower concentrations than at Oonah and appears to be proportional to the TOC content (Fig. 5). Despite having the lowest maturity, the relative amount of extractable organic matter in the Latrobe material is *ca.* three times that of the other samples. This probably reflects a generally higher fossil concentration in these samples, with some being almost 74 % *Tasmanites.*

Total extractable organic matter contained from 56% hydrocarbons in the Latrobe sample to 95% hydrocarbons in the lower shale seam at Oonah; the remainder being attributed to polar material (Table 2).

The high Hydrogen Index (HI) of the Latrobe, Oonah upper seam and Douglas River samples (Table 2) classify the kerogen as containing hydrogen-rich Type I organic matter (TISSOT and WELTE, 1984) wherein over 70 % of the organic matter is convertible to hydrocarbons. The slightly reduced HI value from the Oonah lower seam may be a result of more oxidation/reworking consistent with the elevated Oxygen Index (OI) value.

Hydrocarbon Distributions and Source Characteristics

The GC-FID traces (Fig. 6) of the saturated hydrocarbons from the tasmanite extracts show *n*-alkane distributions dominated by lower molecular weight components with distributions maximising between *n*-C_{11} and *n*-C_{13}, with little odd or even predominance (Table 3). Samples also contained significant amounts of the acyclic isoprenoids pristane and phytane, though in different relative proportions (Table 3). The siltstone sample has a Pr/Ph ratio higher than the oil shales (Table 3), consistent with deposition under more oxic conditions.

For the purposes of this study, detailed analyses were only conducted on three of the samples: a thermally immature rock sample from Latrobe, the *Tasmanites* fossil concentrate from Oonah and the core sample from Douglas River. All the samples contain steranes and diasteranes as shown by the *m/z* 217 mass chromatograms (Fig. 7), which is in contrast to their presence as only "trace components" in a sample from Latrobe (Fig. 1) analysed by SIMONEIT et al. (1990).

The relative proportions of C_{27}, C_{28} and C_{29} steranes show some variation between the samples (Table 3) with C_{29} dominant in the Latrobe sample, C_{27} in Oonah and no preference at Douglas River. Although this may reflect subtle differences in source inputs, maturity will also have an influence. C_{30} 24-*n*-propylcholestanes which are generally accepted to be indicative of a marine source (MOLDOWAN et al., 1990), could not be easily detected in the *m/z* 217 mass chromatogram, but were readily identified (though less so in the Douglas River sample) using MRM together with 2α-methyl and 3β-methyl sterane isomers (Figs. 8-10). The samples also contain relatively high proportions of diasteranes (Fig. 7; Table 3) which were not reported in samples previously analysed (SIMONEIT et al., 1990).

The GC-FID chromatograms and extended *m/z* 191 mass chromatograms for each sample show a high abundance of tricyclic compounds (Figs. 6 & 11) and these extend to at least C_{35}. In the *m/z* 191 chromatograms hopanes occur in trace amounts while C_{21}, C_{23} and C_{24} tricyclic compounds show the greatest intensity. However, the FID chromatogram reveals the predominant tricyclic terpane is a C_{19} compound. In the C_{19} pseudo homologue, the abundance of the *m/z* 191 ion is minor compared with the base peak at m/z 123 (AQUINO NETO et al., 1982). In the MRM reactions used to detect hopanes (Figs. 8-10; e.g. 412 → 191 for the C_{30} hopane), tricyclic terpanes appear as non-quantitative artefacts as a consequence of their high relative abundance and the limitations of the linked scan technique used for the analysis. Only the C_{30} tricyclic is specifically detected using the 416 → 191 reaction. Measurement of the C_{27} Ts/Tm hopane ratios was not possible due to interference from an unknown compound co-eluting with Ts.

Examination of the aromatic fraction of samples from Oonah and Douglas River show they are dominated by a single compound (Fig. 12) which was identified by GC-MS as a C_3-phenanthrene. This was positively identified by co-injection with an authentic standard as 1,2,8-trimethylphenanthrene. This compound is seen as one end member of an identifiable aromatisation sequence as indicated by the presence of partially aromatized intermediates in the less mature samples from Latrobe (Fig. 12; Scheme 1).

Maturity

The samples from Latrobe and the *Tasmanites* concentrate from Oonah exhibit a predominance of the thermodynamically less stable $5\alpha,14\alpha,17\alpha(H)$ (*c.f.* $5\alpha,14\beta,17\beta(H)$) sterane isomers (Table 3) indicating that they are thermally immature. This is further emphasised by the greater proportion of the $5\alpha,14\alpha,17\alpha(H)$ 20R epimer compared with the 20S epimer and the presence of small amounts of $5\beta(H)$-steranes (as determined by metastable reaction monitoring, MRM). A value of 0.54 for the 20 S/S+R sterane ratio (Table 3) suggests the Douglas River sample is within the oil window (PETERS and MOLDOWAN, 1993). An $\alpha\beta\beta/\alpha\alpha\alpha$ ratio of 0.5 is consistent with this, the onset of the oil window occurring at about 0.25 (PETERS and MOLDOWAN, 1993).

Maturity estimates based on phenanthrenes (*viz.* the methylphenanthrene index, MPI; Table 3) showed little discrimination. The uniformity in the MPI has been observed previously for low maturity and hydrogen-rich marine organic matter (RADKE et al., 1986; BOREHAM et al., 1988). The presence of aromatic compounds which appear to be derived from the tricyclic precursors in such immature samples (both this study, AZEVEDO et al., 1992 and REVILL et al., 1993) suggests that aromatisation has occurred early in the maturation process. This possibly reflects the unusual nature of the organic matter or microbial influences on the aromatisation processes (TRENDEL, 1985; LOHMANN, 1988; TRENDEL et al., 1989; WOLFF et al., 1989).

There is little evidence to suggest which tricyclic compound is being preferentially converted to the aromatic compounds. The only noticeable correlation being a relative decrease in the complexity of the *m/z* 191 mass chromatogram in the C_{20} region in the Douglas River sample compared with the Oonah *Tasmanites* concentrate (Fig. 11), which is assumed to be a maturity driven decrease in the three stereoisomers relative to the 13β(H),14α(H) compound (CHICARELLI et al., 1988).

The plot of T_{max} *vs.* HI (Fig. 13) shows very similar T_{max} (443 - 446 °C) values for the Latrobe, Oonah fossil concentrate and Douglas River samples. However, the siltstone from above and below the oil shale has a similar maturity but shows a much lower T_{max} (436 °C), equivalent to a vitrinite reflectance of 0.5 % for Type III kerogen (Fig. 13). This emphasises the limited use of the T_{max} parameter in assessing the thermal maturity of Type I kerogens (TISSOT et al., 1987).

The Production Index (PI) for the most thermally mature sample (Douglas River) is only 0.04 (4 %; Table 2), which indicates an immature kerogen (BORDENAVE et al., 1993). This suggests that the biomarker data (steranes) are over-estimating the thermal maturity of the samples, which is consistent with recent results. MARZI and RULLKÖTTER (1992) calculated an activation energy for sterane isomerization at C_{20} of 169 kJ / mol, while kinetic data derived for the tasmanite indicates a typical Type I distribution (TISSOT et al., 1987). There is a very narrow distribution of activation energies for kerogen transformation (Fig. 14) which, in combination with the frequency factor of 8.9×10^{13}, indicates a relatively labile kerogen once generation commences. When these data are used to model maturity it becomes clear that the 20 S/ 20 R isomerisation is complete before the onset of significant hydrocarbon generation (Fig. 15). In contrast, the kinetic data for sterane isomerisation calculated by MACKENZIE and MCKENZIE (1983) predicts over 50 % kerogen conversion for the Douglas River sample (Fig. 15), clearly inconsistent with its high HI value.

Calculation of the Transformation Ratio (TR) according to hydrogen index (HI) values:

$$TR = \frac{HI_o - HI_z}{HI_o}$$

Where HI_0 and HI_Z are the initial HI value and the HI at a depth z respectively. HIo is taken as the value for Latrobe (Table 2).

shows the Douglas River sample to have a TR value of 0.1, considered to define the onset of petroleum generation. Thus, from the kinetic data curve (Fig. 14) it is clear that this sample has only just started hydrocarbon production, but significantly, an increase of only 10-15 °C to exceed the activation energy, would see a rapid increase in the amount of petroleum production. The production curve (Fig. 15) shows that some hydrocarbons have been produced quite early in the maturation sequence, and this is probably due to the presence of weaker bonds within the kerogen. These are represented by the lower activation energies (205 and 209 kJ /mol; Fig. 14) and probably reflect the sulphur content of the kerogen. Clearly, the depth of the oil shale at Douglas River (320 m) is insufficient to produce this level of thermal maturity, even given a high geothermal gradient for this area of around 30 °C / km (GREEN, 1989). This could reflect significant erosion of Tertiary material, or be due to past and localised heating of the organic matter. Too little is currently known about the geology of this region of Tasmania to assess which is the more likely of these two alternatives.

The high TOC and HI values confirm that the tasmanite has the potential to generate large amounts of hydrocarbons but importantly, in the east of Tasmania, as shown by the data from Douglas River, its thermal maturity is near the oil window. This result contradicts previous assumptions that the oil shale in Tasmania is too immature to represent a possible petroleum source, although the present day areal extent of mature strata is unknown.

Inferred Environment of Deposition

BANKS (1962), KANSTLER (1980) and CALVER et al. (1984) suggested that *Tasmanites* represents the "cysts" of a planktonic organism living in a restricted environment, generally littoral and associated with reduced salinity due to a high fresh water input. It has been suggested that much of present-day Tasmania was covered during the Late Carboniferous by an ice sheet flowing from the west (BANKS AND CLARKE, 1987). At that time Tasmania was positioned in high southern latitudes (ca. 75° - 80° S; SMITH et al., 1981). As the glaciers retreated, black muds were deposited on the sea floor in front of the ice, and it was in these muds that beds of tasmanite were formed. The occasional presence of fossil brachiopods and starfish in the tasmanite shale indicates a marine setting. Deposition in quiescent shallow to very shallow water is indicated by fine-scale cross lamination, scouring and lensing-out over very short distances of both the siltstone and *Tasmanites*-rich layers in oil shale from Oonah and by the close association with lenticular sand and well-sorted granule bodies in the Douglas River core. It is suggested that deposition occurred in water depths of 100 m or less (Fig. 3); a nearshore deposition is further suggested by the presence of desmocollinite at Oonah and collinite at Latrobe. The overall fine grain size of the oil shale-bearing sequence shows that very low current strengths existed at the site of deposition. Lonestones, some of which are demonstrably dropstones (Fig. 4b), may have been transported to the site by shore ice as their shapes are characteristic of fluvial and beach environments with little evidence for transport by glacial ice (DOMACK et al., 1993).

Estimates of sea surface temperature for early Permian Tasmania of -1.8 °C (RAO and GREEN, 1982), are close to the present average near the Antarctic ice shelf of -1.9 °C. DOMACK et al. (1993) propose that the tasmanite beds record a period of enhanced primary productivity coupled with polar to sub-polar glacial marine conditions characterised by very cold waters, seasonal sea ice and shore-ice rafting. Cold water deposition is consistent with the low diversity of the invertebrate fauna and strongly indicated by the presence of glendonites, pseudomorphs after ikaite (calcium carbonate hexahydrate; $CaCO_3.6H_2O$). This mineral is suggested to be an authigenic precipitate, forming at low temperatures from interstitial waters of organic-rich sediments, undergoing microbial degradation and accumulated rapidly in cold bottom waters (SUESS et al., 1982; SHEARMAN and SMITH, 1985; JANSEN et al., 1987).

It is notable that the sediments where *Tasmanites* is abundant, in the Late Ordovician-Early Silurian of the Sahara, the Devonian of Brazil, the Late Carboniferous-Early Permian tasmanite of Tasmania and the *Tasmanites*-rich deposits of the Jurassic/Cretaceous of the Brooks Range, Alaska, all have palaeolatitudes, inferred from palaeomagnetic work, of about 75° (SMITH et al., 1981). Sediments where *Tasmanites* is of low abundance seem to have had a wider latitudinal range. For example its occurrence at about 10°S in the Devonian of Indiana and Ohio (SMITH et al., 1981), indicates that it was a wide ranging organism comparable to some diatoms and prasinophytes in contemporary oceans.

Pyrite occurs within some fossils, but also separately in the fine siltstone and between fossils. The pyrite is predominantly framboidal and seems to have been an early diagenetic deposit, especially in associated conglomerates. This indicates a reducing environment soon after deposition, which is also supported by the presence of glendonites. Identifiable burrows in the sediments suggest only mild bioturbation and that bottom waters were depleted in oxygen at the time of deposition which, combined with low temperatures, reduced the rate of oxidation of the organic matter such that little was oxidised prior to burial. Low pristane/phytane ratios are often associated with low-oxygen environments such as the tasmanite (Table 3; DIDYK et al., 1978), although other factors can be important (TEN HAVEN et al., 1987). In contrast, the siltstone above and below the tasmanite shale which represents deposition in an oxic environment exhibits a relatively high pristane/phytane ratio of 3.1. Our data is consistent with earlier models of tasmanite deposition, suggesting that the sum of the physical properties indicates deposition in a dysaerobic environment with a dissolved oxygen content less than 0.5 ml L^{-1} at the sediment-water interface (ARTHUR et al., 1984).

SIMONEIT et al. (1992; 1993) reported high ^{13}C enrichment for the tricyclic compounds ($\delta^{13}C$ values of -9.9‰ to -12.2‰) extracted from an immature sample from Latrobe (Fig. 1) which was attributed to bloom conditions prevailing at the time of deposition. Phytoplankton from cold, high latitude waters are typically depleted in ^{13}C due to the elevated pCO_2 caused by increased CO_2 solubility at these temperatures (reviewed by SACKETT, 1991). Low atmospheric pCO_2 associated with global glaciation (RAU et al., 1991a) in the Early Permian, possibly combined with additional pCO_2 drawdown during algal blooms provides a possible explanation for the ^{13}C enrichments of tasmanite kerogen reported here and by SIMONEIT et al. (1993). However RAU et al. (1991b) showed that particulate organic matter associated with sea ice could also be significantly enriched in ^{13}C ($\delta^{13}C$ -16‰ to -28‰) relative to the seawater. Within the sea-ice the physical isolation from re-equilibration with the atmosphere may reduce CO_2 availability and therefore significantly reduce isotopic fractionation. SIMONEIT et al. (1993) reported a tasmanite kerogen with a $\delta^{13}C$ value of -16.6‰ and our samples have $\delta^{13}C$ values of -13‰ to -11‰ (Fig. 16). Thus, in view of the depositional setting implied by geological evidence we propose that *Tasmanites* in this instance may have occupied an environment very similar to that of present day sea-ice algae. Thus, by analogy with present day sea-ice diatom communities, the *Tasmanites* bloomed within the ice as the light intensity increased during the spring. As the ice melted, algae from the bloom were released into the water column and subsequently sedimented. The fine scale laminations and rarity of bioturbation are consistent with a quiescent water column, which may be assisted by persistent ice cover. To test this hypothesis we measured the $\delta^{13}C$ for sea ice diatoms collected from ice cores taken in Antarctica, during November 1991. These gave a $\delta^{13}C$ value of -7‰ (Fig. 16) which supports this interpretation. Further studies of sea ice algae from several Antarctic locations have confirmed their ^{13}C enrichment compared to algae isolated from the associated water column (R. E. SUMMONS and P. D. NICHOLS unpublished data). The taxonomic assignment of *Tasmanites* with the Prasinophyceae (Chlorophyta) (WALL, 1962; PARKE, 1966) and the observations of TAPPAN (1980), who suggested that the fossil prasinophytes are a "disaster species", somehow surviving the widespread extinctions of the middle Palaeozoic and, perhaps most importantly, thriving in the absence of other phytoplankton, are all consistent with our model.

Origins of Biomarkers in the Tasmanite Oil Shale

Recently COLLISTER *et al.* (1992) reported isotopic values for tricyclic compounds in the Green River oil shale which ranged from -33.7‰ to -27.3‰. This range corresponds to the values generally associated with photoautotrophs, but there was no correlation with the values for β–carotane or steranes in the same samples, indicating different source organisms. The difference between the isotopic values of COLLISTER et al. (1992) and those reported here and by SIMONEIT et al. (1993) may be due to the source organism occupying a different niche in the very different environments of deposition.

The high proportion of preserved organic remains in the tasmanite oil shale, and the dominance of tricyclic compounds in the hydrocarbon fractions, has often led to *Tasmanites* to be proposed as the likely source for these compounds (e.g. VOLKMAN et al., 1989; SIMONEIT et al., 1992; 1993). However, tricyclic compounds have been identified in a wide range of sediments and petroleum from a range of geological ages, and do not appear to be limited to areas of high *Tasmanites* content (see AQUINO NETO et al., 1983), so other sources must be examined. A consideration of $\delta^{13}C$ values of tricyclic compounds in the extracts and pyrolysates of the tasmanite oil shale provides evidence for a source distinct from the accompanying algaenan.

GC-IRMS analysis of tricyclics in previous studies (SIMONEIT et al., 1993) and the present study yielded $\delta^{13}C$ values of -9.9‰ to -12.2‰ and -6.4‰ to -11.3‰ respectively, which shows that these compounds are enriched in ^{13}C compared with the corresponding kerogen (Fig. 16). The light and variable isotopic composition for the *n*-alkanes ($\delta^{13}C$ values -18 ‰ to -30 ‰) suggests multiple sources. There is a general trend for ^{13}C depletion in higher *n*-alkane homologues, suggesting a possible contribution from allochthonous bacterial or plant waxes. For the lower *n*-alkane homologues, algal and cyanobacterial sources may become increasingly important.

Closed-system pyrolysis of tasmanite kerogen for 72 hours at increasingly higher temperatures showed a number of interesting trends (Table 4). Recovery of bitumen maximised at 68 % at 330 °C and decreased to 59 % at 350 °C, probably as a result of the generation of a larger proportion of gas resulting from cracking of liquid hydrocarbons. The composition of the bitumen also changed markedly. At 350 °C almost 96 % of the bitumen could be recovered from the chromatographic column, as saturates, aromatics and weakly polar materials. At 300 °C and 330 °C the recoveries from column chromatography were only 52 % and 57 % respectively, indicating that the pyrolysate comprised a major proportion of asphaltic or strongly polar material which bound irreversibly to the silica gel. The proportions of saturates, aromatics and weakly polar fractions in the material recovered from column chromatography did not change significantly as the pyrolysis temperature increased.

A comparison of GC traces for the C_{10+} saturated hydrocarbons (Fig. 17) shows a low abundance of *n*-alkanes compared to tricyclanes in the extract and the 300 °C pyrolysate. At the higher temperatures, *n*-alkanes dominate the GC-FID chromatogram, consistent with flash pyrolysis-GC results which revealed the aliphatic nature of the tasmanite kerogen (C. J. BOREHAM, unpublished data). There is also a progression in *n*-alkane generation leading to reduced waxy *n*-alkane contents and lower molecular weight predominance as the temperature increases to 350 °C. In the 300 °C pyrolysate, the *n*-alkane envelope maximises at C_{18} compared with C_{14} in the 350 °C pyrolysate. Evidence for this evolution is also shown by $\delta^{13}C$ analysis of the alkanes (Fig. 18) and comparison with those in the extract. The *n*-alkanes produced at 300 °C exhibit an isotopic composition closest to those of the extract with a progression to "heavier" compounds with an increase in pyrolysis temperature. Note that at 350 °C the $\delta^{13}C$ values of C_{15}-C_{24} *n*-alkanes are in the range -12‰ to -15‰, compared with the kerogen at -12‰. The C_{13} and C_{14} *n*-alkanes are now prominent (Fig. 16) and are slightly "heavier" than the starting kerogen at -10‰ to -11.5‰, although this could be due, in part, to isotopic fractionation on evaporative loss of some of the volatile *n*-alkanes.

The observations from the pyrolysis experiments are consistent with the concept of generation of an asphaltene- and polar-rich material during the initial stages of kerogen conversion (EVANS and FELBECK, 1983), and subsequent cracking of this to lower molecular weight components, including gaseous products. The main information conveyed by the isotope data is, however, that the $\delta^{13}C$ values of the *n*-alkanes produced by kerogen pyrolysis are significantly different from those in the extract of immature tasmanite. Pyrolytically generated *n*-alkanes and *n*-alkylcyclohexanes (data not shown) are isotopically similar to the kerogen consistent with earlier observations (BURWOOD et al., 1988) of a close correlation between ^{13}C contents of sapropellic kerogens and their pyrolysates. Based on experience with other algal-derived kerogens (e.g. GOTH et al., 1988; TEGELAAR et al., 1989; DERENNE et al., 1992; BOREHAM et al., 1994), these compounds are probably derived from an *n*-alkyl based biopolymer, algaenan, which forms part of the structure of the tasmanite fossils. Indeed, the $\delta^{13}C$ values are constant for the C_{17} - C_{27} *n*-alkanes from the 330 °C pyrolysate. Here, yields are high, secondary cracking is minimal and the isotopic value is considered to represent that of the *Tasmanites* algaenan. This is also consistent with the reported aliphatic nature of the preserved organic matter (KJELLSTRÖM, 1968).

Saturated tricyclic alkanes did not appear to be generated during the 330 °C and 350 °C pyrolyses where the *n*-alkanes were mostly produced. Their abundance relative to the *n*-alkanes decreased as the temperature increased. Caution should be exercised however. Tricyclic hydrocarbons may have been converted to aromatics at higher pyrolysis temperatures. Furthermore, the composition of the aromatic fractions generated in the pyrolysis experiments became much simpler with increasing temperature and at 350 °C was dominated by 1,7-dimethylphenanthrene and 1,2,8-trimethylphenanthrene with $\delta^{13}C$ values of -7.9 ‰ and -5.7 ‰ respectively, which are within the range for tricyclic compounds in the tasmanite extracts of different maturities (Fig. 16). The isotopic similarity in the tricyclic hydrocarbons from pyrolysis and tasmanite extracts (Scheme 1 and Fig. 18) suggest that they are almost certainly derived from the same precursors. A proposed genetic relationship between the tricyclic hydrocarbons is shown in Scheme 1. It is uncertain at present whether this process is mediated by bacteria or by heating in the natural environment (LOHMANN, 1988; FREEMAN, 1991; FREEMAN et al., 1994). Certainly, the latter process is indicated by the bias towards the fully aromatised tricyclics in both the pyrolysates and the higher maturity Oonah and Douglas River extracts.

However, the occurrence of the monoaromatic des-A-triterpane (-8.5 ‰; Fig. 12; FREEMAN et al., 1994) suggests a contribution from the former process (LOHMANN, 1988).

The isotopic dissimilarity of the tricyclic hydrocarbons (mean -8 ‰) to the kerogen and kerogen-derived *n*-alkanes suggests a source distinct from the *Tasmanites* themselves.

Interestingly, the difference in kerogen $\delta^{13}C$ data in this study with that of SIMONEIT et al. (1993) is matched by differences of a similar magnitude in the tricyclic compounds, aromatic derivatives and *n*-alkanes in the extracts. This, in conjunction with the previously noted differences in sterane and hopane observations, suggests that there were fluctuations in the source and depositional environment of organic matter within the oil shale seam which affected both biomarker distributions and their ^{13}C isotopic values.

CONCLUSIONS

This study represents the first organic geochemical comparison of thermally mature and immature tasmanite oil shale samples in conjunction with a detailed geological evaluation of the sedimentary setting.

1). This study has shown, for the first time, that at least some deposits of the tasmanite shale in Tasmania are near the "oil window".

2). Geological, isotopic and biomarker analysis indicates that *Tasmanites* thrived in an environment of ice cover and bloomed in conditions analogous to those experienced by present-day sea-ice diatoms. The algal cells were subsequently deposited in sediments overlain with oxygen-depleted waters, induced by restricted water movement.

3). Closed-system pyrolysis suggests that there is little correlation between the temperature profiles for production of *n*-alkanes and the tricyclic compounds from the kerogen precursors. The *n*-alkanes are mainly derived from thermal cracking of algal aliphatic biopolymer whereas the tricyclic alkanes and aromatic hydrocarbons are generated earlier, possibly from a different source.

ACKNOWLEDGEMENTS

Dr. S.J. Rowland, University of Plymouth, is thanked for kindly supplying a sample of authentic 1,2,8-trimethylphenanthrene. Peter Baillie (Tasmanian Department of Mines) provided the Latrobe sample (BMR #1995) and Janet Hope carried out closed-system pyrolysis on this sample. We would like to thank Dr. Peter Nichols (CSIRO) for providing the sea-ice diatom sample and Malcolm Bendall for information about the Douglas River core. ATR thanks the CSIRO Institute of Natural Resources and Environment for a post-doctoral fellowship. Andrew Murray and Dr. Clinton Foster (AGSO) provided valuable reviews of early versions of the manuscript and AM is thanked for providing the data for Fig. 15. We are grateful to Professor B.R.T. Simoneit for a pre-print of unpublished data and to Dr. J. W. De Leeuw, Dr. H. L. ten Haven, Dr. J. M. Moldowan and Dr. M. Radke for very helpful reviews of the manuscript. RES and CJB publish with permission of the Director, AGSO.

REFERENCES

AQUINO NETO F. R., RESTLE A., CONNAN J., ALBRECHT P. and OURISSON G. (1982) Novel tricyclic terpanes (C_{19}, C_{20}) in sediments and petroleums. *Tetrahedron Lett.* **23,** 2027-2030.

AQUINO NETO F. R., TRENDEL J. M., RESTLE A., CONNAN J. and ALBRECHT P. (1983) Occurrence and formation of tricyclic and tetracyclic terpanes in sediments and petroleums. In *Advances in Organic Geochemistry 1981* (ed. M. BJORØY et al.), pp. 659-667. Wiley.

AQUINO NETO F. R., TRIGÜIS D. A., AZEVEDO D. A., RODRIGUES R. and SIMONEIT B. R. T. (1992) Organic geochemistry of geographically unrelated *Tasmanites*. *Org. Geochem.* **18,** 791-03.

ARTHUR M. A., DEAN W. E. and STOW D. A. V. (1984) Models for the deposition of Mesozoic-Cenezoic fine-grained organic-rich sediment in the deep sea. In *Fine-grained* *sediments: Deep-water processes and facies* (ed. D. A. V. STOW and D. J. W. PIPER), Geological Society Special Publication, pp. 527-560.

AZEVEDO D. A., AQUINO NETO F. R. and SIMONEIT B. R. T. (1990) Mass spectrometric characteristics of a novel series of ring-C monoaromatic tricyclic terpanes found in Tasmanian tasmanite. *Org. Mass Spectrom.* **25,** 475-480.

AZEVEDO D. A., AQUINO NETO F. R., SIMONEIT B. R. T. and PINTO A. C. (1992) Novel series of tricyclic aromatic terpanes characterized in Tasmanian tasmanite. *Org. Geochem.* **18,** 9-16.

BANKS M. R. (1962) Permian (Tasmania). *J. Geol. Soc. Aust.* **9,** 189-216.

BANKS M. R. and CLARKE M. J. (1987) Changes in the geography of the Tasmania Basin in the late Paleozoic. In *Gondwana Six: Stratigraphy, Sedimentology and Paleontology.* (ed. G. D. McKENZIE) Amer. Geophys. Union Geophys. Monograph 41.

BENDALL M. R., VOLKMAN J. K., LEAMAN D. E. and BURRETT C. F. (1991) Recent developments in exploration for oil in Tasmania. *APEA J part 1* **31,** 74-84.

BOALCH G. T. and GUY-OHLSON D. (1992) *Tasmanites*, the correct name for *Pachysphaera* (Prasinophyceae, *Pterospermataceae*). *Taxon* **41,** 529-531.

BORDENAVE M. L., ESPITALIÉ J., LEPLAT P., OUDIN J. L. and VANDENBROUCKE M. (1993) Screening Techniques for Source Rock Evaluation. In *Applied Petroleum Geochemistry* (ed. M. L. BORDENAVE), Editions Tecnip, Ch. II-2.

BOREHAM C. J., CRICK I. H. and POWELL T. G. (1988) Alternative calibration of the Methylphenanthrene Index against vitrinite reflectance: application to maturity measurements on oils and sediments. *Org. Geochem.* **12,** 289-294.

BOREHAM C. J., SUMMONS R. E., ROKSANDIC Z., DOWLING L. M. and HUTTON A. C. (1994) Chemical, molecular and isotopic differentiation of organic facies in the tertiary lacustrine Duaringa oil shale deposit, Queensland, Australia. *Org. Geochem.* In press.

BURLINGAME A. L., WSZOLEK P. C. and SIMONEIT B. R. T. (1969) The fatty acid content of tasmanites. In *Advances in Organic Geochemistry 1968* (ed. P. A. SCHENCK and I. HEVENAAR), pp. 131-155. Pergamon-Vieweg.

BURWOOD R., DROZD R. J., HALPERN H. I. and SEDIVY R. A. (1988) Carbon isotopic variations of kerogen pyrolysates. *Org. Geochem.* **12,** 195-205.

CALVER C. R., CLARKE M. J. and TRUSWELL E. M. (1984) The stratigraphy of a late Palaeozoic bore hole section at Douglas River, eastern Tasmania: a synthesis of marine macro-invertebrate and palynological data. *Pap. Proc. R. Soc. Tasm.* **118,** 137-161.

CHICARELLI M. I., AQUINO NETO F. R. and ALBRECHT P. (1988) Occurrence of four stereoisomeric tricyclic terpane series in immature Brazilian shales. *Geochim. Cosmochim. Acta* **52,** 1955-1959.

CLARKE M. J. (1989) Lower Parmeener Supergroup. In *Geology and Mineral Resources of Tasmania.* (ed. C. F. BURRETT and E. L. MARTIN), Chap. 8, pp. 295-309. Geological Society of Australia, Special Publication 15.

CLARKE M. J. (1992) Hellyerian and Tamarian (Late Carboniferous-Lower Permian) invertebrate faunas from Tasmania. *Tasm. Geol. Surv. Bull.* 69.

CLARKE M. J. and BANKS M. R. (1975) The stratigraphy of the Lower (Permo-Carboniferous) parts of the Parmeener super-group, Tasmania. In *Gondwana Geology* (ed. K. S. W. CAMPBELL) pp. 453-467. A.N.U. Press.

CLARKE M. J. and FARMER N. (1976) Biostratigraphic nomenclature for late Palaeozoic rocks in Tasmania. *Pap. Proc. R. Soc. Tasm.* **110,** 91-109.

COLLISTER J. W., SUMMONS R. E., LICHTFOUSE E. and HAYES J. M. (1992) An isotopic biogeochemical study of the Green River oil shale. *Org. Geochem.* **19,** 265-276.

DERENNE S., LE BERRE F., LARGEAU C., HATCHER P., CONNAN J. and RAYNAUD J. F. (1992) Formation of ultralaminae in marine kerogens via selective preservation of thin resistant outer walls of microalgae. *Org. Geochem.* **19,** 345-350.

DIDYK B. M., SIMONEIT B. R. T., BRASSELL S. C. and EGLINTON G. (1978) Organic geochemical indicators of palaeoenvironmental conditions of sedimentation. *Nature (Lond.)* **272,** 216-222.

DOMACK E. W., BURKLEY L. A. DOMACK C. R. and BANKS M. R. (1993) Facies analysis of glacial marine pebbly mudstones in the Tasmania Basin: Implications for regional paleoclimates during the late Paleozoic. In *Gondwana Eight: Proceedings of the Eighth Gondwana Symposium* (ed. R. H. FINDLAY et al.) pp.471-484. Balkema.

EVANS R. J. and FELBECK Jr. G. T. (1983) High temperature simulation of petroleum formation - 1. The pyrolysis of Green River shale. *Org. Geochem.* **4,** 135-144.

FOSTER C. B. and WATERHOUSE J. B. (1988) The Granulatisporites confluens Oppel-zone and Early Permian marine faunas from the Grant Formation on the Barbwire Terrace, Canning Basin, Western Australia. *Aust. J. Earth Sci.* **35,** 135-157.

FREEMAN K. H. (1991) The carbon isotopic composition of individual compounds from ancient and modern depositional environments. Ph.D. thesis, Indiana University, Bloomington, Indiana, USA.

FREEMAN K. H., BOREHAM C. J., SUMMONS R. E. and HAYES J. M. (1994) The effect of aromatisation on the isotopic compositions of hydrocarbons during early diagenesis. *Org. Geochem.*, submitted.

GREEN D. C. (1989) Heat flow and heat production in Tasmania. In *Geology and Mineral Resources of Tasmania.* (ed. C. F. BURRETT and E. L. MARTIN), Chap. 13, pp. 461-463. Geological Society of Australia, Special Publication 15.

GOTH K., DE LEEUW J. W., PÜTTMANN W. and TEGELAAR E. W. (1988) Origin of Messel Oil Shale kerogen. *Nature (Lond.)* **336,** 759-761.

GOULD C. (1861) Resinous shales (Dysodile at Latrobe). *Tasm. House of Assembly Pap.* 8.

GUY-OHLSON D. (1988) Developmental stages in the life cycle of Mesozoic *Tasmanites. Bot. Mar.* **31,** 447-456.

GUY-OHLSON D. and BOALCH G. T. (1992) Comparative morphology of the genus *Tasmanites* (Pterospermales, Chlorophyta). *Phycologia* **31,** 523-528.

HARLAND W. B., ARMSTRONG R. L., COX A. V., CRAIG L. E. SMITH A. G. and SMITH D. G. (1990) *A Geological Timescale 1989.* Cambridge University.

HAYES J. M., FREEMAN K. H., POPP B. N. and HOHAM C. H. (1990) Compound-specific isotope analysis: a novel tool for reconstruction of ancient biogeochemical processes. In *Advances in Organic Geochemistry 1989* (ed. B. DURAND and F. BEHAR), pp. 1115-1128. Pergamon Press.

JAMES C., GEPP H. W., AIKENHEAD A., SCOTT J. B., NYE P. B., PURVES S. S. B., CHAMBERS C. O., JUDE T. M. and REES H. W. (1932) *Report of the Tasmanian Shale Oil Investigation Committee.* Tasmania Department of Mines, Geological Survey, Mineral Resources, No. 8, vol. II. (Reprinted 1950).

JANSEN J. H. F., WOENSDREGT C. F., KOOISTRA M. J. and VAN DER GAAST S. J. (1987) Ikaite pseudomorphs in the Zaire deep-sea fan: an intermediate between calcite and porous calcite. *Geology* **15,** 245-248.

KANTSLER A. J. (1980) Aspects of organic petrology with particular reference to the exinite group of macerals. In *Oil Shale Petrology Workshop, Wollongong, 1980* (ed. A. C. COOK and A. J. KANSTLER), pp. 16-41. Keiraville Kopiers.

KJELLSTRÖM G. (1968) Remarks on the chemistry and ultrastructure of the cell wall of some Palaeozoic Leiospheres. *Geolog. Förenin. Stockh. Förhandlin.* **90,** 221-228.

LOHMANN F. (1988) Aromatisations microbiennes de triterpenes vegetaux. Ph.D. dissertation, L'Université Louis Pasteur de Strasbourg, France.

MACKENZIE A. S. and MCKENZIE D. P. (1983) Aromatization and isomerization of hydrocarbons in sedimentary basins formed by extension. *Geol. Magazine* **120**, 417-470.

MARZI R. and RULLKÖTTER J. (1992) Qualitative and quantitative evolution and kinetics of biological marker transformations - laboratory experiments and application to the Michigan Basin. In *Biological Markers in Sediments and Petroleum* (ed. J. M. MOLDOWAN, P. ALBRECHT and R. P. PHILP), pp. 18-41, Prentice-Hall.

MILLIGAN J. (1852) Report on the coal said to have been found at the Don River, and upon the west bank of the Tamar River, in Tasmania. *Pap. Proc. R. Soc. V.D.L.* **II**, 90-106.

MOLDOWAN J. M., FAGO F. J., LEE C. Y., JACOBSON S. R., WATT D. S., SLOUGUI N. E., JEGANATHAN A. and YOUNG D. C. (1990) Sedimentary 24-*n*-propylcholestanes, molecular fossils diagnostic of marine algae. *Science* **247**, 309-312.

PARKE M. (1966) The genus *Pachysphaera* (Prasinophyceae). In *Some Contemporary Studies in Marine Science.* (ed. H. BARNES), pp. 555-563. Allen and Unwin.

PARKE M. and HARTOG-ADAMS I. (1965) Three species of *Halosphaera. J. Mar. Biol. Ass. U.K.* **45**, 537-557.

PARKE M., BOALCH G. T., JOWETT R. and HARBOUR D. S. (1978) The genus *Pterosperma* (Prasinophyceae): Species with a single equatorial ala. *J. Mar. Biol. Ass. U.K.* **58**, 239-276.

PETERS K. E. and MOLDOWAN J. M. (1993) *The Biomarker Guide. Interpreting Molecular Fossils in Petroleum and Ancient Sediments.* Prentice-Hall, 363 pp.

PHILP R. P., GILBERT T. D. and RUSSELL N. J. (1982) Characterization by pyrolysis-gas chromatography-mass spectrometry of the insoluble organic residues derived from the hydrogenation of *Tasmanites* sp. oil shale. *Fuel* **61**, 221-226.

RADKE M., WELTE D. H. and WILLSCH H. (1986) Maturity parameters based on aromatic hydrocarbons: influence of organic matter type. In *Advances in Organic Geochemistry 1985. Part I: Petroleum Geochemistry* (ed. D. LEYTHAEUSER and J. RULLKÖTTER), pp. 51-64. Pergamon Press.

RAO C. P. and GREEN D. C. (1982) Oxygen and carbon isotopes of Early Permian cold-water carbonates, Tasmania, Australia. *J. Sediment. Petrol.* **52,** 1111-1125.

RAU G. H., FROELICH P. N., TAKAHASHI T. and DES MARAIS D. J. (1991a) Does sedimentary organic $\delta^{13}C$ record variations in Quaternary ocean $[CO_2(aq)]$?. *Paleoceanography* **6,** 335-347.

RAU G. H., SULLIVAN C. W. and GORDON L. I. (1991b) $\delta^{13}C$ and $\delta^{15}N$ variations in Weddell Sea particulate organic matter. *Mar. Chem.* **35,** 355-369.

REVILL A. T., VOLKMAN J. K., O'LEARY T. and SUMMONS R. E. (1993) Aromatic hydrocarbon biomarkers in tasmanite oil shales from Tasmania, Australia. In *Organic Geochemistry: Poster sessions from the 16th International Meeting on Organic Geochemistry, Stavanger 1993* (ed. K. Øygard.). pp. 3-6. Falch Hurtigtrykk.

SACKETT W. M. (1991) A history of the $\delta^{13}C$ composition of oceanic plankton. *Mar. Chem.* **34,** 153-156.

SHEARMAN D. and SMITH A. J. (1985) Ikaite, the parent material of jarrowite-type pseudomorphs. *Proc. Geol. Assoc.* **96,** 305-314.

SIMONEIT B. R. T. and BURLINGAME A. L. (1973) Carboxylic acids derived from Tasmanian tasmanite by extractions and kerogen oxidations. *Geochim. Cosmochim. Acta* **37,** 595-610.

SIMONEIT B. R. T., LEIF R. N., AQUINO NETO F. R., AZEVEDO A. D., PINTO A. C. and ALBRECHT P. (1990) On the presence of tricyclic terpane hydrocarbons in Permian tasmanite algae. *Naturwissenschaften* **77,** 380-383.

SIMONEIT B. R. T., SCHOELL M. and AQUINO NETO F. R. (1992) Sources of biomarkers in Permian tasmanite based on carbon isotope compositions of individual compounds. Abstract of a presentation at American Chemical Society meeting, San Francisco.

SIMONEIT B. R. T., SCHOELL M., DIAS R. F. and AQUINO NETO F. R. (1993) Unusual carbon isotope compositions of biomarker hydrocarbons in a Permian tasmanite. *Geochim. Cosmochim. Acta* **57,** 4205-4211.

SMITH A. G., HURLEY A. M. and BRIDEN J. C. (1981) *Phanerozoic Palaeocontinental World Maps.* Cambridge University Press.

SUESS E., BALZER W., HESSE K.-F., MÜLLER P. J., UNGERER C. A. and WEFER G. (1982) Calcium carbonate hexahydrate from organic-rich sediments of the Antarctic shelf: precursors of glendonites. *Science* **216,** 1128-1131.

TAPPAN H. (1980) *The Paleobiology of Plant Protists.* Freeman.

TEGELAAR E. W., DE LEEUW J. W., DERENNE S. and LARGEAU C. (1989) A reappraisal of kerogen formation. *Geochim. Cosmochim. Acta* **53,** 3103-3106.

TEN HAVEN H. L., DE LEEUW J. W., RULLKÖTTER J. and SINNINGHE DAMSTÉ J. S. (1987) Restricted use of the pristane/phytane ratio as a palaeoenvironmental indicator. *Nature (Lond.)* **330,** 641-643.

TISSOT B. P. and WELTE D. H. (1984) *Petroleum Formation and Occurrence.* Springer-Verlag. 699 pp.

TISSOT B. P., PELET R. and UNGERER P. (1987) Thermal history of sedimentary basins, maturation indices, and kinetics of oil and gas generation. *Amer. Assoc. Pet. Geol. Bull.* **71,** 1445-1466.

TRENDEL J. -M. (1985) Degradation de triterpenes dans les sediments: aspects photochemique et microbiologiques. Ph.D. dissertation, L'Université Louis Pasteur de Strasbourg, France.

TRENDEL J. -M., LOHMANN F., KINTZINGER J. P. and ALBRECHT P. (1989) Identification of des-A-triterpenoid hydrocarbons occurring in surface sediments. *Tetrahedron* **45,** 4457-4470.

TRUSWELL E. M. (1978) *Palynology of the Permo-Carboniferous in Tasmania: an interim report.* Tas. Geol. Survey Bull. No. 56. 31pp. Dept. Mines, Hobart, Tasmania.

TWELVETREES W. H. (1917) The search for petroleum in Tasmania. *Tasm. Mines Dept. Circ.* **2,** 1-18.

VOLKMAN J. K., EVERITT D. A. and ALLEN D. I. (1986) Some analyses of lipid classes in marine organisms, sediments and seawater using thin-layer chromatography-flame ionisation detection. *J. Chromatogr.* **356,** 147-162.

VOLKMAN J. K., BANKS M. R., DENWER K. and AQUINO NETO F. R. (1989) Biomarker composition and depositional setting of tasmanite oil shale. *Poster presentation.* 14th International Meeting on Organic Geochemistry, Paris, France.

VOLKMAN J. K., O'LEARY T., SUMMONS R. E. and BENDALL M. R. (1992) Biomarker composition of some asphaltic coastal bitumens from Tasmania, Australia. *Org. Geochem.* **18,** 669-682.

WALL D. (1962) Evidence from recent plankton regarding the biological affinities of *Tasmanites* Newton 1875 and *Leiospaeridea* Eisenack 1958. *Geol. Mag.* 94, 353-362.

WOLFF G. A., TRENDEL J. -M. and ALBRECHT P. (1989) Novel monoaromatic triterpenoid hydrocarbons occurring in sediments. *Tetrahedron* **45,** 6721-6728.

Table 1. Examples of oil shale characteristics at Oonah.

	Lower bed- lower seam	Lower bed - Upper seam	Middle bed - Upper seam	Upper bed - Lower seam
Thickness of oil shale (m)	0.28-0.42	0.3-0.7	0.38-0.59	0.24-0.28
Thin walled : thick walled fossils	16:1	6.5:1	10.5:1	5.6:1
% Matrix	48.9	71.4	48.8	74.8
% Fossils	36.5	10.1	32.2	5.4
% Spherical fossils	<0.2	0.4	0.2	0.6
% Pyrite framboids	3.5	2.0	4.3	3.7
% Non-framboidal pyrite	1.3	<0.2	<0.2	<0.2
% Vitrinite	0.5	0.2	0.4	n/d
% Elongate burrows	1.2	0.6	1.4	0.6
% Other*	7.9	15.5	12.5	15.3

* Predominantly clay and silt
n/d = not detected
Percentages are from point counts using approximately 500 data points

Table 2. Bulk parameters for tasmanite samples

Sample	Sample No.†	TOC (% whole sample)	EOM (mg/g TOC)	Iatroscan TLC-FID Hydrocarbons (%, (mg/g TOC))	Iatroscan TLC-FID Polars (%)	Rock-Eval T_{max} (°C)	Rock-Eval S_1 (kg/Tonne)	Rock-Eval S_2 (kg/Tonne)	Rock-Eval S_3 (kg/Tonne)	PI	HI	OI
Latrobe	1	31.3	52	56* (29)	44	444	12.5	304.2	5.6	0.039	972	18
Oonah												
Upper Seam												
Total	2	6.9	66	94 (62)	6	443	3.6	65.2	0.3	0.052	937	4
fossil Concentrate	3	63.0	23	85 (19)	15	446	30.8	590.8	2.3	0.050	937	3
Siltstone above seam	9	1.01	n.m.	n.m.	n.m.	437	0.04	0.89	0.73	0.04	88	72
Siltstone between seams	7	0.78	n.m.	n.m.	n.m.	440	0.07	1.30	0.34	0.05	166	43
Lower Seam												
Total	6	8.1	32	95 (30)	5	440	1.4	54.4	2.2	0.025	675	27
fossil Concentrate	4	61.3	n.m.	n.m.	n.m.	444	22.82	534.94	3.23	0.04	872	5
Siltstone below seam	8	1.1	35	73 (25)	27	436	0.1	1.8	0.6	0.052	163	51
Douglas River	5	17	34	90 (31)	10	446	6.3	147.5	0.2	0.041	868	1

† Sample number refers to Fig. 13

n.m. = not measured

* determined by gravimetry

PI = Production Index = S_1 / S_1 + S_2

Table 3: Molecular data for tasmanite samples

859057

				Parameter				
Sample	1 Pr/Ph	2 Pr/C_{17}	3 CPI	4* steranes $C_{27:28:29}$	5* Diasteranes	6* 20S/S+R	7* αββ/αββ + ααα	8 MPI
trobe	0.45	0.62	n.d.	1.4:1:2.6	0.12	0.11	n.d.†	n.d.‡
onah								
Upper Seam								
Total	1.6	0.69	0.92	n.m.	n.m.	0.30	0.15	n.m.
ssil concentrate	1.5	0.60	1.03	2.2:1:1.9	0.35	0.35	0.15	0.46
Lower Seam								
Total	1.4	0.48	0.83	n.m.	n.m.	0.31	n.m.	n.m.
Siltstone	3.1	0.91	1.40	n.m.	n.m.	n.m.	n.m.	n.m.
uglas River	0.7	0.45	0.98	2:1:2	0.64	0.54	0.5	0.36

alculated from MRM data, † αββ probably absent, isomer is 20R 5β,14α,17α(H), .‡ MPI not applicable at this maturity

d. = Not detected; n.m. = Not measured

rameters:

Pristane / Phytane

Pristane / n-C_{17}

Carbon Preference Index $= \dfrac{(\%C_{25}-C_{33}\text{ odd})+(\%C_{23}-C_{31}\text{ odd})}{2(\%C_{24}-C_{32}\text{ even})}$

5α,14α,17α(H) 20R steranes

C_{29} Diasteranes (βα 20S + 20R) / (ααα + αββ 20S & 20R)

C_{29} ααα sterane 20S / 20S + 20R

C_{29} αββ 20R steranes / C_{29} 20R (ααα +αββ) steranes

Methyl Phenanthrene Index $= \dfrac{1.5(2\text{-}MP+3\text{-}MP)}{P+1\text{-}MP+9\text{-}MP}$

Table 4. Comparison of whole rock extract and kerogen pyrolysate of tasmanite from Latrobe, Tasmania

72 hr Pyrolysis Temp. (°C)	EOM (mg/g TOC)#	C_{12} + Saturates* (%)	Aromatics* (%)	Polars* (%)	Asphaltenes‡ (%)
unheated	51.4	19.0	30.5	38.8	11.7
300	190.8	7.0	13.3	31.3	48.4
330	1019.2	8.5	13.9	39.3	38.3
350	879.1	14.9	42.1	39.7	3.3

TOC (kerogen) = 67.1 %

* Based on pre-chromatography weight

‡ Taken as that fraction not eluting from the chromatographic column

FIGURE LEGENDS

Fig. 1. Sample locations

Fig. 2. Correlation chart for the lower (Carboniferous and Permian) sections of the Parmeener Supergroup for Latrobe and Douglas River (adapted from BANKS and CLARKE, 1987). Sst = Sandstone, CMs = Coal Measure Formation

Fig. 3. Suggested paleogeography of Tasmania during the Early Tamarian stage. Dashed lines = isopachs, numbers = thicknesses in metres, T = occurrence of tasmanite oil shale, ▨ = land areas, ░ = areas of unknown geography. (Adapted from BANKS and CLARKE, 1987).

Fig. 4. (a) Fossil *Tasmanites* filled with pyrite from Oonah, (diameter = ca. 0.5 mm) and (b) Dropstone in tasmanite shale from Oonah. Note how the stone breaks the bedding of the shale, (magnification = x 10).

Fig. 5. Relationship between TOC and sulphur content in tasmanite samples. The upper graph shows the relationship with height above the Wynard tillite in a sample from Oonah. T indicates the oil shale seams. The lower graph shows the general relationship in samples taken from Latrobe.

Fig. 6. Gas chromatograms of the aliphatic fractions of extracts from samples taken from Latrobe, Oonah and Douglas River and an example tricyclic (cheilanthane) structure. Numbers refer to carbon number; Pr = pristane; Ph = phytane; T = tricyclic alkane. Note that the Latrobe fraction was analysed using a different temperature program.

Fig. 7. Extended *m/z* 217 mass chromatograms for samples from Oonah and Douglas River. Numbers refer to carbon number; D = diasteranes; 20S and 20R refer to stereochemistry at carbon 20. Those denoted $\alpha\alpha\alpha$ 20R have biological stereochemistry, i.e. $5\alpha,14\alpha,17\alpha(H)$-20R with the other signals arising from "geological" isomers.

Fig. 8. Distribution of sterane and terpane biomarkers in the saturated hydrocarbon fraction isolated from the Latrobe sample. The data were acquired by gas chromatography-mass spectrometry using metastable reaction monitoring (MRM). Each trace is identified with the carbon number, the reaction as determined by the masses of the parent and daughter ions, and a normalised relative abundance. The last peak to elute in each sterane trace (i.e. those denoted ααα-20R) have 5α,14α,17α(H) - 20R stereochemistry with the other signals arising from "geological" isomers. The desmethyl steranes are 24-*n*-propylcholestane (C_{30}), 24-ethylcholestane (C_{29}), 24-methylcholestane (C_{28}) and cholestane (C_{27}). The C_{30} methylsteranes are 24-ethylcholestanes with an additional methyl group in ring-A i.e. 2α-methyl and 3β-methyl which are denoted 2α(Me), 3β(Me) respectively. Hopanes are denoted H, tricyclics T and unknown compounds U. Tricyclic terpenoids appear in each hopane reaction as artefacts of the MRM analysis using the linked scan technique. For example, T_{30} is specifically detected in the 416→191 reaction. It also appears as an artefact, along with T_{31} in the 412 →191 reaction.

Fig. 9. Distribution of sterane and terpane biomarkers in the saturated hydrocarbon fraction isolated from the Oonah sample, from GC-MS analysis with MRM (see Fig. 8 legend for an explanation of symbols).

Fig. 10. Distribution of sterane and terpane biomarkers in the saturated hydrocarbon fraction isolated from the Douglas River sample, from GC-MS analysis with MRM (see Fig. 8 legend for an explanation of symbols).

Fig. 11. Extended m/z 191 mass chromatogram for extracts from Latrobe, Oonah and Douglas River. Numbers refer to carbon number; T = Tricyclics; H = Hopane. Symbols refer to isomerisation at carbons 13 and 14. For example, βα refers to 13β(H), 14α(H). Assignments are taken from CHICARELLI et al. (1988). T_{25} structure is shown in Fig. 6.

Fig. 12. Gas chromatograms of the aromatic fractions isolated from samples collected at Latrobe, Oonah and Douglas River. Peak assignments are indicated by structures. The peak assigned as des-A-gammacerane was identified by the major ions in it's mass spectrum M^+ 274 (36 %), 259 (100), 244 (8), 230 (15), 229 (25), 228 (11), 215 (16).

Fig. 13. HI/Tmax plot showing the relative positions of the samples. Note the difference in maturity shown by the algal kerogen and the associated siltstone. The standard 0.5% Vitrinite reflectance contour is shown. 1 = Latrobe, 2 = Oonah upper seam whole rock, 3 = Oonah *Tasmanites* concentrate, 4 = Oonah lower seam *Tasmanites* concentrate, 5 = Oonah lower seam whole rock, 6 = Douglas River whole shale, 7,8,9 = Siltstone samples from above and below the oil shale at Oonah.

Fig. 14. Plot showing the distribution of activation energies in the Latrobe tasmanite kerogen. FF = Frequency Factor.

Fig. 15. Simulated maturation of the Latrobe tasmanite kerogen, compared with sterane isomerisation at C_{20}. Sterane activation energies used are those of MACKENZIE and McKENZIE (1983) -•- and MARZI and RULLKÖTTER (1992) -♦-, at 8 °C per million years. Tasmanite maturation is shown at 8 °C (-□-) and 2 °C (-■-) per million years.

Fig. 16. Plot showing the variation in $\delta^{13}C$ values for kerogen and for *n*-alkanes, tricyclic compounds and aromatic derivatives vs. carbon number. Data from this study are represented as: -■- Latrobe; -O- Oonah; -□- Douglas River; and -x- Sea-ice diatoms. Data previously reported by Simoneit et al. (1993) are represented as -●-. Groups of compounds are indicated as *n*-alkanes and cyclic compounds (tricyclic alkanes and aromatic derivatives). Numerals refer to structures in scheme 1, tricyclic alkanes are all of type I. Note that the $\delta^{13}C$ values of kerogen from Latrobe and Oonah are almost identical.

Fig. 17. Gas chromatograms showing the aliphatic hydrocarbons from (a) the original extract and from closed-system pyrolysis of *tasmanite* kerogen, isolated from a sample collected at Latrobe, at (b) 300 °C, (c) 330 °C and (d) 350 °C. Note the progressive increase in low molecular weight *n*-alkanes and the relative decrease in tricyclic compounds.

Fig. 18. Chart showing the $\delta^{13}C$ values of :

a) *n*-alkanes liberated by pyrolysis at 300 °C -◇-, 330 °C -◆- and 350 °C -□- of tasmanite kerogen from Latrobe (AGSO sample # 1995), compared with the original extract -■-.

b) tricyclic hydrocarbons (structures I-VII in scheme 1) from Latrobe (extract and pyrolysate, symbols as in (a)).

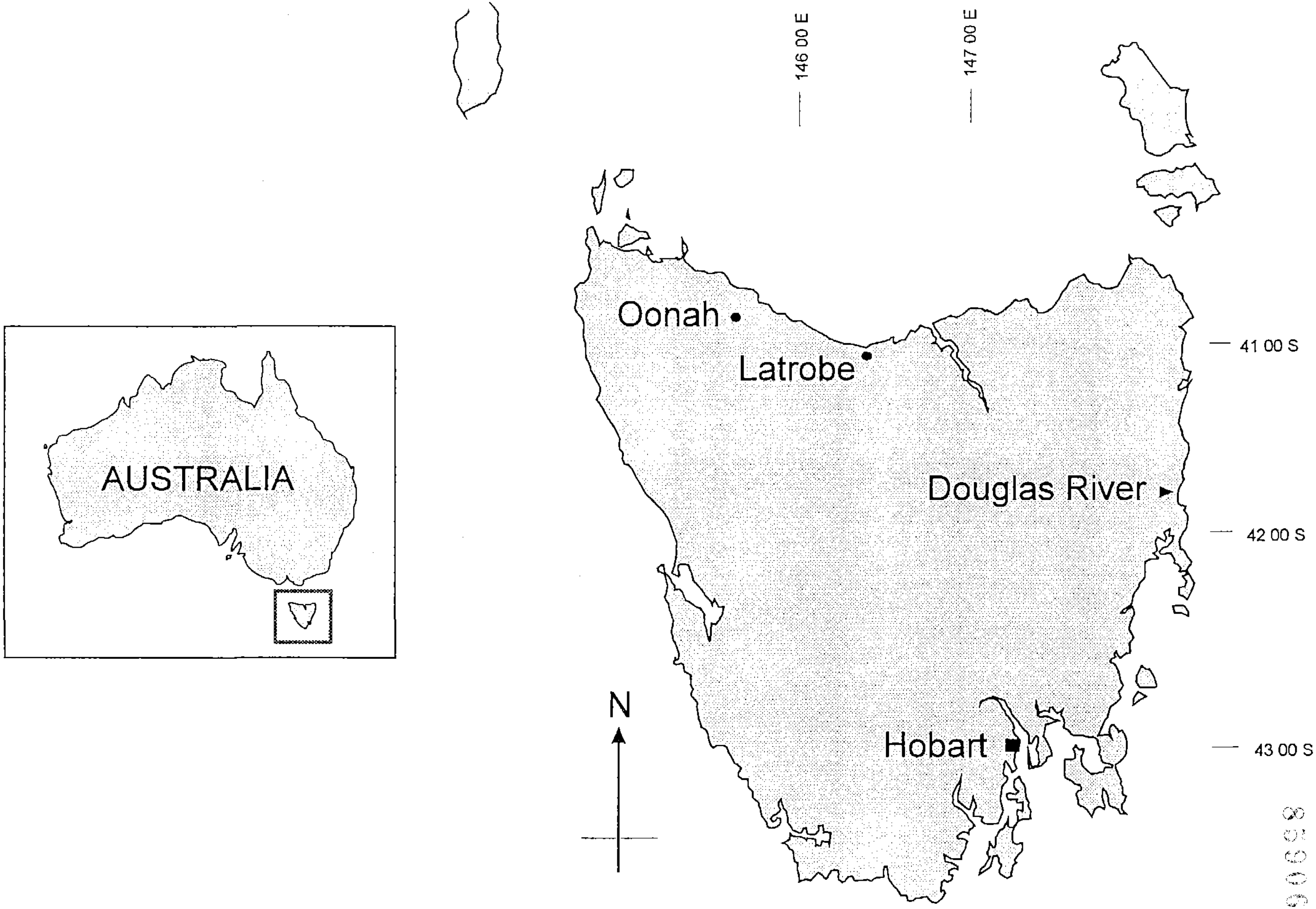
146 00 E
147 00 E
AUSTRALIA
Oonah
Latrobe
Douglas River
Hobart
N
41 00 S
42 00 S
43 00 S

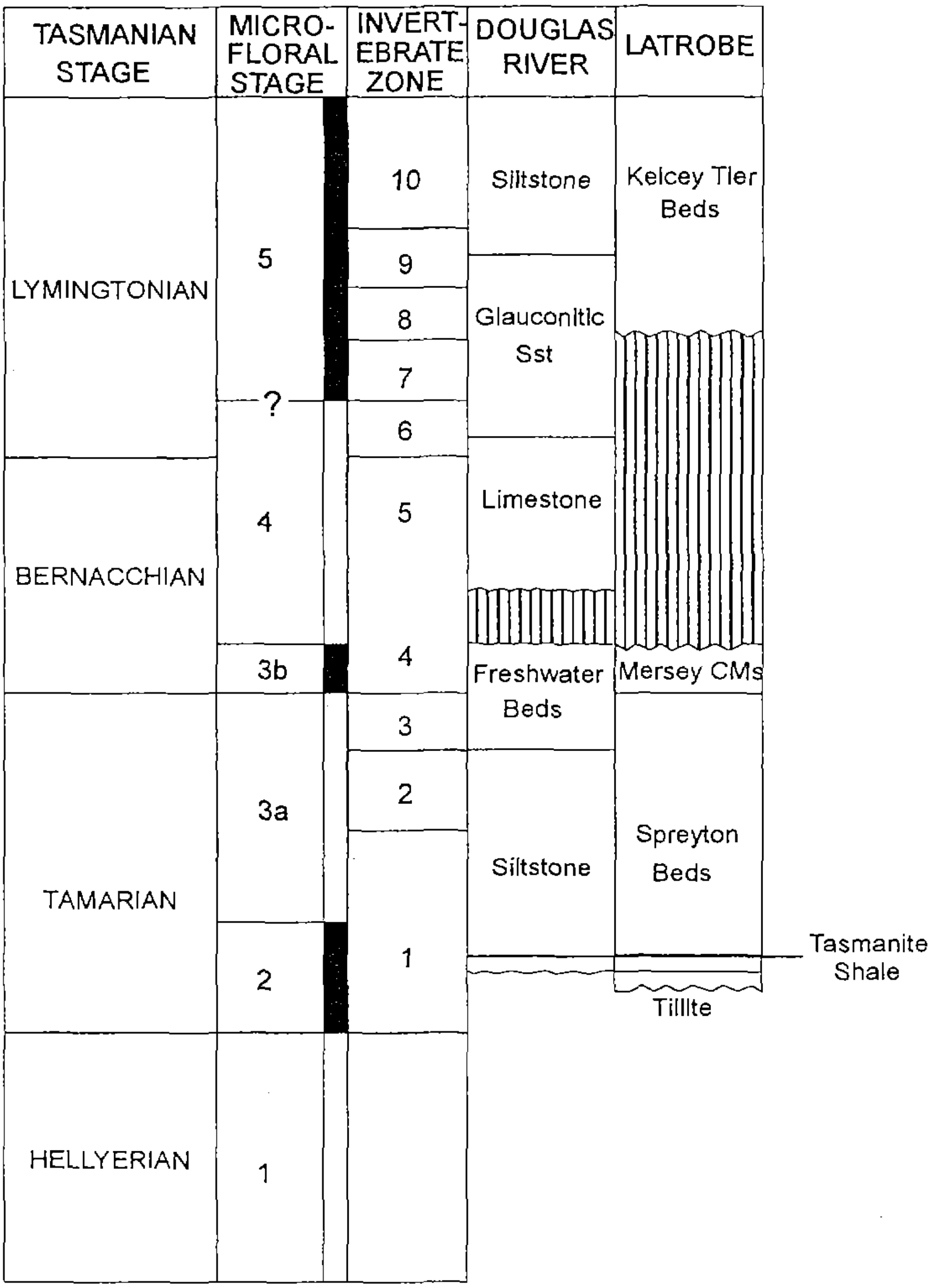
TASMANIAN STAGE
MICRO-FLORAL STAGE
INVERT-EBRATE ZONE
DOUGLAS RIVER
LATROBE
LYMINGTONIAN
BERNACCHIAN
TAMARIAN
HELLYERIAN
5
?
4
3b
3a
2
1
10
9
8
7
6
5
4
3
2
1
Siltstone
Glauconitic Sst
Limestone
Freshwater Beds
Siltstone
Kelcey Tier Beds
Mersey CMs
Spreyton Beds
Tasmanite Shale
Tillite

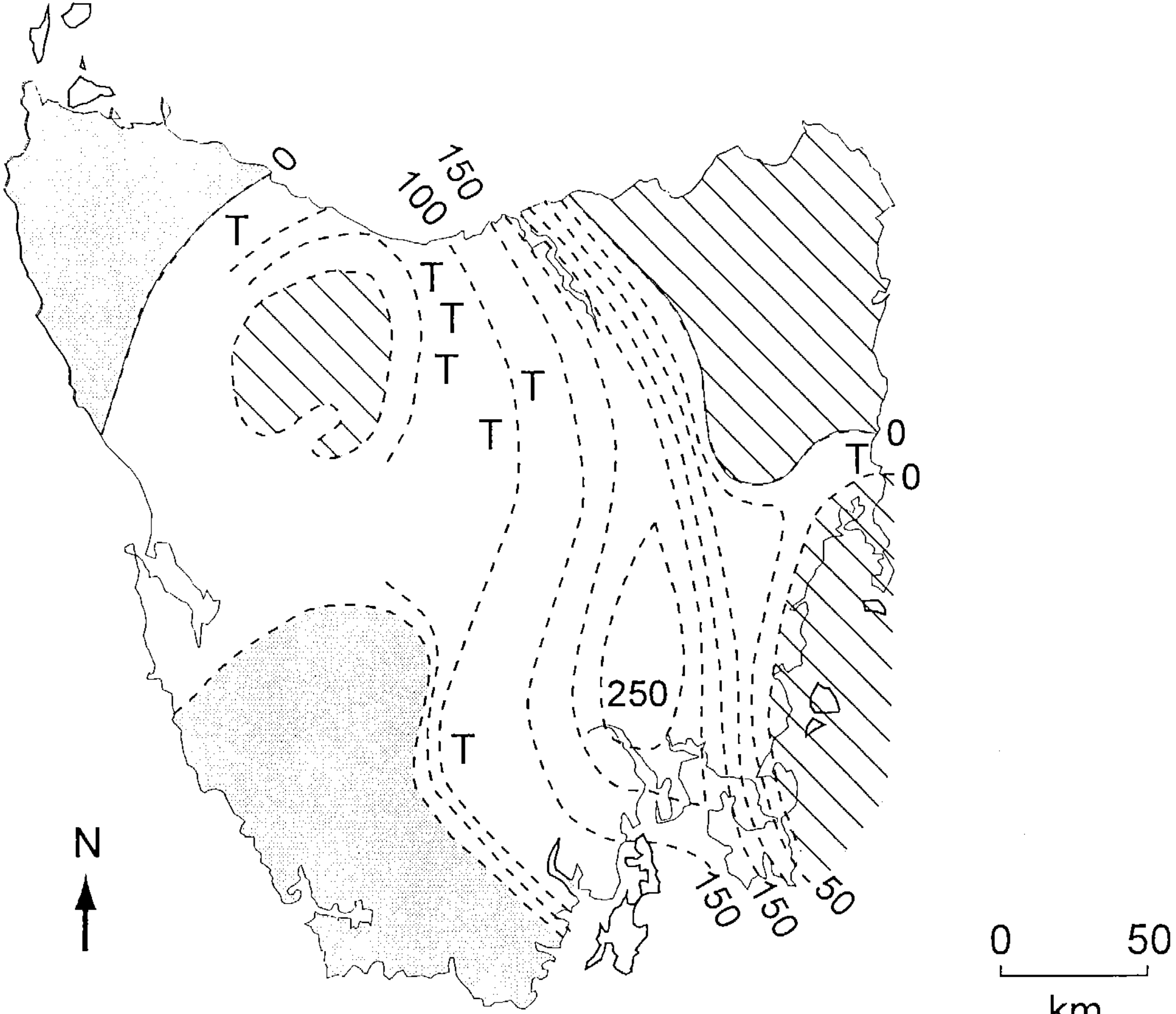
0
150
100
T
T
T
T
T
T
0
T
0
250
T
150
150
50
N
0
50
km
859065

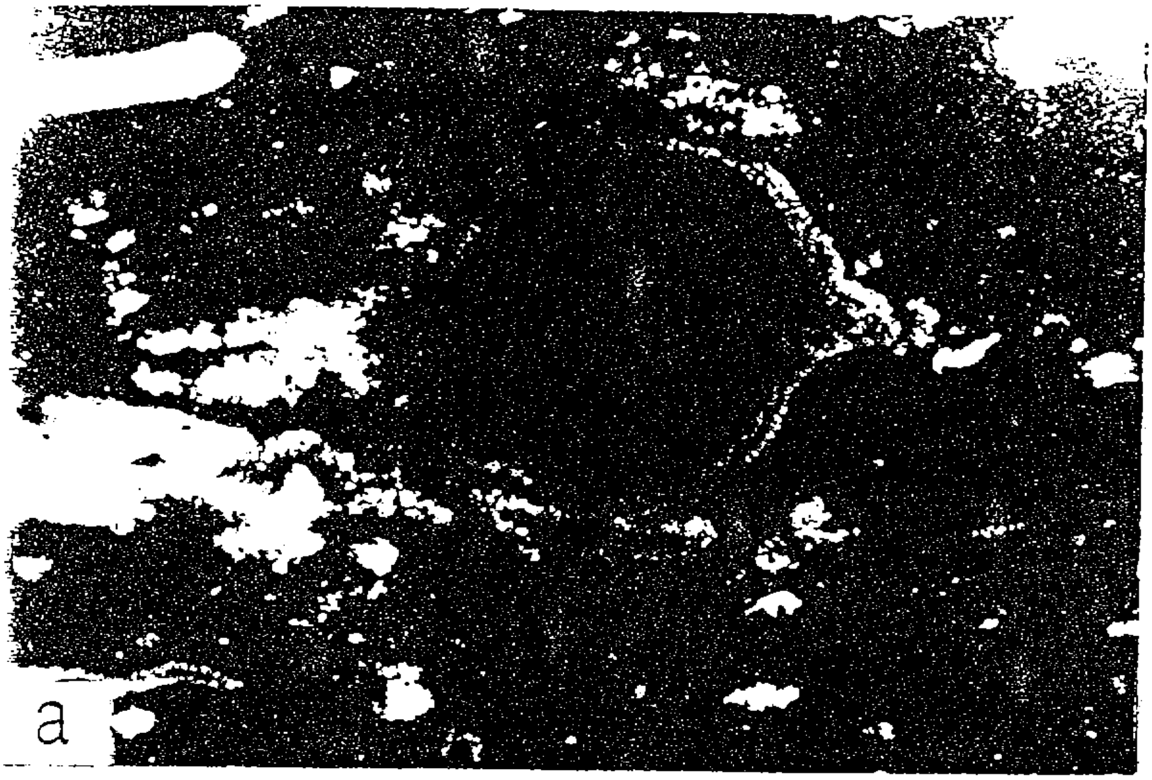
a

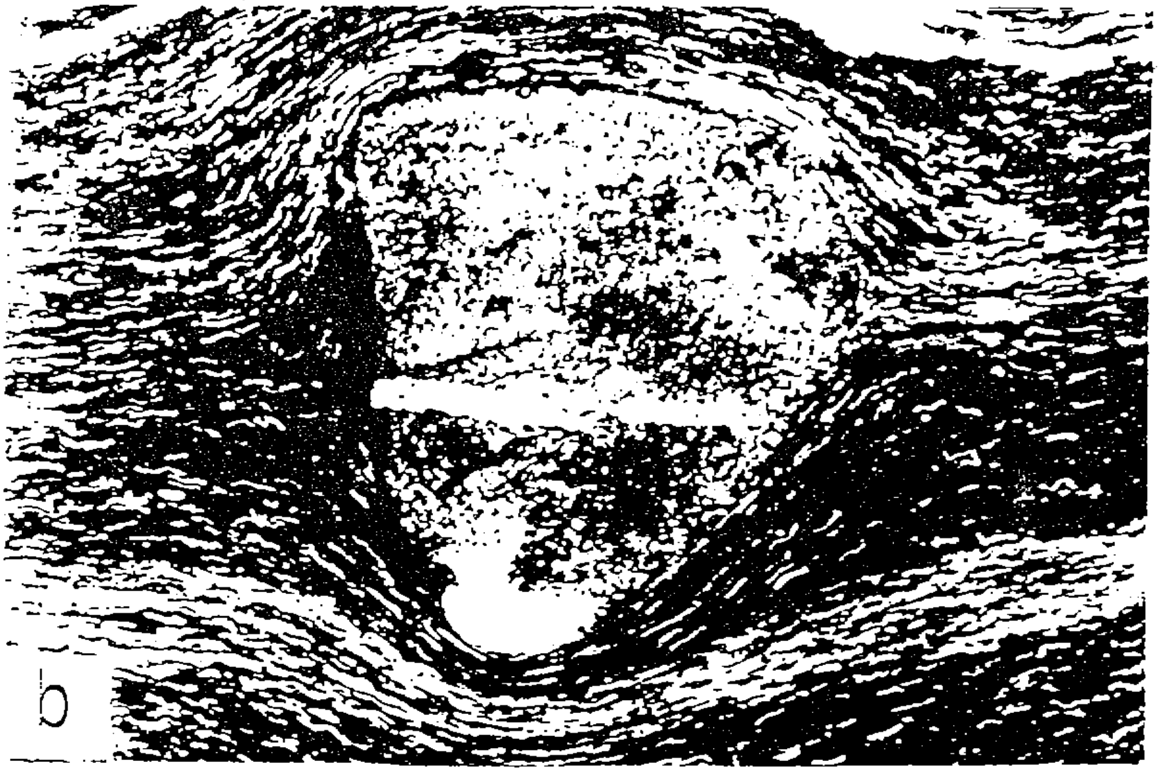
b

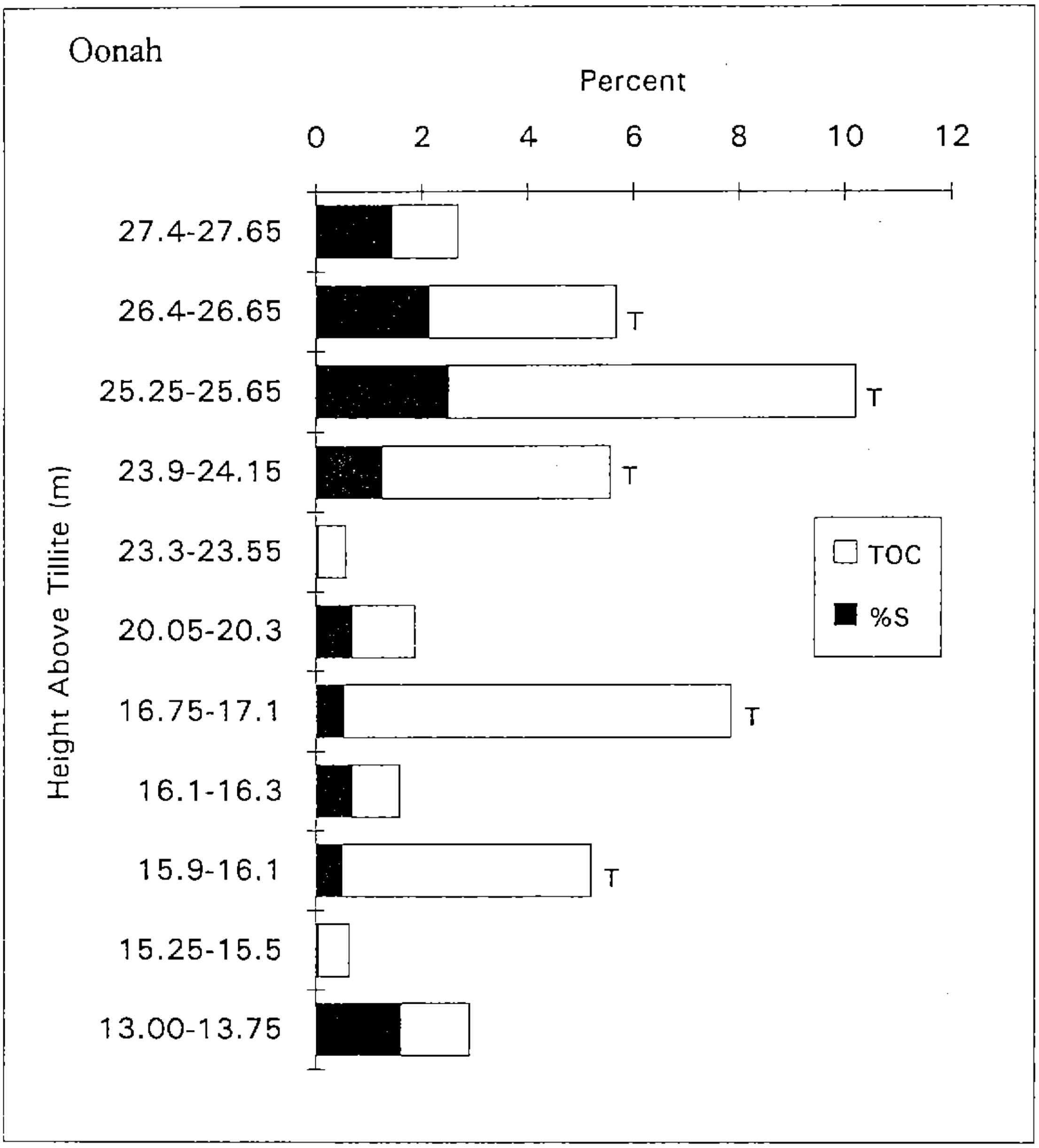
Oonah
Percent
0
2
4
6
8
10
12
27.4-27.65
26.4-26.65
25.25-25.65
23.9-24.15
23.3-23.55
20.05-20.3
16.75-17.1
16.1-16.3
15.9-16.1
15.25-15.5
13.00-13.75
Height Above Tillite (m)
T
T
T
T
T
☐ TOC
■ %S

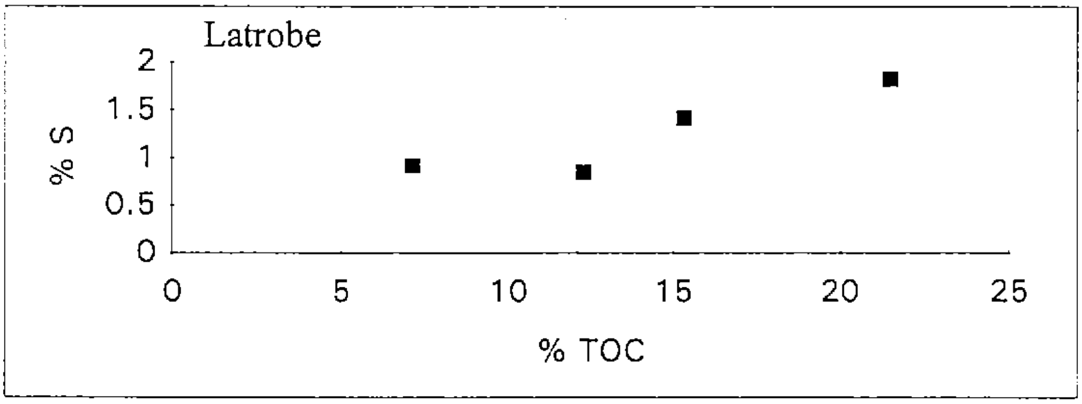
Latrobe
2
1.5
1
0.5
0
% S
0
5
10
15
20
25
% TOC

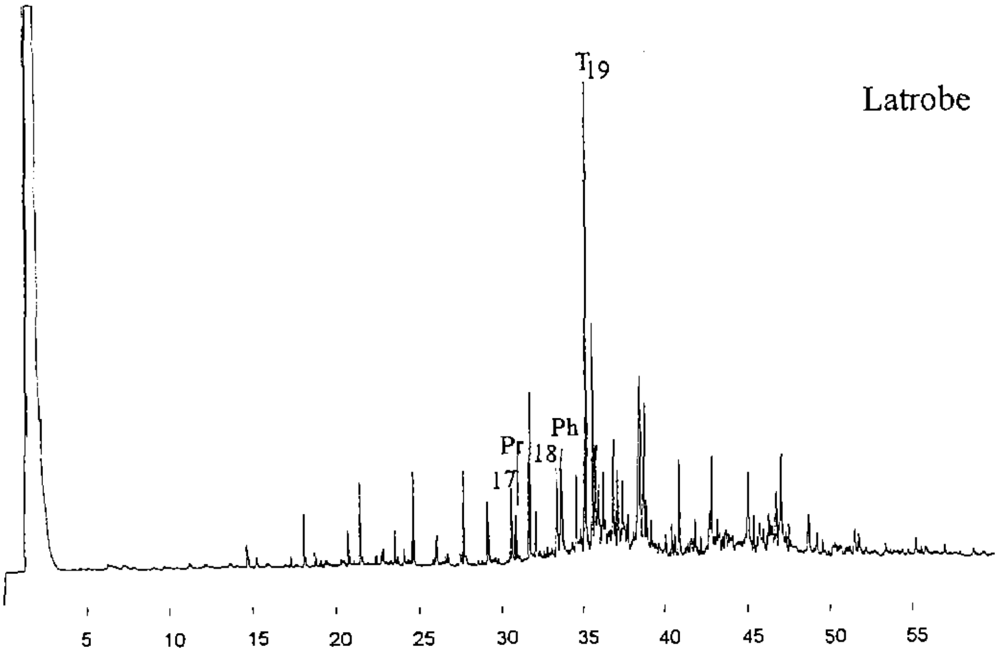
Latrobe
T_{19}
Pr
Ph
17
18
5
10
15
20
25
30
35
40
45
50
55

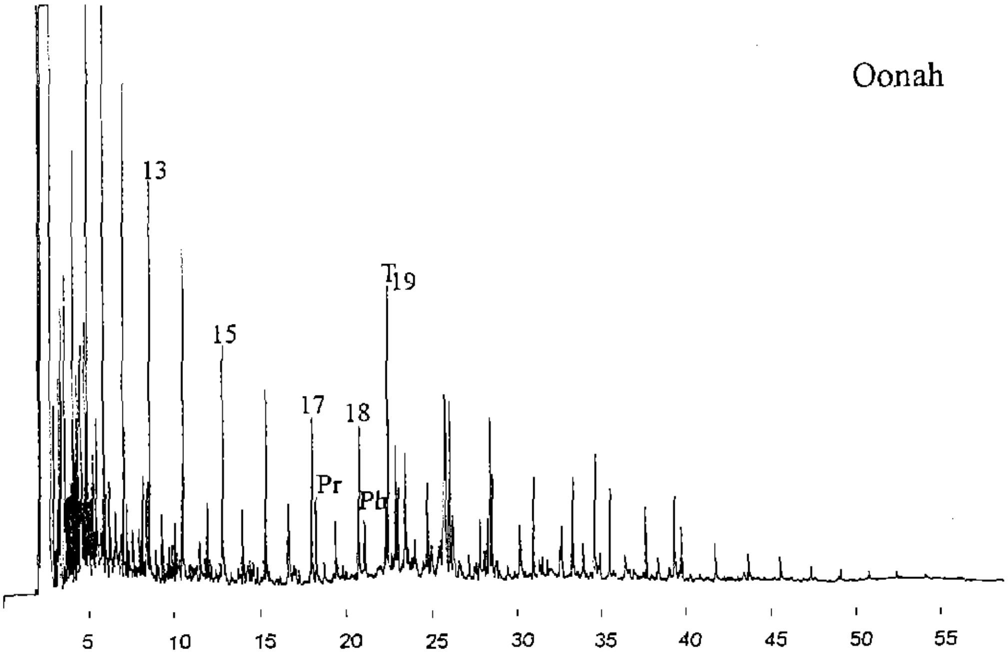
Oonah
13
15
T_{19}
17
18
Pr
Ph
5
10
15
20
25
30
35
40
45
50
55

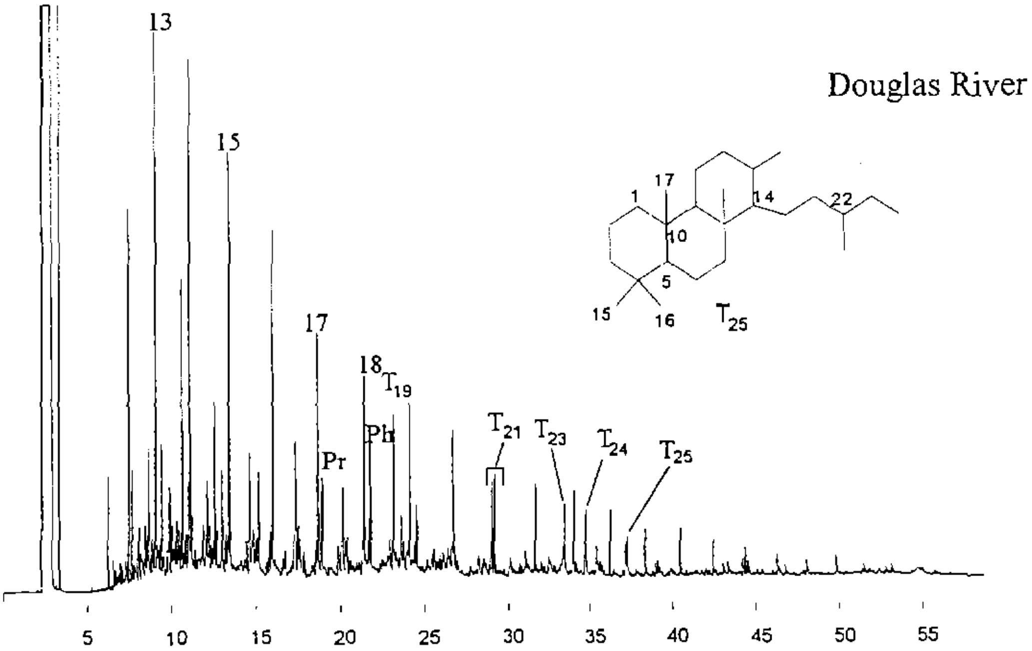
Douglas River
13
15
17
18
T_{19}
Pr
Ph
T_{21}
T_{23}
T_{24}
T_{25}
1
17
10
14
22
5
15
16
T_{25}
5
10
15
20
25
30
35
40
45
50
55

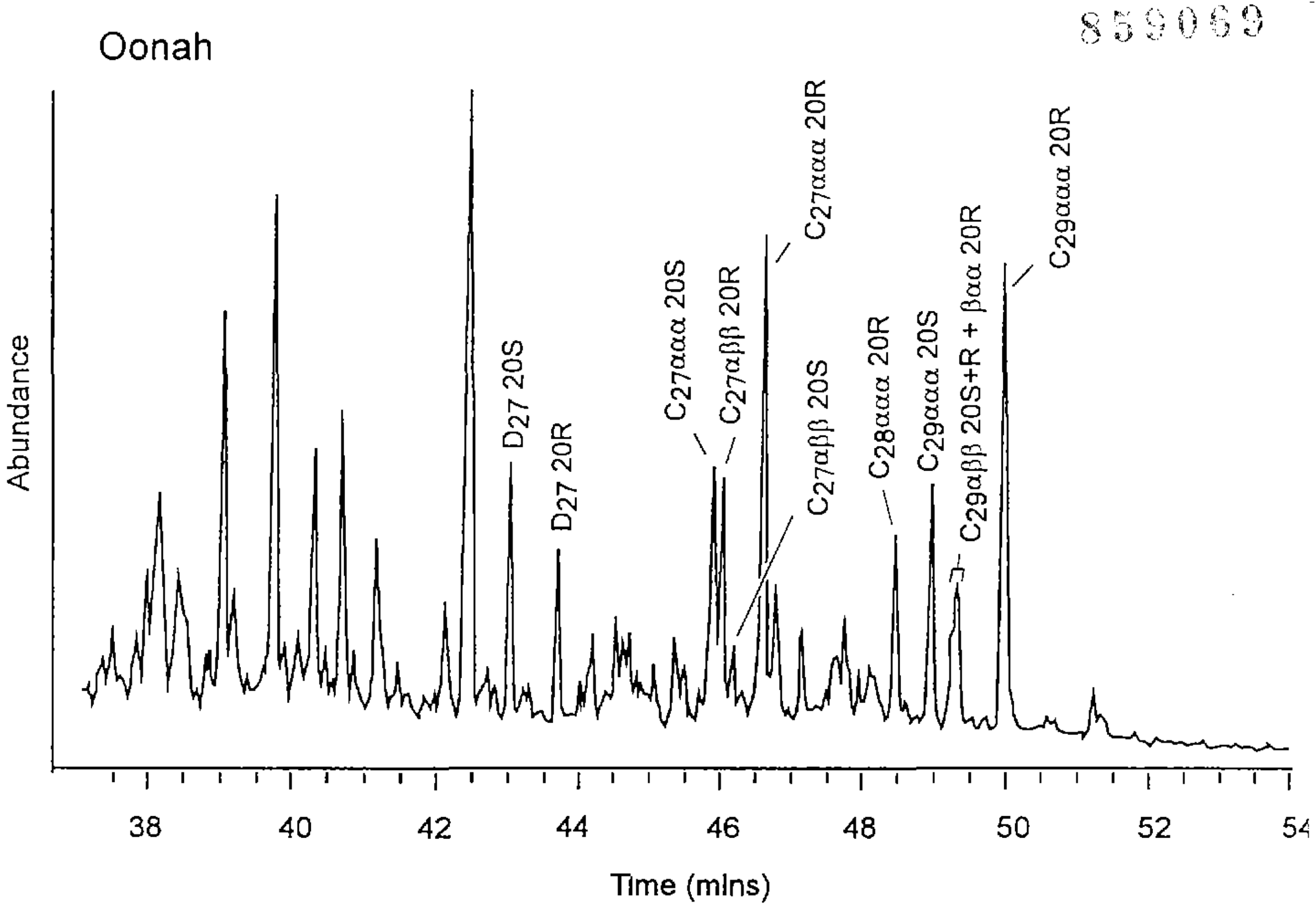
Oonah
Abundance
D$_{27}$ 20S
D$_{27}$ 20R
C$_{27}\alpha\alpha\alpha$ 20S
C$_{27}\alpha\beta\beta$ 20R
C$_{27}\alpha\alpha\alpha$ 20R
C$_{27}\alpha\beta\beta$ 20S
C$_{28}\alpha\alpha\alpha$ 20R
C$_{29}\alpha\alpha\alpha$ 20S
C$_{29}\alpha\beta\beta$ 20S+R + $\beta\alpha\alpha$ 20R
C$_{29}\alpha\alpha\alpha$ 20R
38
40
42
44
46
48
50
52
54
Time (mins)

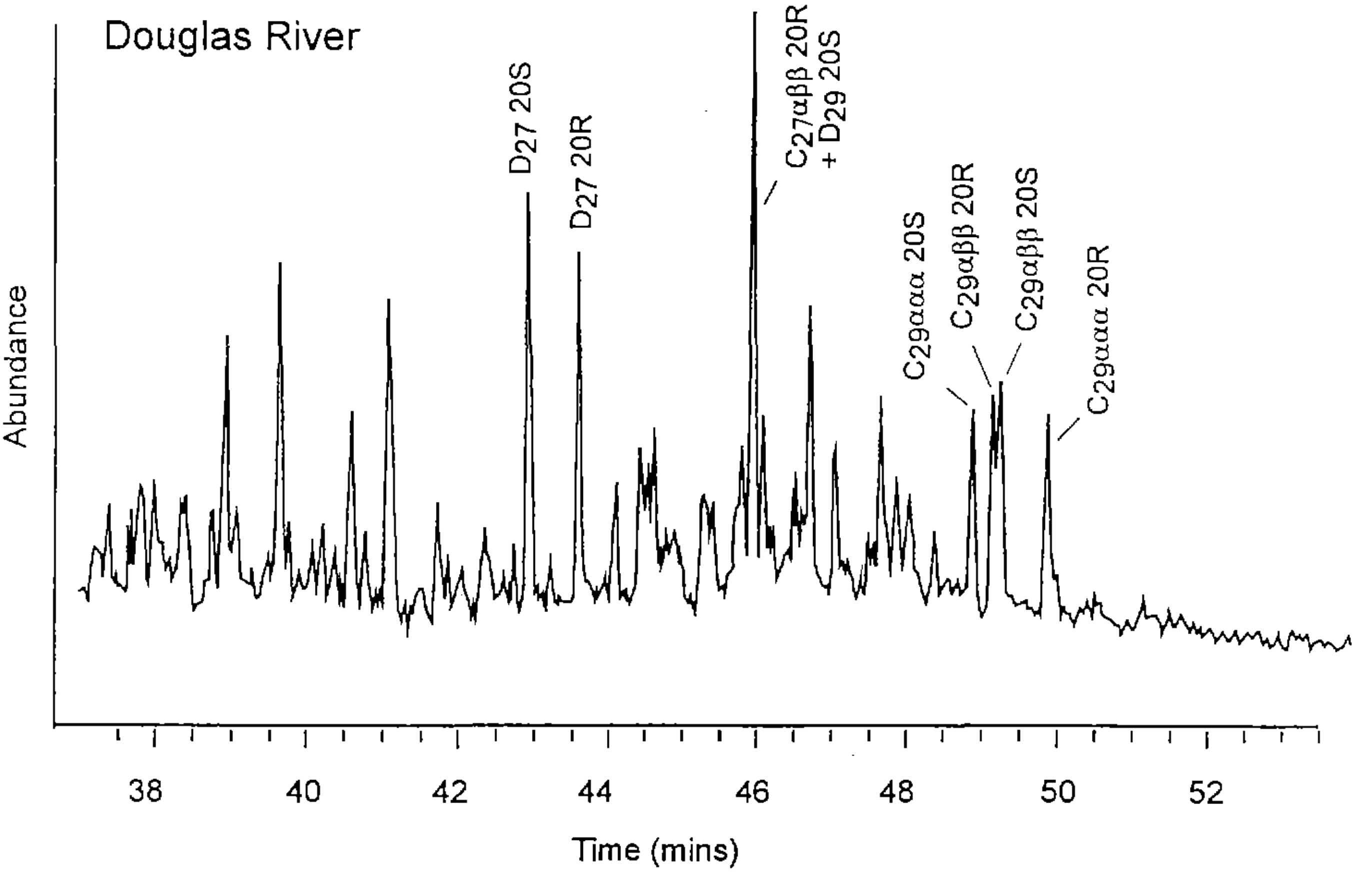
Douglas River
Abundance
D$_{27}$ 20S
D$_{27}$ 20R
C$_{27}\alpha\beta\beta$ 20R + D$_{29}$ 20S
C$_{29}\alpha\alpha\alpha$ 20S
C$_{29}\alpha\beta\beta$ 20R
C$_{29}\alpha\beta\beta$ 20S
C$_{29}\alpha\alpha\alpha$ 20R
38
40
42
44
46
48
50
52
Time (mins)

AGSO #1995 Latrobe tasmanite

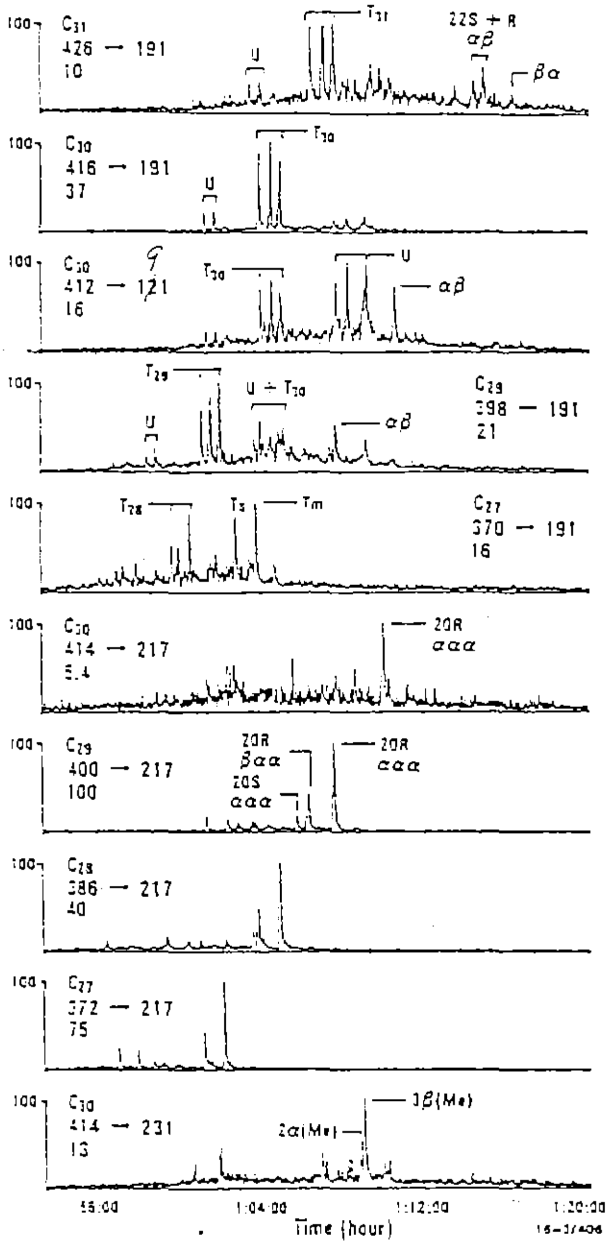

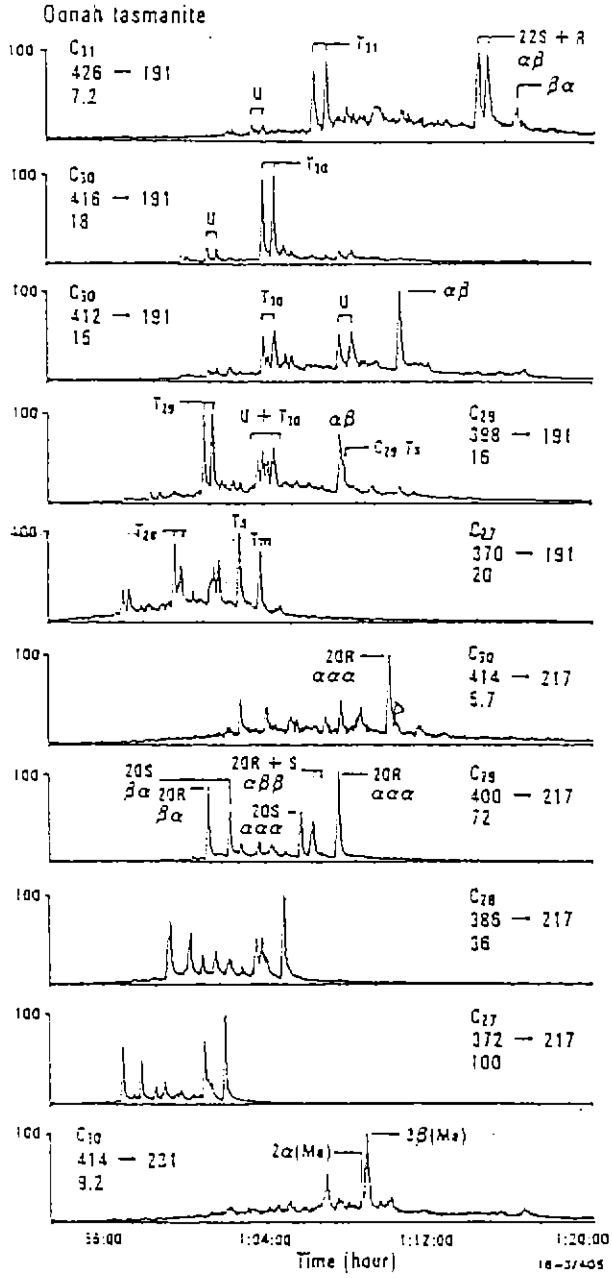
Oonah tasmanite
100
C31
426 → 191
7.2
U
T31
22S + R
αβ
βα
C30
416 → 191
18
U
T30
C30
412 → 191
15
T30
U
αβ
T29
U + T30
αβ
C29 Ts
C29
398 → 191
16
T28
Ts
Tm
C27
370 → 191
20
20R
ααα
C30
414 → 217
5.7
20S
βα
20R
βα
20R + S
αββ
20S
ααα
20R
ααα
C29
400 → 217
72
C28
386 → 217
36
C27
372 → 217
100
C30
414 → 231
9.2
2α(Me)
3β(Me)
56:00
1:04:00
1:12:00
1:20:00
Time (hour)
16-3/405

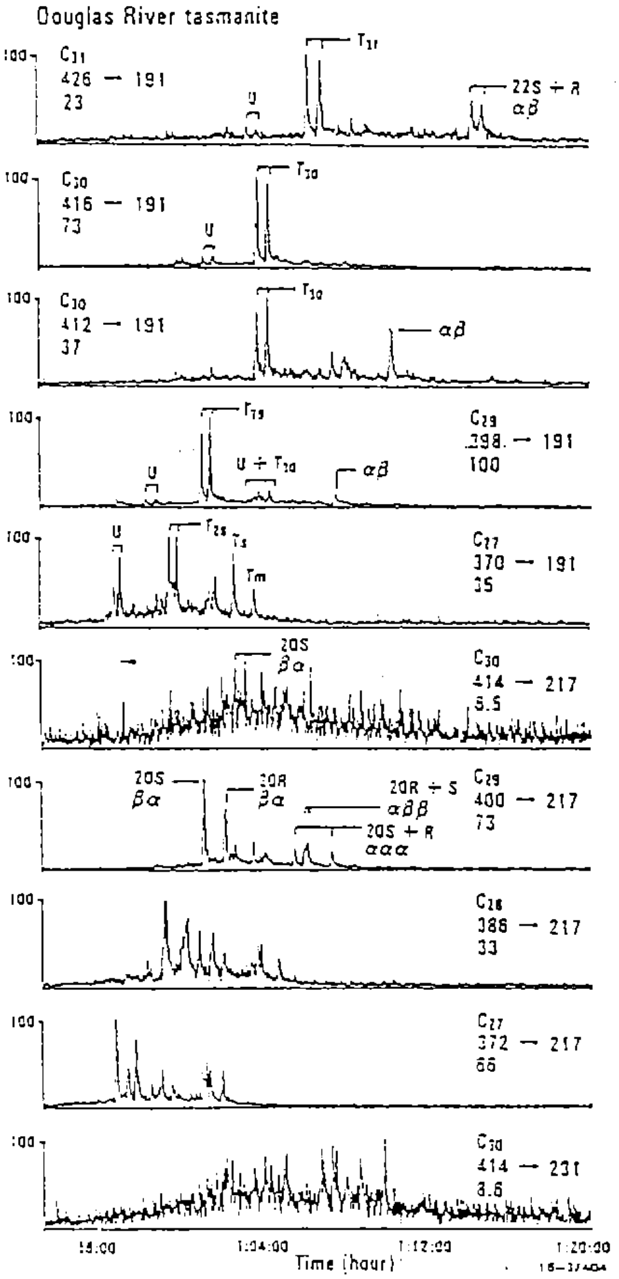
Douglas River tasmanite
100
C31
426 → 191
23
U
T31
22S + R
αβ
C30
416 → 191
73
U
T30
C30
412 → 191
37
T30
αβ
C29
398 → 191
100
U
T29
U + T30
αβ
C27
370 → 191
35
U
T28
Ts
Tm
C30
414 → 217
5.5
20S
βα
C29
400 → 217
73
20S
βα
20R
βα
20R + S
αββ
20S + R
ααα
C28
386 → 217
33
C27
372 → 217
66
C30
414 → 231
8.6
56:00
1:04:00
1:12:00
1:20:00
Time (hour)
16-37404

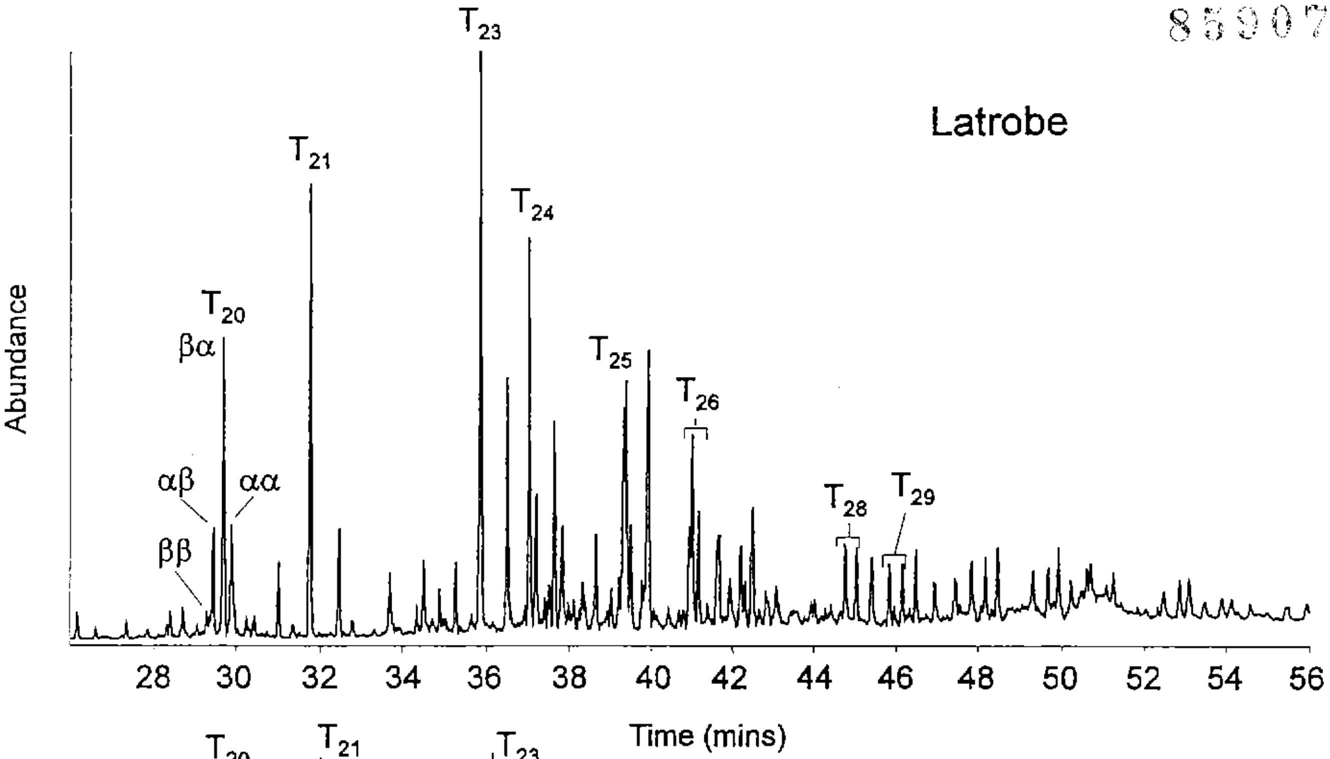
Latrobe
Abundance
T$_{23}$
T$_{21}$
T$_{24}$
T$_{20}$
βα
T$_{25}$
T$_{26}$
αβ
αα
ββ
T$_{28}$
T$_{29}$
28
30
32
34
36
38
40
42
44
46
48
50
52
54
56
Time (mins)

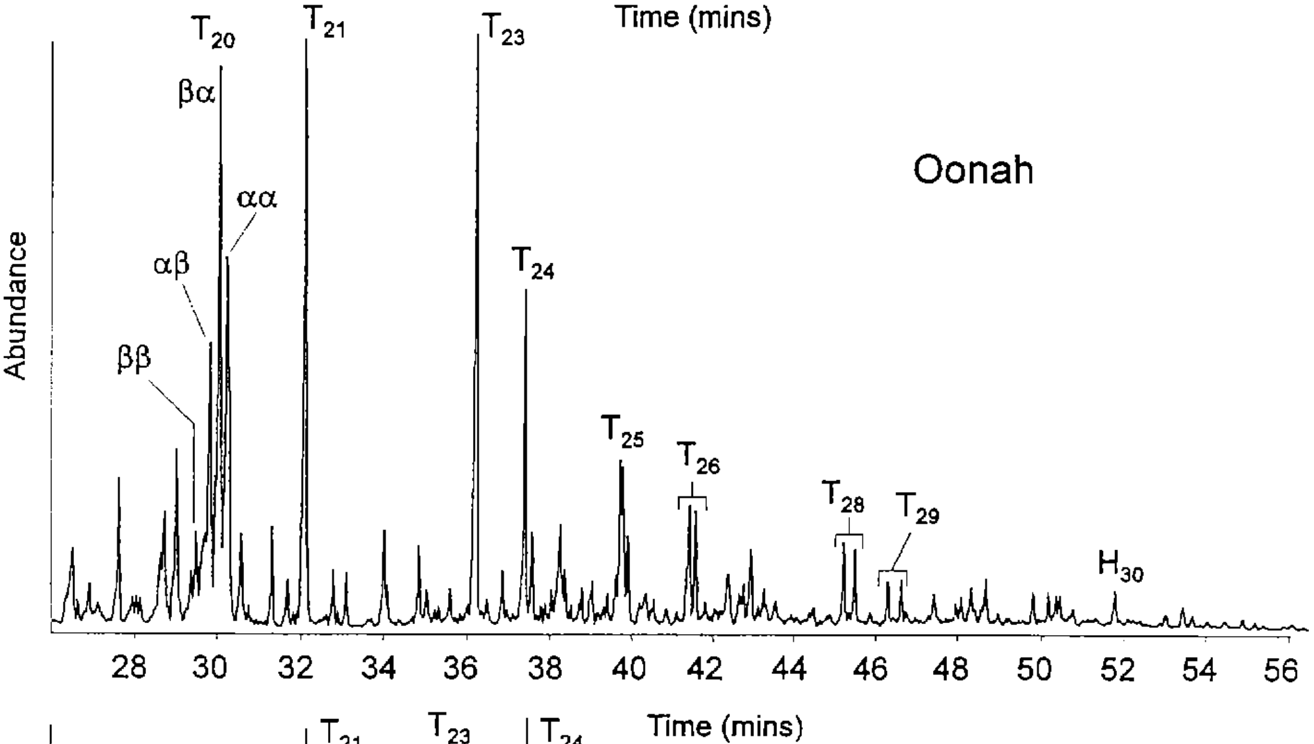
Oonah
Abundance
T$_{20}$
T$_{21}$
T$_{23}$
βα
αα
αβ
T$_{24}$
ββ
T$_{25}$
T$_{26}$
T$_{28}$
T$_{29}$
H$_{30}$
28
30
32
34
36
38
40
42
44
46
48
50
52
54
56
Time (mins)

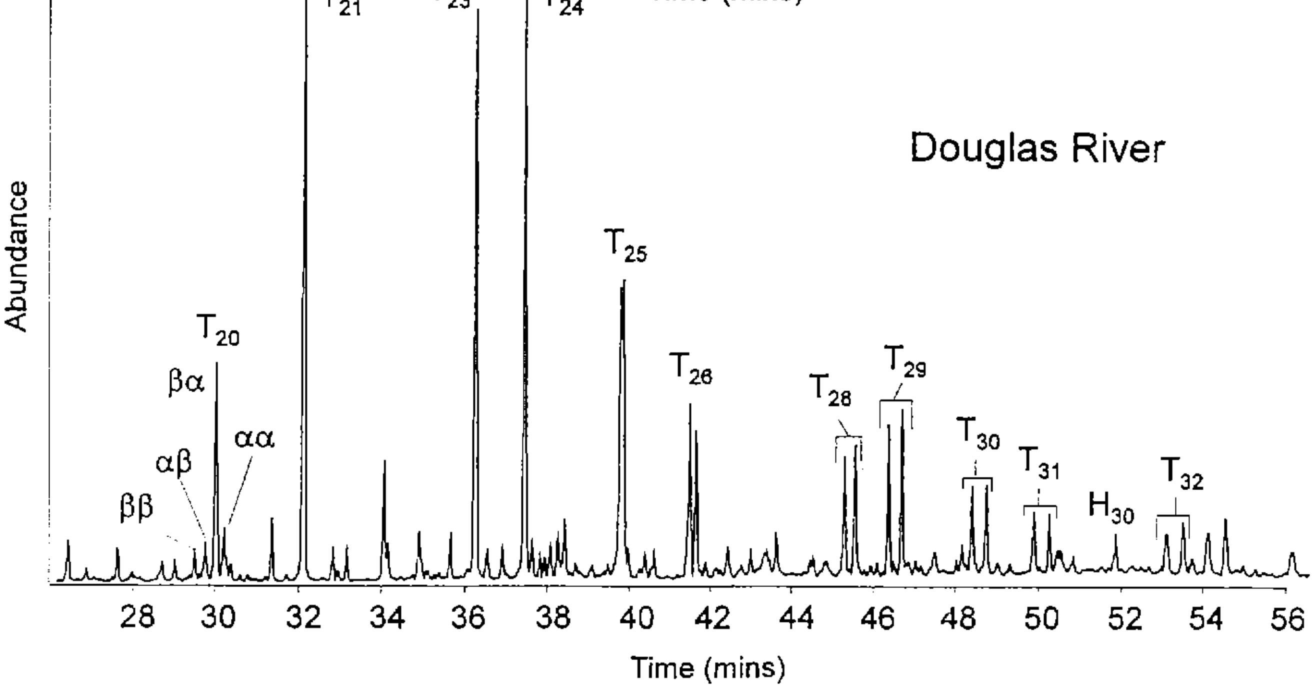
Douglas River
Abundance
T$_{21}$
T$_{23}$
T$_{24}$
T$_{25}$
T$_{20}$
βα
αβ
αα
ββ
T$_{26}$
T$_{28}$
T$_{29}$
T$_{30}$
T$_{31}$
H$_{30}$
T$_{32}$
28
30
32
34
36
38
40
42
44
46
48
50
52
54
56
Time (mins)

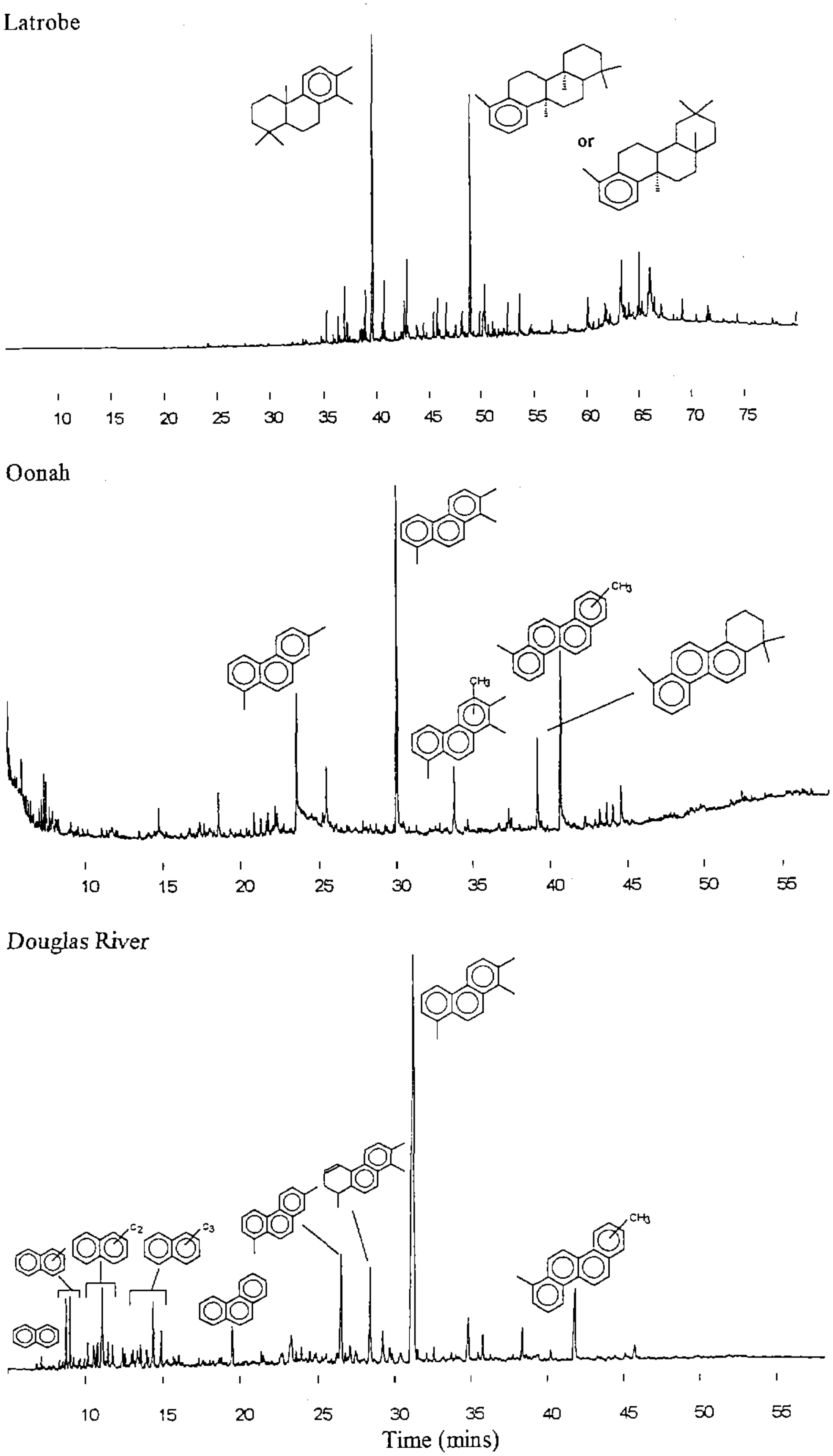
Latrobe
or
10 15 20 25 30 35 40 45 50 55 60 65 70 75
Oonah
CH3
CH3
10 15 20 25 30 35 40 45 50 55
Douglas River
C2
C3
CH3
10 15 20 25 30 35 40 45 50 55
Time (mins)

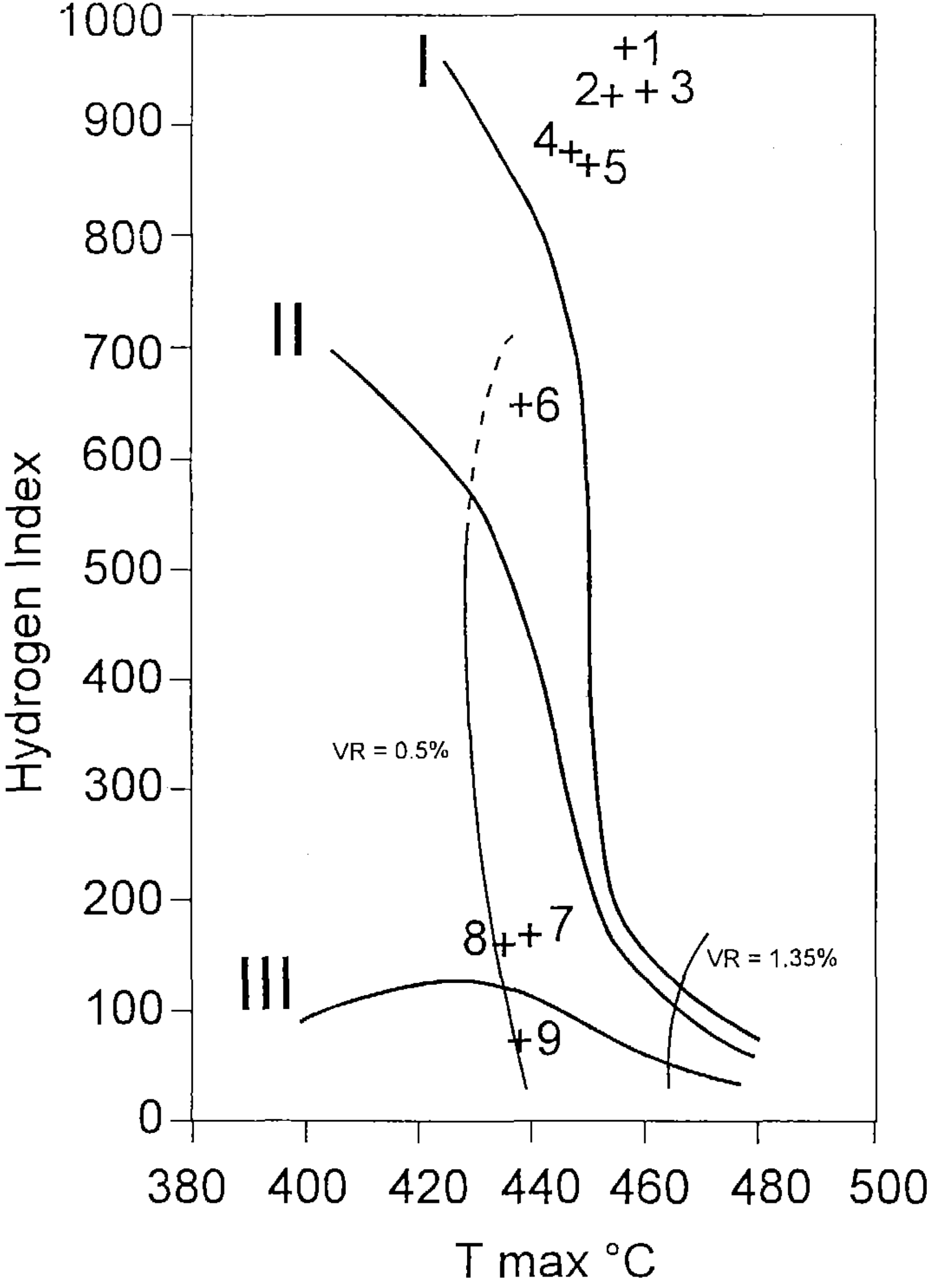
1000
900
800
700
600
500
400
300
200
100
0
Hydrogen Index
380
400
420
440
460
480
500
T max °C
I
II
III
+1
2+
+ 3
4+
+5
+6
8+
+ 7
+9
VR = 0.5%
VR = 1.35%

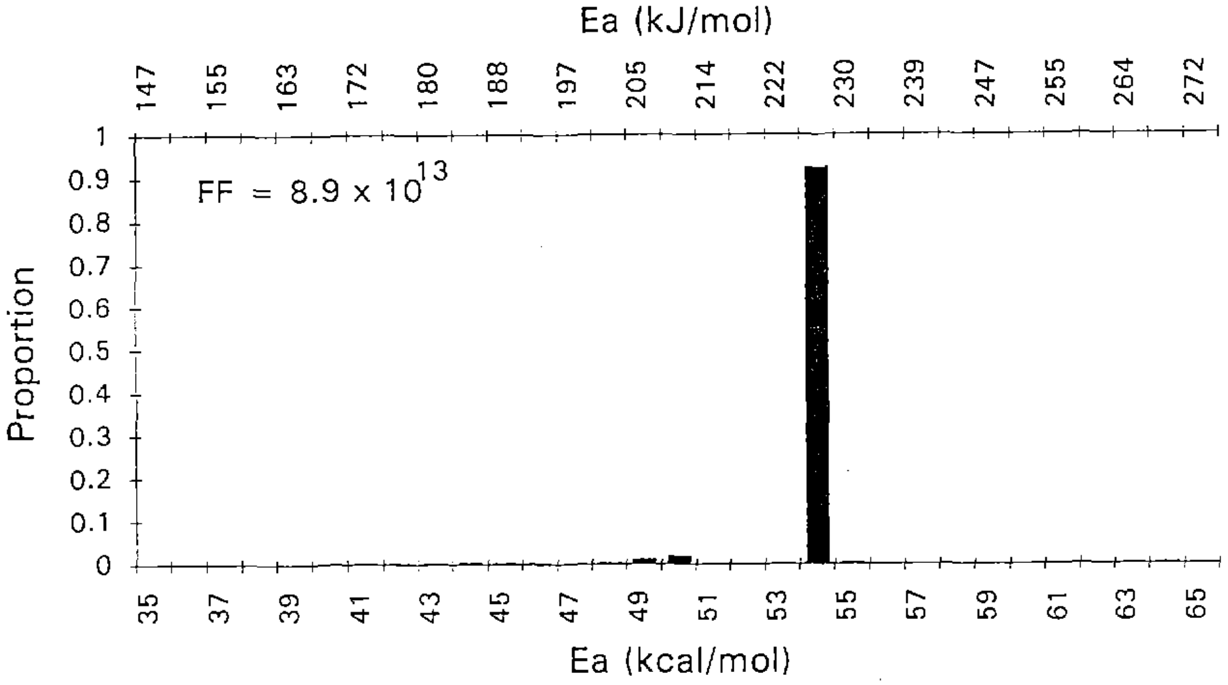
Ea (kJ/mol)
147
155
163
172
180
188
197
205
214
222
230
239
247
255
264
272
FF = 8.9 x 10^{13}
Proportion
1
0.9
0.8
0.7
0.6
0.5
0.4
0.3
0.2
0.1
0
35
37
39
41
43
45
47
49
51
53
55
57
59
61
63
65
Ea (kcal/mol)

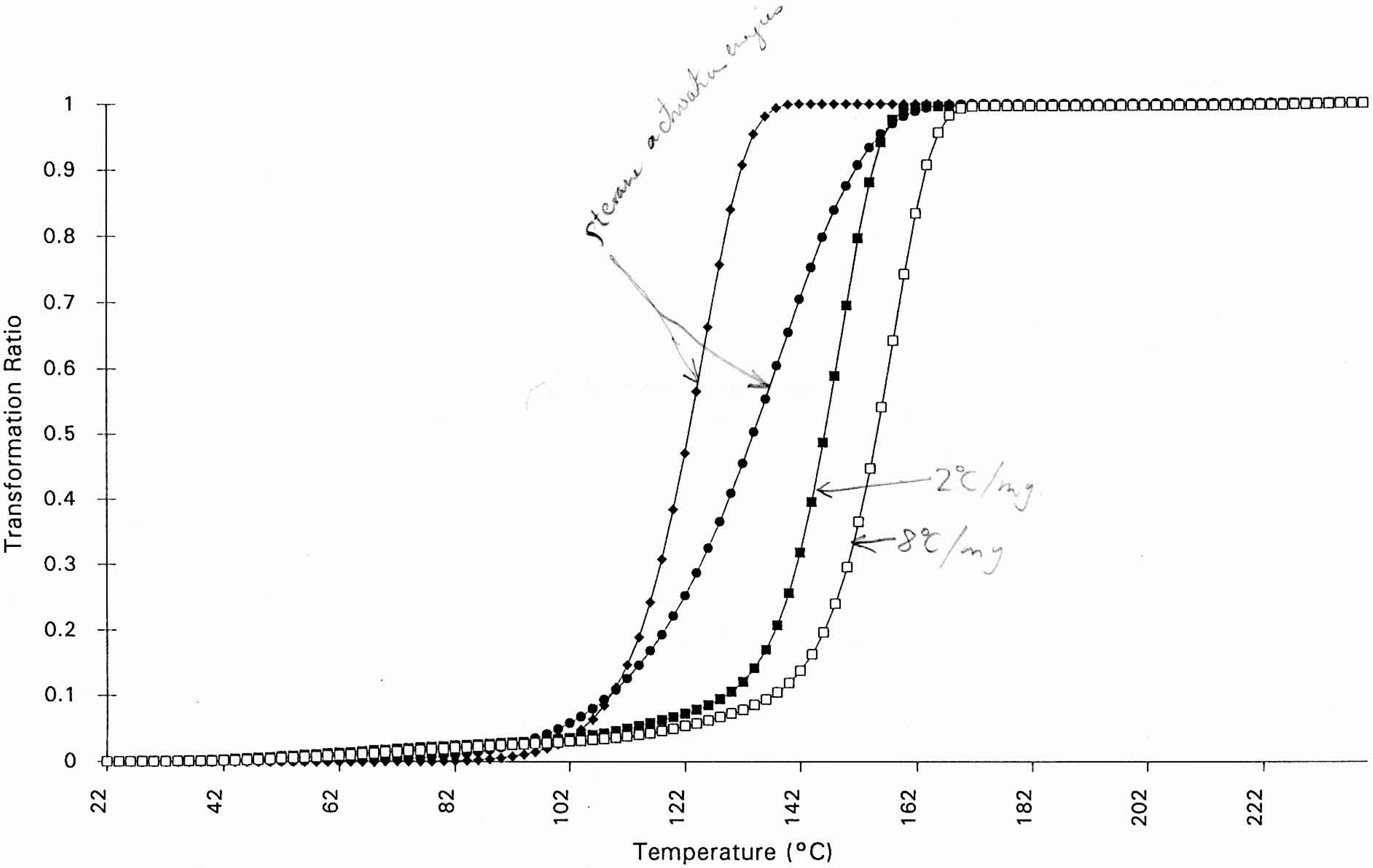
Sterane activation energies
2°C/my
8°C/my
Transformation Ratio
0
0.1
0.2
0.3
0.4
0.5
0.6
0.7
0.8
0.9
1
22
42
62
82
102
122
142
162
182
202
222
Temperature (°C)

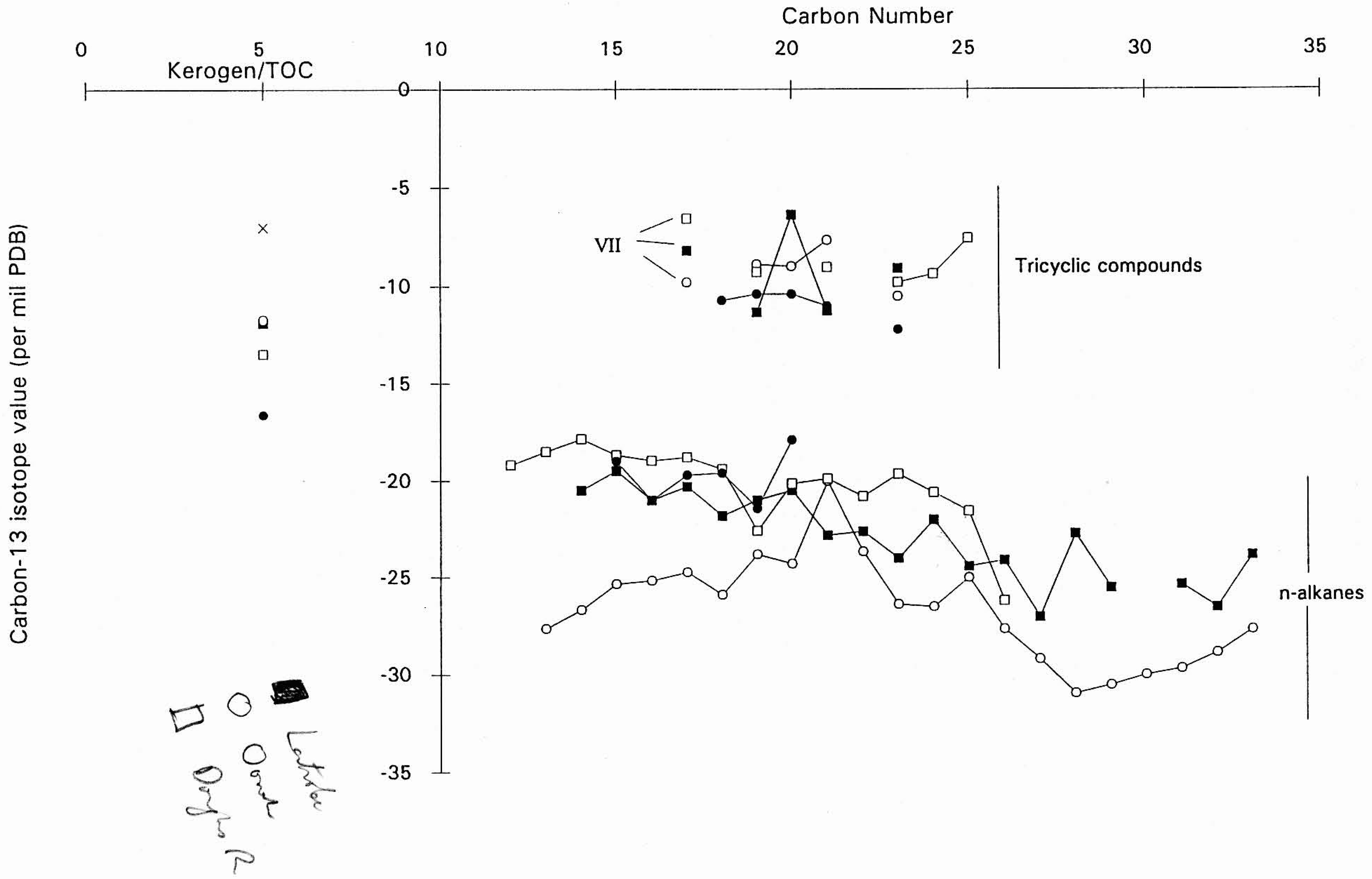
Carbon Number
0
5
10
15
20
25
30
35
Kerogen/TOC
0
-5
-10
-15
-20
-25
-30
-35
Carbon-13 isotope value (per mil PDB)
VII
Tricyclic compounds
n-alkanes
■ Latrobe
○ Oonah
□ Douglas R

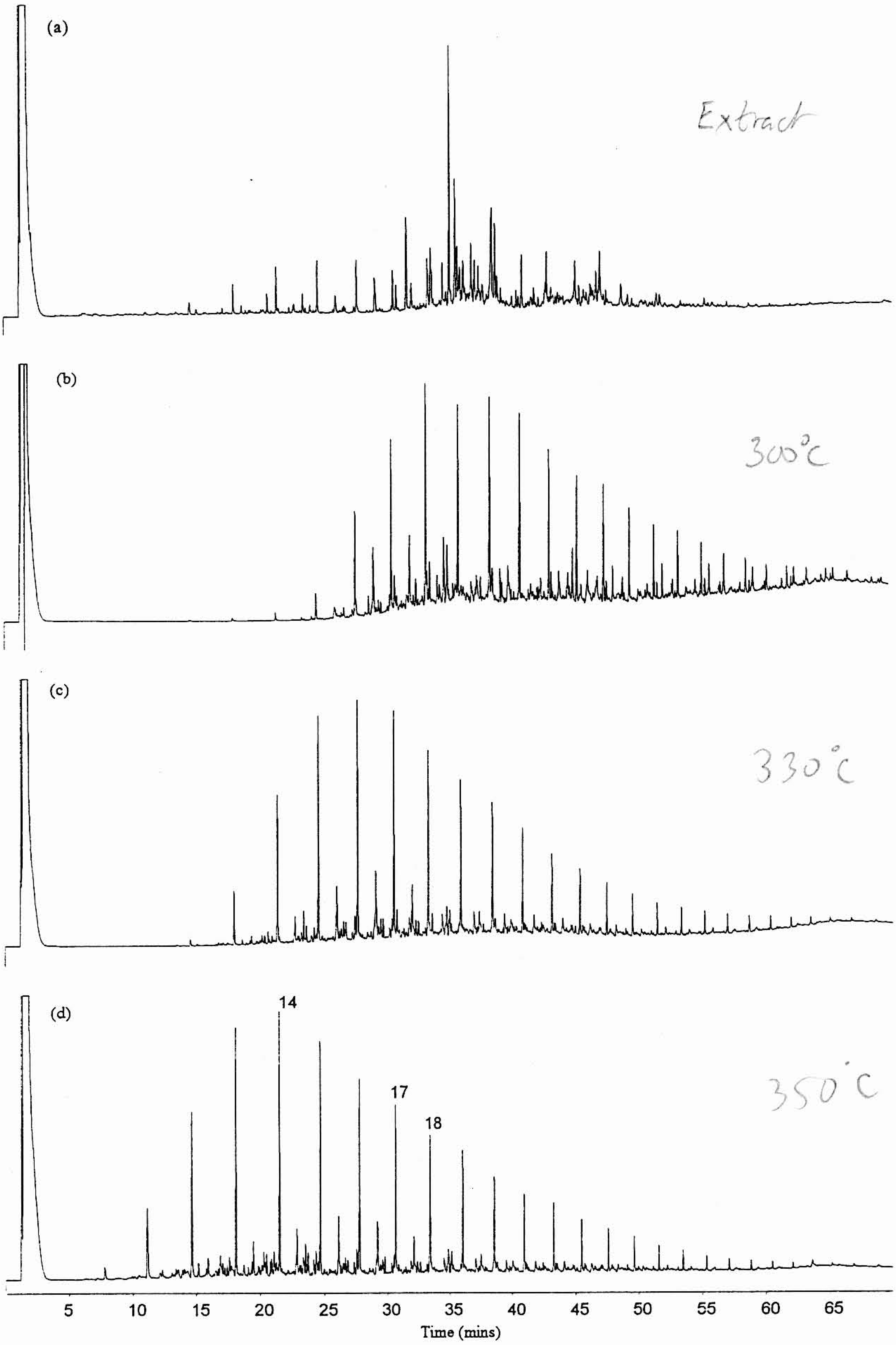
(a)
Extract
(b)
300°C
(c)
330°C
(d)
14
17
18
350°C
5
10
15
20
25
30
35
40
45
50
55
60
65
Time (mins)

44

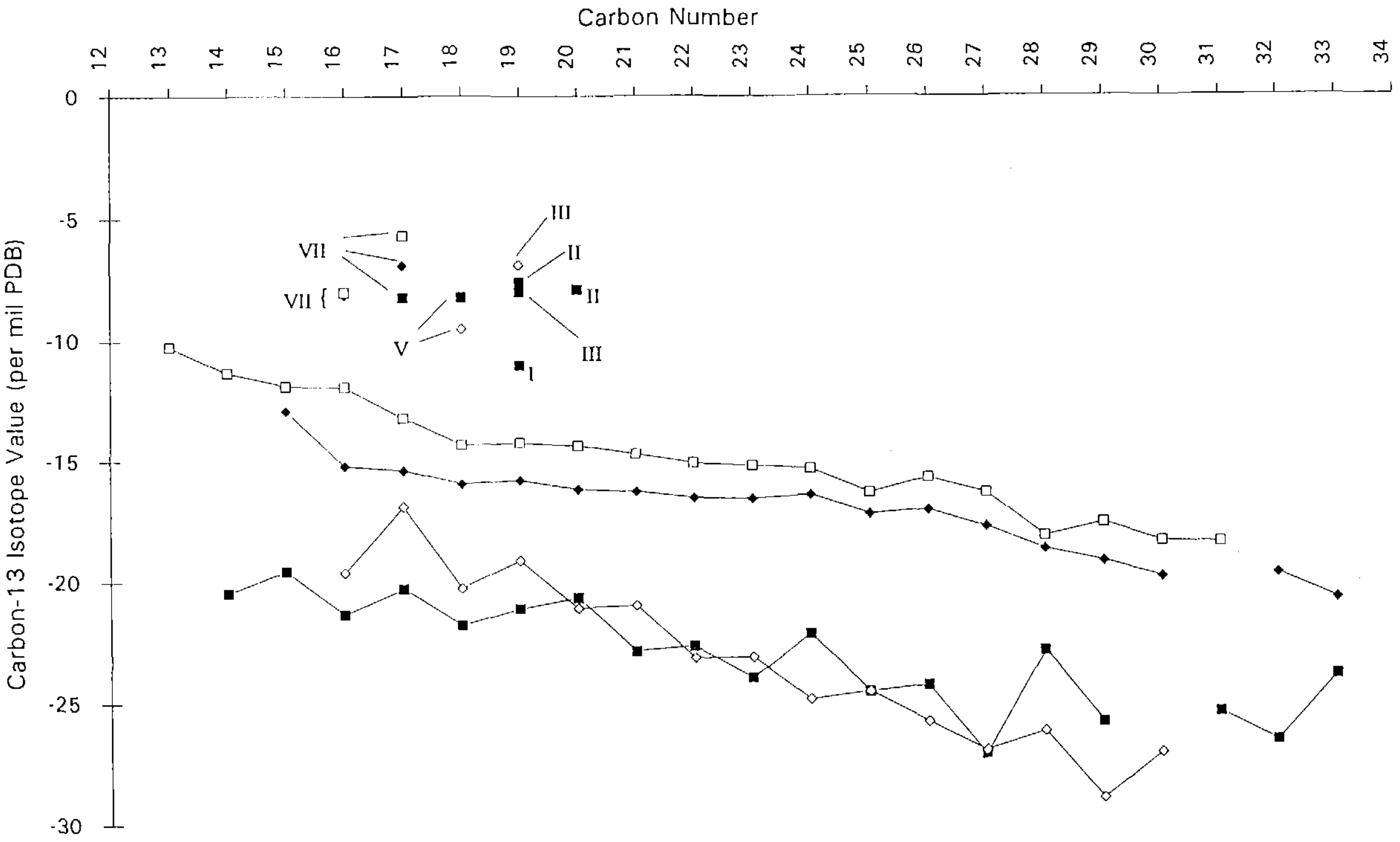
Carbon Number
12
13
14
15
16
17
18
19
20
21
22
23
24
25
26
27
28
29
30
31
32
33
34
Carbon-13 Isotope Value (per mil PDB)
0
-5
-10
-15
-20
-25
-30
VII
VII {
V
III
II
II
III
I

859083

Scheme 1

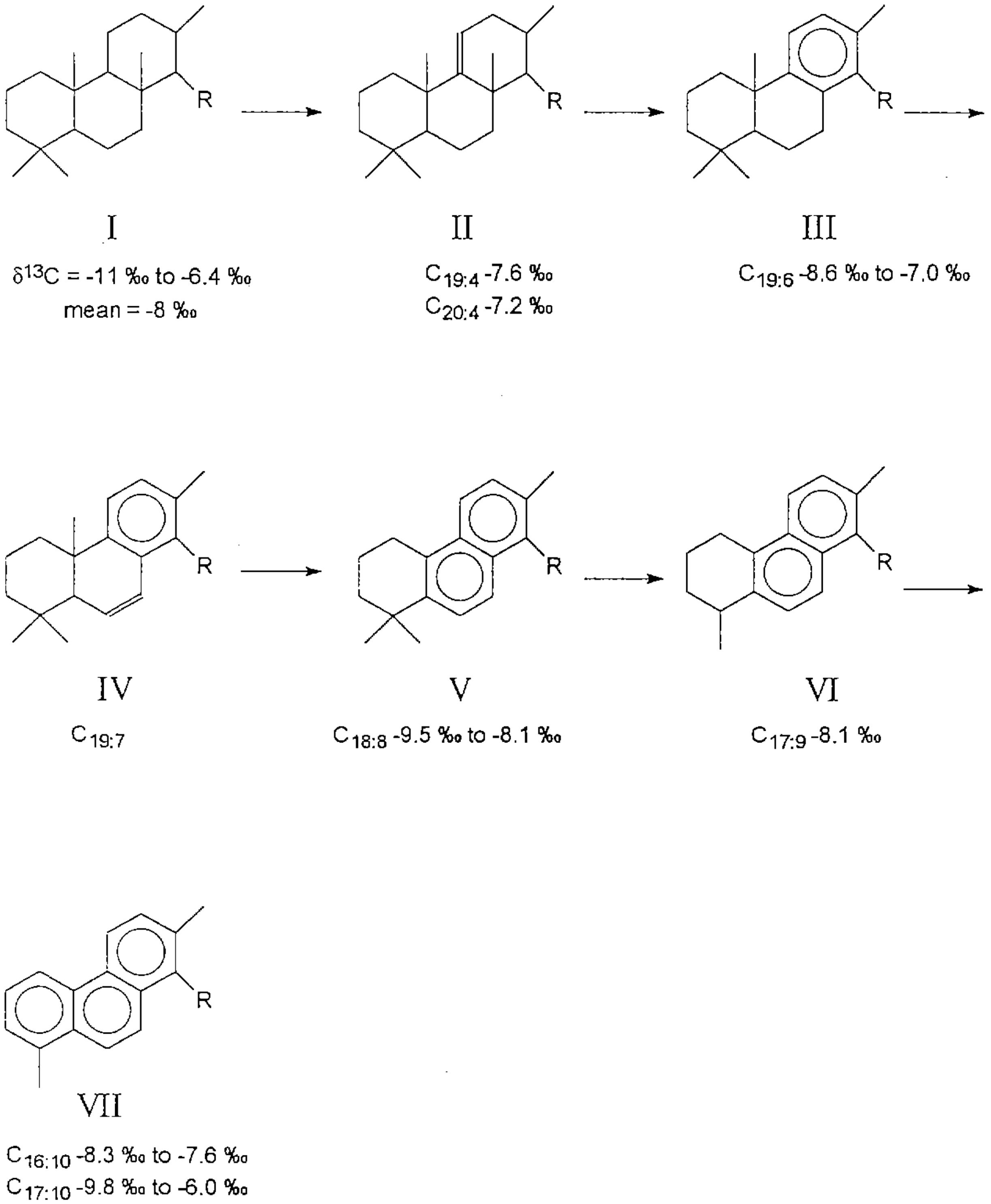

Proposed general scheme for tricyclic compound aromatisation. R = H or alkyl chain, Cn:x, n = carbon number, x = rings + double bonds. Compound IV could be identified but no isotopic data could be obtained. Compounds I, III and V-VII had mass spectra comparable to published data. For type II ($C_{19:4}$) M^+ 260 (27 %), 245 (100), 189 (8), 175 (29), 163 (15), 149 (67), 119 (21); type IV ($C_{19:7}$) M^+ 254 (35), 239 (45), 183 (42), 169 (100).